UNIVERSIDADE FEDERAL DE VIÇOSA

ISABELLA VASCONCELLOS GOULART

EVALUATION OF PANCHELONIOIDEA (TESTUDINES: CRYPTODIRA) EVOLUTION BASED ON PHYLOGENETIC MORPHOMETRICS

VIÇOSA – MINAS GERAIS
2021

ISABELLA VASCONCELLOS GOULART

EVALUATION OF PANCHELONIOIDEA (TESTUDINES: CRYPTODIRA) EVOLUTION BASED ON PHYLOGENETIC MORPHOMETRICS

Dissertação apresentada à Universidade Federal de Viçosa, como parte das exigências do Programa de Pós-Graduação em Biologia Animal, para obtenção do título de *Magister Scientiae*.

Orientador: Pedro Seyferth Ribeiro Romano

VIÇOSA – MINAS GERAIS
2021

Ficha catalográfica elaborada pela Biblioteca Central da Universidade Federal de Viçosa - Campus Viçosa

T

G694e
2021

Goulart, Isabella Vasconcellos, 1995-
Evaluation of Panchelonioidea (Testudines: Cryptodira) evolution based on phylogenetic morphometrics / Isabella Vasconcellos Goulart. - Viçosa, MG, 2021.
96 f. : il. (algumas color.) ; 29 cm.

Inclui apêndices.
Orientador: Pedro Seyferth Ribeiro Romano.
Dissertação (mestrado) - Universidade Federal de Viçosa.
Referências bibliográficas: f. 55-58.

1. Tartaruga-marinha. 2. Evolução. 3. Filogenética. 4. Morfometria. I. Universidade Federal de Viçosa. Departamento de Biologia Animal. Programa de Pós-Graduação em Biologia Animal. II. Título.

CDD 22. ed. 597.9209813

ISABELLA VASCONCELLOS GOULART

EVALUATION OF PANCHELONIOIDEA (TESTUDINES: CRYPTODIRA) EVOLUTION BASED ON PHYLOGENETIC MORPHOMETRICS

Dissertação apresentada à Universidade Federal de Viçosa, como parte das exigências do Programa de Pós-Graduação em Biologia Animal, para obtenção do título de *Magister Scientiae*.

APROVADA: 13 de janeiro de 2021

Assentimento:

Isabella Vasconcellos Goulart
Autora

Pedro Seyferth Ribeiro Romano
Orientador

Dedico esse trabalho ao meu noivo, Fernando Elias, por sua compreensão e apoio incondicionais.

AGRADECIMENTOS

Meu primeiro e maior agradecimento vai à minha família *sensu lato*, porque família não são só os "de sangue" – não posso colocar minha família em um clado monofilético porque ela vai muito além disso. Então meu muito obrigada aos que sempre me apoiaram em todos os sentidos, que me estimularam a dar o meu melhor e a continuar mesmo quando as coisas parecem difíceis. Minha família de Valença por me manter alegre, saudável e motivada, a família de Curitiba por me acolher e sempre se preocupar comigo e a de Viçosa, em especial ao meu orientador e ao pessoal do LAPOC, por me ajudarem a lidar com o vespeiro. Agradeço até ao vespeiro (o apelido dessa dissertação, no sentido de que sempre em que se mexe, sai mais coisa para resolver), por me ensinar que eu talvez seja mais capaz do que eu acredito ser.

Muito obrigada aos participantes da banca: Santiago Catalano pelo aconselhamento e revisão ao longo do processo e Gustavo Oliveira por fazer parte da comissão avaliadora e ajudar no aprimoramento deste projeto.

Agradeço o auxílio do professor Leonardo Bherig, por permitir a utilização do cluster do Laboratório de Processamento Biométrico para realização das análises filogenéticas; F. James Rohlf e Stony Brook Morphometrics por tornarem a série de software TPS disponível gratuitamente, e Willy Hennig Society por tornar possível o acesso gratuito ao software TNT.

Sou muito grata também pela ajuda de Serjoscha Evers por fornecer fotos de vários espécimes adicionados a esta amostra. Obrigada também pelo o acesso ao acervo de quelônios da UNIVALI e a ajuda dos curadores Jules, Bibiana e Gerson.

Um muito obrigada também à Universidade Federal de Viçosa e ao Programa de Pós-Graduação em Biologia Animal por tornarem essa pesquisa possível.

O presente trabalho foi realizado com apoio da Coordenação de Aperfeiçoamento de Pessoal de Nível Superior – Brasil (CAPES) – Código de Financiamento 001.

"Although stability is often considered an important quality of classifications, I believe that it is often a spurious and misleading indication of the attainment of phylogenetic "truth." All of our notions about phylogeny are hypotheses that could be wrong; they can never be proved correct. If a classification is to have wide-ranging biologic usefulness, it must be susceptible to change."

E. Gaffney, 1977

Estudar Biologia sem o conhecimento da Paleontologia é como ler um livro do qual só se têm as duas últimas páginas.

RESUMO

GOULART, Isabella Vasconcellos, M.Sc., Universidade Federal de Viçosa, janeiro de 2021. **Avaliação da Evolução de Panchelonioidea (Testudines: Cryptodira) Baseada em Filogenia Morfométrica.** Orientador: Pedro Seyferth Ribeiro Romano.

Nesse estudo é apresentada uma hipótese cladística baseada em marcos anatômicos, conhecida como Morfometria Filogenética. A análise foi conduzida investigando 11 configurações de marcos anatômicos (carapaça, coracoide, úmero, ílio, ísquio, mandíbula, plastrão, púbis e crânio – dorsal, ventral e lateral) de 31 espécies de tartarugas marinhas. Essas configurações representam um conjunto de coordenadas que retêm a forma geral de uma estrutura e, pode-se dizer, permitem mapear diferenças morfológicas entre táxons com menos subjetividade do que com caracteres discretos. Embora algumas inconsistências persistam, como as relações internas e a definição filogenética de Cheloniidae, os resultados permitem elucidar algumas questões sobre a evolução de Panchelonioidea. *Ctenochelys procax* e *Toxochelys latiremis* foram resgatadas como, respectivamente, os dois primeiros nós de divergência de Panchelonioidea Os Cheloniidae estemáticos do Cretáceo, *Euclastes wielandi* e *Allopleuron hofmanni*, foram aninhados separados das demais espécies de Cheloniidae, mostrando mais afinidade com os clados do Cretáceo Superior do que com tartarugas marinhas cenozoicas. Portanto, *E. wielandi* foi realocado para Ctenochelyidae. A composição de Dermochelyoidea *sensu* Evers & Benson, 2019 é suportada por nossos dados e *Allopleuron* presumivelmente tem maior afinidade com esse clado do que com Pancheloniidae. Os Cheloniidae do Paleogeno foram posicionados em dois grupos fortemente suportados, com o primeiro táxon a divergir sendo *Eochelone*. *Ocepechelon bouyai* foi recuperada em Protostegidae e os resultados confirmam que os antigos membros de "Osteopygidae" possuem origens distintas (linhagens independentes). O fato de Protostegidae ser recuperado dentro do grupo coroa Chelonioidea é controverso e implica em uma extensa linhagem-fantasma para a maioria de Cheloniidae, portanto é possível que este posicionamento seja resultado de convergência evolutiva, provavelmente constituindo especializações ao modo de vida pelágico que mascararam parte do sinal filogenético dos dados analisados.

Palavras-chave: Panchelonioidea. Tartarugas marinhas. Fósseis. Paleontologia. Parcimônia. Procrustes. Sistemática Filogenética. Morfometria Geométrica. TNT.

ABSTRACT

GOULART, Isabella Vasconcellos, M.Sc., Universidade Federal de Viçosa, January, 2021. **Evaluation of Panchelonioidea (Testudines: Cryptodira) evolution based on phylogenetic morphometrics.** Advisor: Pedro Seyferth Ribeiro Romano.

This study presents a cladistic hypothesis based on morphogeometric data, known as Phylogenetic Morphometrics. The analysis was conducted investigating 11 landmark configurations (carapace, coracoid, humerus, ilium, ischium, jaw, plastron, pubis and skull - dorsal, ventral and lateral) of 31 species of sea turtles. These configurations represent a set of anatomical landmarks that retain the general shape of a structure and allow to map morphological differences between taxa with less subjectivity than with discrete characters. Although some inconsistencies persist, such as internal relationships and the phylogenetic definition of Cheloniidae, the results elucidate some aspects about the evolution of Panchelonioidea. *Ctenochelys procax* and *Toxochelys latiremis* were recovered as, respectively, the first two divergence nodes of Panchelonioidea. The Cretaceous stem-Cheloniidae, *Euclastes wielandi* and *Allopleuron hofmanni*, were nested separately from the other species of Cheloniidae, showing more affinity with the Upper Cretaceous clades than with Cenozoic sea turtles, so, *E. wielandi* was reallocated to Ctenochelyidae. The composition of Dermochelyoidea *sensu* Evers & Benson, 2019 is supported by our data and *Allopleuron* presumably has a greater affinity with this clade than with Panchelonioidae. The Paleogene Cheloniidae were placed in two strongly supported groups, with *Eochelone* as the first diverging taxon. Despite being positioned outside Panchelonioidea, there is no concrete evidence supporting *Mesodermochelys undulatus* as stem-Cryptodira. *Ocepechelon bouyai* was recovered in Protostegidae and the results confirm that the former members of "Osteopygidae" have different origins (independent lineages). The fact that Protostegidae is recovered within the Chelonioidea crown-group is controversial and implies an extensive ghost lineage for most Cheloniidae, so it is possible that this positioning is the result of evolutionary convergence, probably comprising pelagic specializations that masked part of the phylogenetic signal in the analysed data.

Keywords: Panchelonioidea. Sea turtle. Fossil turtle. Palaeontology. Parsimony. Procrustes. Phylogenetic Morphometrics. Geometric Morphometrics. TNT.

LISTA DE FIGURAS

Figure 1. Schematic reference of landmark configurations shown in *Chelonia mydas* (humerus based on MOVI27799 and all the other bones based on MZUFV0068-C). Descriptions of all landmarks illustrated in here are presented in Appendix A. Legend: A: skull in dorsal view, B: skull in ventral view, C: skull in lateral view, D: jaw in dorsal view, E: carapace in dorsal view, F: plastron in ventral view, G: right coracoid in dorsal view, H: right pubis in dorsal view, I: right ilium in dorsal view, J: right ischium in dorsal view, K: left humerus in ventral view. Scale 5 cm. 24

Figure 2. Cutout of the dorsal view of the skull from Figure 1, detailing osteological structures and anatomical reference for landmark digitisation. Scale 5 cm.. 59

Figure 3. Cutout of the ventral view of the skull from Figure 1, detailing osteological structures and anatomical reference for landmark digitisation. Scale 5 cm. 60

Figure 4. Cutout of the lateral view of the skull from Figure 1, detailing osteological structures and anatomical reference for landmark digitisation. Scale 5 cm. 61

Figure 5. Cutout of the jaw from Figure 1, detailing osteological structures and anatomical reference for landmark digitisation. Scale 5 cm. 62

Figure 6. Cutout of the carapace from Figure 1, detailing osteological structures and anatomical reference for landmark digitisation. Scale 5 cm. 63

Figure 7. Cutout of the coracoid from Figure 1, detailing osteological structures and anatomical reference for landmark digitisation. Scale 5 cm. 64

Figure 8. Cutout of the humerus from Figure 1, detailing osteological structures and anatomical reference for landmark digitisation. Scale 5 cm. 65

Figure 9. Cutout of the plastron from Figure 1, detailing osteological structures and anatomical reference for landmark digitisation. Scale 5 cm. 66

Figure 10. Cutout of the pubis from Figure 1, detailing osteological structures and anatomical reference for landmark digitisation. Scale 5 cm. 67

Figure 11. Cutout of the ischium from Figure 1, detailing osteological structures and anatomical reference for landmark digitisation. Scale 5 cm. 68

Figure 12. Cutout of the ischium from Figure 1, detailing osteological structures and anatomical reference for landmark digitisation. Scale 5 cm. 68

Figure 13. Flowchart summarizing the steps taken in this analysis from raw data to the most parsimonious tree (MPT). LM's – landmarks; ch. – characters; conf. – configurations. 29

Figure 14. Relative Warps Analysis of the skull (dorsal view). The colors and icons represent the clades: green – Protostegidae; blue – Pancheloniidae; red – Dermochelyidae; black – Chelydridae; purple – Ctenochelyidae; pink – *Toxochelys latiremis.* The numbers represent the species: 2 – *Ashleychelys palmeri †,* 3 – *Caretta caretta,* 4 – *Carolinochelys wilsoni †,* 5 – *Chelonia mydas,* 6 – *Eochelone brabantica †,* 7 – *Eretmochelys imbricata,* 8 – *Lepidochelys kempii,* 9 – *Lepidochelys olivacea,* 10 – *Natator depressus,* 12 – *Procolpochelys charlestonensis †,* 13 – *Procolpochelys grandaeva †,* 14 – *Puppigerus camperi †,* 15 – *Dermochelys coriacea,* 17 – *Eosphargis gigas †,* 22 – *Desmatochelys lowii †,* 24 – *Santanachelys gaffneyi †,* 27 – *Erquelinnesia gosseleti †,* 29 – *Toxochelys latiremis †,* 32 – *Chelydra serpentina.* The polygons represent the shape range of each clade. Along the x and y axes, thin plate splines are placed indicating the shape represented by each extreme of that axis. RW_1 = 33,34% of the variance and RW_2 = 24,16%.. 69

Figure 15. Relative Warps Analysis of the skull (ventral view). The colors and icons represent the clades: green – Protostegidae; blue – Pancheloniidae; red – Dermochelyidae; black – Chelydridae; purple – Ctenochelyidae; pink – *Toxochelys latiremis.* The numbers represent the species: 1 – *Allopleuron hofmanni †,* 2 – *Ashleychelys palmeri †,* 3 – *Caretta caretta,* 4 – *Carolinochelys wilsoni †,* 5 – *Chelonia mydas,* 6 – *Eochelone brabantica †,* 7 – *Eretmochelys imbricata,* 8 – *Lepidochelys kempii,* 9 – *Lepidochelys olivacea,* 10 – *Natator depressus,* 11 – *Euclastes wielandi †,* 12 – *Procolpochelys charlestonensis †,* 13 – *Procolpochelys grandaeva †,* 14 – *Puppigerus camperi †,* 15 – *Dermochelys coriacea,* 20 – *Archelon ischyros †,* 21 – *Bouliachelys suteri †,* 23 – *Protostega gigas †,* 25 – *Ctenochelys acris †,* 26 – *Ctenochelys procax †,* 27 – *Erquelinnesia gosseleti †,* 28 – *Erquelinnesia planimentum †,* 29 – *Toxochelys*

latiremis †, 30 – *Prionochelys matutina †,* 31 – *Ctenochelys stenoporus †,* 32 – *Chelydra serpentina.* The polygons represent the shape range of each clade. Along the x and y axes, thin plate splines are placed indicating the shape represented by each extreme of that axis.RW_1 = 28,29% of the variance and RW_2 = 22,43%.. 71

Figure 16. Relative Warps Analysis of the skull (lateral view). The colors and icons represent the clades: green – Protostegidae; blue – Pancheloniidae; red – Dermochelyidae; black – Chelydridae. The numbers represent the species: 3 – *Caretta caretta,* 5 – *Chelonia mydas,* 6 – *Eochelone brabantica †,* 7 – *Eretmochelys imbricata,* 8 – *Lepidochelys kempii,* 9 – *Lepidochelys olivacea,* 10 – *Natator depressus,* 14 – *Puppigerus camperi †,* 15 – *Dermochelys coriacea,* 24 – *Santanachelys gaffneyi †,* 32 – *Chelydra serpentina.* The polygons represent the shape range of each clade. Along the x and y axes, thin plate splines are placed indicating the shape represented by each extreme of that axis.RW_1 = 24,66% of the variance and RW_2 = 23,84%. 70

Figure 17. Relative Warps Analysis of the jaw. The colors and icons represent the clades: green – Protostegidae; blue – Pancheloniidae; red – Dermochelyidae; black – Chelydridae; purple – Ctenochelyidae. The numbers represent the species: 3 – *Caretta caretta,* 4 – *Carolinochelys wilsoni †,* 5 – *Chelonia mydas,* 6 – *Eochelone brabantica †,* 7 – *Eretmochelys imbricata,* 8 – *Lepidochelys kempii,* 9 – *Lepidochelys olivacea,* 10 – *Natator depressus,* 12 – *Procolpochelys charlestonensis †,* 15 – *Dermochelys coriacea,* 17 – *Eosphargis gigas †,* 18 – *Mesodermochelys undulatus †,* 21 – *Bouliachelys suteri †,* 22 – *Desmatochelys lowii †,* 27 – *Erquelinnesia gosseleti †,* 31 – *Ctenochelys stenoporus †,* 32 – *Chelydra serpentina.* The polygons represent the shape range of each clade. Along the x and y axes, thin plate splines are placed indicating the shape represented by each extreme of that axis.RW_1 = 66,93% of the variance and RW_2 = 18,14%.. 73

Figure 18. Relative Warps Analysis of the carapace. The colors and icons represent the clades: green – Protostegidae; blue – Pancheloniidae; red – Dermochelyidae; black – Chelydridae; purple – Ctenochelyidae. The numbers represent the species: 1 – *Allopleuron hofmanni †,* 2 – *Ashleychelys palmeri †,* 4 – *Carolinochelys wilsoni †,* 5 – *Chelonia mydas,* 8 – *Lepidochelys kempii,* 9 – *Lepidochelys olivacea,* 12 – *Procolpochelys charlestonensis †,* 13 – *Procolpochelys grandaeva †,* 16 – *Eosphargis breineri †,* 19 – *Ocepechelon bouyai †,* 20 – *Archelon ischyros †,* 22 – *Desmatochelys lowii †,* 23 – *Protostega gigas †,* 25 – *Ctenochelys acris †,* 31 – *Ctenochelys stenoporus †,* 32 – *Chelydra serpentina.* The polygons represent the shape range of each clade. Along the x and y axes, thin plate splines are placed indicating the shape represented by each extreme of that axis.RW_1 = 53,74% of the variance and RW_2 = 14,21%. 72

Figure 19. Relative Warps Analysis of the plastron. The colors and icons represent the clades: green – Protostegidae; from blue – Pancheloniidae; black – Chelydridae; purple – Ctenochelyidae. The numbers represent the species: 2 – *Ashleychelys palmeri †,* 3 – *Caretta caretta,* 5 – *Chelonia mydas,* 9 – *Lepidochelys olivacea,* 10 – *Natator depressus,* 12 – *Procolpochelys charlestonensis †,* 13 – *Procolpochelys grandaeva †,* 22 – *Desmatochelys lowii †,* 30 – *Prionochelys matutina †,* 31 – *Ctenochelys stenoporus †,* 32 – *Chelydra serpentina.* The polygons represent the shape range of each clade. Along the x and y axes, thin plate splines are placed indicating the shape represented by each extreme of that axis.RW_1 = 37,90% of the variance and RW_2 = 26,91%. 75

Figure 20. Relative Warps Analysis of the coracoid. The colors and icons represent the clades: blue – Pancheloniidae; red – Dermochelyidae; purple – Ctenochelyidae. The numbers represent the species: 3 – *Caretta caretta,* 5 – *Chelonia mydas,* 7 – *Eretmochelys imbricata,* 9 – *Lepidochelys olivacea,* 10 – *Natator depressus,* 15 – *Dermochelys coriacea,* 18 – *Mesodermochelys undulatus †,* 25 – *Ctenochelys acris †,* 31 – *Ctenochelys stenoporus †.* The polygons represent the shape range of each clade. Along the x and y axes, thin plate splines are placed indicating the shape represented by each extreme of that axis. RW_1 = 80,79% of the variance and RW_2 = 7,39%.. 74

Figure 21. Relative Warps Analysis of the humerus. The colors and icons represent the clades: green – Protostegidae; blue – Pancheloniidae; red – Dermochelyidae; purple – Ctenochelyidae. The numbers represent the species: 1 – *Allopleuron hofmanni †,* 3 – *Caretta caretta,* 7 – *Eretmochelys imbricata,* 9 – *Lepidochelys olivacea,* 10 – *Natator depressus,* 11 – *Euclastes wielandi †,* 15 – *Dermochelys coriacea,* 18 – *Mesodermochelys undulatus †,* 20 – *Archelon ischyros †,* 22 – *Desmatochelys lowii †,* 30 – *Prionochelys matutina †.* The polygons represent the shape range of each clade. Along the x and y axes, thin plate splines are placed indicating the shape represented by each extreme of that axis.RW_1 = 58,37% of the variance and RW_2 = 14,17%. 77

Figure 22. Relative Warps Analysis of the pubis. The colors and icons represent the clades: blue – Pancheloniidae; red – Dermochelyidae; black – Chelydridae; purple – Ctenochelyidae. The numbers represent the species: 3 – *Caretta caretta,* 5 – *Chelonia mydas,* 7 – *Eretmochelys imbricata,* 9 – *Lepidochelys olivacea,* 10 – *Natator depressus,* 15 – *Dermochelys coriacea,* 18 – *Mesodermochelys undulatus †,*

19 – *Ocepechelon bouyai †,* 25 – *Ctenochelys acris †,* 30 – *Prionochelys matutina †,* 31 – *Ctenochelys stenoporus †,* 32 – *Chelydra serpentina.* The polygons represent the shape range of each clade. Along the x and y axes, thin plate splines are placed indicating the shape represented by each extreme of that axis. RW_1 = 46,94% of the variance and RW_2 = 24,48%.. 76

Figure 23. Relative Warps Analysis of the ilium. The colors and icons represent the clades: blue – Pancheloniidae; red – Dermochelyidae; black – Chelydridae; purple – Ctenochelyidae. The numbers represent the species: 3 – *Caretta caretta,* 5 – *Chelonia mydas,* 7 – *Eretmochelys imbricata,* 9 – *Lepidochelys olivacea,* 10 – *Natator depressus,* 15 – *Dermochelys coriacea,* 18 – *Mesodermochelys undulatus †,* 25 – *Ctenochelys acris †,* 30 – *Prionochelys matutina †,* 31 – *Ctenochelys stenoporus †,* 32 – *Chelydra serpentina.* The polygons represent the shape range of each clade. Along the x and y axes, thin plate splines are placed indicating the shape represented by each extreme of that axis.RW_1 = 58,70% of the variance and RW_2 = 23,70%. 79

Figure 24. Relative Warps Analysis of the ischium. The colors and icons represent the clades: blue – Pancheloniidae; red – Dermochelyidae; black – Chelydridae; purple – Ctenochelyidae. The numbers represent the species: 5 – *Chelonia mydas,* 7 – *Eretmochelys imbricata,* 10 – *Natator depressus,* 15 – *Dermochelys coriacea,* 25 – *Ctenochelys acris †,* 30 – *Prionochelys matutina †,* 31 – *Ctenochelys stenoporus †,* 32 – *Chelydra serpentina.* The polygons represent the shape range of each clade. Along the x and y axes, thin plate splines are placed indicating the shape represented by each extreme of that axis. RW_1 = 69,28% of the variance and RW_2 = 10,45%.. 78

Figure 25. Cladograms of the most parsimonious trees of the carapace and skull (dorsal view) preliminary analyses. Legend: green – Protostegidae; blue – Pancheloniidae; red – Dermochelyidae; black – Chelydridae; purple – Ctenochelyidae; pink – *Toxochelys latiremis.* *80*

Figure 26. Cladogram of the most parsimonious tree of the skull (ventral view) preliminary analysis. Legend: green – Protostegidae; blue – Pancheloniidae; red – Dermochelyidae; black – Chelydridae; purple – Ctenochelyidae; pink – *Toxochelys latiremis.* *81*

Figure 27. Cladograms of the most parsimonious trees of the skull (lateral view), coracoid and ilium preliminary analyses. Legend: green – Protostegidae; blue – Pancheloniidae; red – Dermochelyidae; black – Chelydridae; purple – Ctenochelyidae. 82

Figure 28. Cladograms of the most parsimonious trees of the ischium and jaw preliminary analyses. Legend: green – Protostegidae; blue – Pancheloniidae; red – Dermochelyidae; black – Chelydridae; purple – Ctenochelyidae. 83

Figure 29. Cladograms of the most parsimonious trees of the plastron, pubis and humerus preliminary analyses. Legend: green – Protostegidae; blue – Pancheloniidae; red – Dermochelyidae; black – Chelydridae; purple – Ctenochelyidae. *84*

Figure 30. Cladogram of the most parsimonious trees of the "head" = skull (all views) + jaw preliminary analysis. Legend: green – Protostegidae; blue – Pancheloniidae; red – Dermochelyidae; black – Chelydridae; purple – Ctenochelyidae; pink – *Toxochelys latiremis.* *85*

Figure 31. Cladograms of the most parsimonious trees of the shell = carapace + plastron, pelvic girdle = ilium + ischium + pubis, and pectoral girdle = coracoid + humerus preliminary analyses. Legend: green – Protostegidae; blue – Pancheloniidae; red – Dermochelyidae; black – Chelydridae; purple – Ctenochelyidae. 86

Figure 32. Cladograms of the most parsimonious trees of the appendices = pelvic + pectoral girdles, and post-cranium = shell + appendices preliminary analyses. Legend: green – Protostegidae; blue – Pancheloniidae; red – Dermochelyidae; black – Chelydridae; purple – Ctenochelyidae.. 87

Figure 33. Cladogram of the most parsimonious trees of the "turtle" = all LM configurations preliminary analysis. Legend: green – Protostegidae; blue – Pancheloniidae; red – Dermochelyidae; black – Chelydridae; purple – Ctenochelyidae; pink – *Toxochelys latiremis.* *88*

Figure 34. Strict consensus of the 2 most parsimonious trees of the reanalysis of Gentry *et al.,* 2019 pruned matrix. The purple dots point changes in the nodes in contrast to the original tree. Legend: green – Protostegidae; blue – Pancheloniidae; red – Dermochelyidae; black – Chelydridae; purple – Ctenochelyidae; pink – *Toxochelys latiremis.* *89*

Figure 35. Cladogram of the most parsimonious tree of the first global preliminary analysis. Legend: green – Protostegidae; blue – Pancheloniidae; red – Dermochelyidae; black – Chelydridae; purple – Ctenochelyidae; pink – *Toxochelys latiremis.* *90*

Figure 36. Cladogram of the most parsimonious tree of the second global preliminary analysis. Legend: green – Protostegidae; blue – Pancheloniidae; red – Dermochelyidae; black – Chelydridae; purple – Ctenochelyidae; pink – *Toxochelys latiremis.* Species with only LM data are marked with an asterisk. . . 91

Figure 37. Cladogram of the most parsimonious tree of the third global preliminary analysis. Legend: green – Protostegidae; blue – Pancheloniidae; red – Dermochelyidae; black – Chelydridae; purple – Ctenochelyidae; pink – *Toxochelys latiremis.* *92*

Figure 38. Cladogram of the most parsimonious tree of the fourth global preliminary analysis. Legend: green – Protostegidae; blue – Pancheloniidae; red – Dermochelyidae; black – Chelydridae; purple – Ctenochelyidae; pink – *Toxochelys latiremis.* *93*

Figure 39. Cladogram of the most parsimonious tree of the fifth global preliminary analysis. Legend: green – Protostegidae; blue – Pancheloniidae; red – Dermochelyidae; black – Chelydridae; purple – Ctenochelyidae; pink – *Toxochelys latiremis.* *94*

Figure 39. Time-calibrated phylogeny combining all landmark data with Gentry *et al.*, 2019's pruned dataset of discrete morphological characters, aligned to *Natator depressus*. Relative Bremer Supports (above 0.5) are indicated under the nodes, rounded to one decimal place. Legend: I: divergence node of Panchelonioidea; II: crown-Chelonioidea; III: Dermochelyoidea; IV: Carettini; V: K-Pg mass extinction; VI: Eocene-Oligocene cooling event; VII: Pg-N brief glacial event; blue – Pancheloniidae; red – Dermochelyidae; black – Chelydridae; purple – Ctenochelyidae; pink – *Toxochelys latiremis*. The numerical ages are in Ma. Chart from the International Commission on Stratigraphy (1), accessed on December 11, 2020. 46

Figure 40. Cladogram of the most parsimonious tree of the sixth global preliminary analysis. Legend: blue – Pancheloniidae; red – Dermochelyidae; black – Chelydridae; purple – Ctenochelyidae; pink – *Toxochelys latiremis.* *95*

Figure 41. Cladogram of the most parsimonious tree of the sixth global preliminary analysis. Legend: green – Protostegidae; blue – Pancheloniidae; red – Dermochelyidae; black – Chelydridae; purple – Ctenochelyidae; pink – *Toxochelys latiremis.* *96*

LISTA DE TABELAS

Table 1. This table describes the sample used in the phylogenetic analysis, the source of the images for Geometric Morphometrics, taxonomic, locality and geostratigraphic information, as well as the availability of data for each configuration of landmarks. 21

Table 2. This table contains anatomical descriptions of each landmark in Figure 2 and its classification by type, according to Bookstein, 1991: 1 – contact of 3 structures/tissues; 2 – maximum or minimal curvature of a structure; 3 – points located in boundaries, limits or edges. 59

Table 3. This table contains anatomical descriptions of each landmark in Figure 3 and its classification by type, according to Bookstein, 1991: 1 – contact of 3 structures/tissues; 2 – maximum or minimal curvature of a structure; 3 – points located in boundaries, limits or edges. 60

Table 4. This table contains anatomical descriptions of each landmark in Figure 4 and its classification by type, according to Bookstein, 1991: 1 – contact of 3 structures/tissues; 2 – maximum or minimal curvature of a structure; 3 – points located in boundaries, limits or edges. 61

Table 5. This table contains anatomical descriptions of each landmark in Figure 5 and its classification by type, according to Bookstein, 1991: 1 – contact of 3 structures/tissues; 2 – maximum or minimal curvature of a structure; 3 – points located in boundaries, limits or edges. 62

Table 6. This table contains anatomical descriptions of each landmark in Figure 6 and its classification by type, according to Bookstein, 1991: 1 – contact of 3 structures/tissues; 2 – maximum or minimal curvature of a structure; 3 – points located in boundaries, limits or edges. 63

Table 7. This table contains anatomical descriptions of each landmark in Figure 7 and its classification by type, according to Bookstein, 1991: 1 – contact of 3 structures/tissues; 2 – maximum or minimal curvature of a structure; 3 – points located in boundaries, limits or edges. 64

Table 8. This table contains anatomical descriptions of each landmark in Figure 8 and its classification by type, according to Bookstein, 1991: 1 – contact of 3 structures/tissues; 2 – maximum or minimal curvature of a structure; 3 – points located in boundaries, limits or edges. 65

Table 9. This table contains anatomical descriptions of each landmark in Figure 9 and its classification by type, according to Bookstein, 1991: 1 – contact of 3 structures/tissues; 2 – maximum or minimal curvature of a structure; 3 – points located in boundaries, limits or edges. 66

Table 10. This table contains anatomical descriptions of each landmark in Figure 10 and its classification by type, according to Bookstein, 1991: 1 – contact of 3 structures/tissues; 2 – maximum or minimal curvature of a structure; 3 – points located in boundaries, limits or edges. 67

Table 11. This table contains anatomical descriptions of each landmark in Figure 11 and its classification by type, according to Bookstein, 1991: 1 – contact of 3 structures/tissues; 2 – maximum or minimal curvature of a structure; 3 – points located in boundaries, limits or edges. 68

Table 12. This table contains anatomical descriptions of each landmark in Figure 12 and its classification by type, according to Bookstein, 1991: 1 – contact of 3 structures/tissues; 2 – maximum or minimal curvature of a structure; 3 – points located in boundaries, limits or edges. 68

Table 13. Compilation of settings, computational specifications and results of every phylogenetic search in this paper. All matrices and trees (figures and parenthetic notations) can be found in the Supplementary Material. Legend: BIOMETRIA is a cluster run by the Laboratory of Biometrical Processing in Federal University of Viçosa to which we were granted access during the execution of this research; the operational system is Windows Server 2008 R2 enterprise 64 bit, with two processors Intel Xeon CPU E5-2643 0 3.30GHz, memory of 96GB and 4 HD's totalizing 4.6 TB storage. PC Fernando is a personal computer Dell 64bit with processor Intel Core i7-4700MQ CPU 2.4GHz, memory of 16GB, operating with a Windows 10 Home 2020 and 1TB storage. PC Dell is a personal computer Dell 64bit with processor Intel Core i7-6700HQ CPU 2.6GHz, memory of 16GB, operating with a Windows 10 Home 2018 and 1TB storage. PC HP is a personal computer HP Pavilion Sleekbook 14 RW 64bit, with processor Intel Core i3-32171 CPU 1.8GHz, memory of 4GB, operating with a Windows 10 Home version 10.1018363 and 500GB storage. 30

LISTA DE ABREVIATURAS E SIGLAS

Osteological abbreviations

Ac. facet – acetabular facet
Add. cham. – adductor chamber
Ap. narium ext. – apertura narium externa
Ap. narium int. – apertura narium interna
ART – articular
BO – basioccipital
BS – basisphenoid
C – costal
Cap. hum. – capu thumeri
Cav. tymp. – cavum tympani
CO – coracoid
Cond. mand. – condyles mandibularis
Crista supraoc. – crista supraoccipitalis
DEN – dentary
Den. sym. – dentary symphisis
Ect. cond. groove – ectepicondylar groove
EN – entoplastron
EP – epiplastron
EX – exoccipital
FR – frontal
Gl. fossa – glenoid fossa
HO – hyoplastron
HP – hypoplastron
Int. fossa – intertubular fossa
Is. jun. – ischial junction
JU – jugal
Lat. indent. – lateral indentation
Lat. process – lateral process
Med. indent. – medial indentation
Med. process – medial process
MX – maxilla
N – neural
NU – nuchal
OP – opistothic
P – peripheral
PA – parietal
PAL – palatine

PF – prefrontal
PM – premaxilla
PO – postorbital
Post. process – posterior process
Proc. pteryg. ext. – processuspterygoideus externus
PT – pterygoid
PU – pubis
PY – pygal
QJ – quadratojugal
QU – quadrate
Rad. cond. – radial condyle
Scap. jun. – scapular junction
SO – supraoccipital
SP – suprapygal
SQ – squamosal
SUR – surangular
Temp. em. – temporal emargination
Thy. fen. – thyroid fenestra
Ul. cond. – ulnar condyle
Vent. lat. em. – ventrolateral emargination
VO – vomer
XP – xiphiplastron

Configurations

CAD = carapace - dorsal view
CD = skull - dorsal view
CL = skull - lateral view
CO = right coracoid - dorsal view
CV = skull - ventral view
II = right ilium - dorsal view
IS = right ischium - dorsal view
MD = jaw - dorsal view
P = plastron - ventral view
PU = right pubis - dorsal view
UM = left humerus - ventral view
HE = head (cd + cl + cv + md)
SH = shell (cad + p)
PEG = pelvic girdle (ii + is + pu)
PCG = pectoral girdle (co + um)
AP = appendices (PEG + PCG)
PC = post-cranium (AP + SH)

TU = turtle (PC + HE)

Institutional Abbreviations

MZUFV – Museu de Zoologia João Moojen, Universidade Federal de Viçosa
MOVI – MuseuOceanográficoUnivali
FMNH – Field Museum of Natural History
SMNS – Staatliches Museum fürNaturkunde Stuttgart
USNM – National Museum of Natural History, Smithsonian Institution
ZMB – Zoologisches Museum Berlin
AMNH – American Museum of Natural History
QM – Queensland Museum
MNHN – Muséum National d'Histoire Naturelle

SUMÁRIO

1. INTRODUCTION **18**

2. MATERIAL AND METHODS **20**

2.1. Sample and Data 20

2.2. Geometric Morphometrics 20

2.3. Phylogenetic Morphometrics 25

3. RESULTS **40**

3.1. Relative Warps 40

3.2. Preliminary trees 41

3.3. Reanalysis 42

3.4. Landmark plus traditional characters analysis 43

4. DISCUSSION **47**

5. CONCLUSION **52**

6. ACKNOWLEDGMENTS **53**

7. AUTHOR CONTRIBUTIONS **53**

8. DATA ACCESSIBILITY **53**

9. FUNDING **53**

10. COMPETING INTERESTS **54**

11. ETHICAL STATEMENT **54**

12. REFERENCES **55**

APPENDIX A. LM descritions and schematic reference for digitisation 59

APPENDIX B. Plots of the Relative Warps Analyses 69

APPENDIX C. Cladograms of the preliminary analises 80

APPENDIX D. Cladogram of the reanalysis of Gentry *et al.,* 2019's dataset 89

APPENDIX E. Cladograms of the global preliminary analises 90

1. INTRODUCTION

Panchelonioidea Joyce *et al.*, 2004 refers to the panstem clade that includes crown Chelonioidea Baur, 1893 and all relative extinct species, arguably including the Mesozoic marine clades Thalassochelydia Anquentin *et al.*, 2017, Sandownidae Tong & Meylan, 2013, and Protostegidae Cope, 1872 (2). These are highly marine-adapted (3) cryptodiran turtles, characterised by the presence of flippers, salt glands, a tendency to develop a secondary palate and hydrodynamic shell adaptions; present in all extant chelonioids and at some level in the fossil taxa (2,4,5). Modern chelonioids are restricted to seven species, recognised in two families: Dermochelyidae Lydekker, 1889 and Cheloniidae Bonaparte, 1832, along with an extensive fossil record.

Protostegidae Cope, 1872 is an extinct Cretaceous clade of specialised marine turtles and the most dominant chelonioids during Albian to Turonian (3). Studies indicate a phylogenetic proximity with Dermochelyidae, among modern chelonioids (2,3,5–10), whereas others recover Protostegidae at the stem of Panchelonioidea or as an early independent Mesozoic radiation of cryptodiran marine turtles, pre-dating *Toxochelys latiremis* and other chelonioids (11,12). According to Gentry *et al.* (13), the first hypothesis – in which Protostegidae is sister-group to Dermochelyidae – would imply a ghost-lineage of nearly 50 Myr to the first chelydroid. The controversial inclusion of Protostegidae in Panchelonioidea also influences the definition of how far back in time can we trace this sea turtle's clade. One of its most problematic phylogenetic placements is that of *Santanachelys gaffneyi* Hirayama, 1998, considered until recently to be the oldest chelonioid (9). *S. gaffneyi* is often used as sole representative of Protostegidae in global phylogenetic reconstructions (11,14,15). Similarly, *Toxochelys latiremis* Cope 1873 is feasibly considered the earliest unambiguous total-group Chelonioidea (11,15–17), and a key taxon, often used to mark the divergence node of this clade (12,18–21). Both species have well preserved fossils with several visible diagnostic features.

The species formerly assigned to "Toxochelyidae", whose phylogenetic placement is controversial, are often recovered as stem-Cheloniidae or stem-Chelonioidea: *Ctenochelys acris* Zangerl, 1953; *Ctenochelys stenoporus* Hay, 1905; *Ctenochelys procax* Hay, 1905; *Prionochelys matutina* Zangerl, 1953; *Erquelinnesia planimentum* Owen, 1842 and *Erquelinnesia gosseleti* Dollo, 1886. *Ctenochelys* spp. and *Prionochelys* sp. are assigned to Ctenochelyidae, a monophyletic group previously identified by Hirayama (3), but formally named by Gentry (20). Ctenochelyidae is recovered either nested among pancheloniids – as sister-group to the clade including crown-Cheloniidae, *Puppigerus camperi* Gray, 1831 and *Euclastes wielandi* Hay 1908 (13) –, or associated with crown-Cheloniidae (18). *Erquelinnesia gosseleti* and *Erquelinnesia planimentum* are traditionally recovered alongside *Euclastes wielandi*, Hay, 1908, also at the stem of Cheloniidae (22–24).

The clades – *Ctenochelys*, Osteopygis and *Erquelinnesia* – used to be included in "Osteopygidae", representing the oldest cheloniids, with gradual expansion of the secondary palate as a differentiating trait (25). Former "Toxochelyidae" taxa lack the extreme marine adaptation observed in the front limb and girdle elements, but they do possess flipper-like modifications in comparison to chelydrids and other testudinoids (26,27), and since the limb-complex is used as the primary basis for a diagnosis of Chelonioidea, Zangerl and Sloan (28) suggested that the families "Toxochelyidae", Protostegidae, Dermochelyidae and Cheloniidae possess these features in multiple degrees (27). Hirayama (3) considers "toxochelyids" bottom dwellers in the shallow seas instead of having pelagic habits.

Despite its relevance to environmental and paleontological studies, the origin and phylogenetic situation of several fossil marine turtles remains uncertain, impacting on our understanding of turtle evolution and fossil calibration (29).

Recently, phylogenetic studies of turtle's relationships have been increasingly relying on molecular data and even some morphological analysis often use molecular backbone (29–31). However, focusing on morphology is still a valuable way to test phylogenetic hypotheses, especially when most of the species of a given clade are represented by extinct groups, which is the case of marine turtles. Therefore, the consideration of fossil taxa is a key factor for understanding turtle evolution as a whole (2).

Our objective is to test the phylogenetic relationships of Panchelonioidea by including Geometric-Morphometrics-based data. Differently than most attempts to do a phylogenetic inference from landmark data, we used several configurations of landmarks (LM, from now on), instead of only one or two configurations (32–35). As verified in other studies (36–38), the analysis based on a single or in very few LM configurations often show poor conclusions about the evolution of the group. The inclusion of structures with different evolution rates allows the resolution of phylogenetic affinities in several levels of the tree (36,38). Furthermore, this wide variation of anatomical structures can help to reduce the effect of homoplastic characters (39). The method used was Phylogenetic Morphometrics, described in Catalano *et al.* (40), which enables the use of LM data in conventional parsimony analysis (*sensu* Farris, 1983) (36). It heuristically recovers hypothetical ancestral positions for each LM and optimize the data along the tree (41). Because of the continuous nature of landmark data, it can provide much more information about morphological variability than discrete characters, often restricted to a couple of states (36). In contrast to other methods for using LM data in phylogenetic inferences, Phylogenetic Morphometrics was proven empirically to produce results that correspond significantly to those obtained by other sources of evidence (42). This study is the first attempt to use this method on Panchelonioidea.

2. MATERIAL AND METHODS

2.1. Sample and Data

The ingroup is composed of 31 species of the four recognized families of Panchelonioidea, *Toxochelys latiremis*, sole member of the chelonioid stem-group, according to Evers & Benson (2), and former "Toxochelyidae". Geometric Morphometrics (henceforth GM) does not support missing data (43), thus all taxa that have incomplete configurations of LMs, either because of damaged fossil specimens or structures that are not visible in the sampled images – were excluded from the sample.

Chelydra serpentina Linnaeus, 1758 was chosen as outgroup because it possesses all LM configurations and have been consistently recovered inside Chelydroidea (Chelydridae + Kinosternidae), the sister-group of Panchelonioidea in the total-group Americhelydia (17). Illustrations of the species were gathered from published illustrations/ reconstructions and pictures from specimens in museum collections. The data used in this study conform to Viscosi & Cardini (44) protocol for Geometric Morphometrics. Consensus of superimposed configurations were used to represent species with more than one specimen digitized – since our aim is to study the interspecific relations. The source list for all species along with structures available for each terminal taxon can be found in Table 1, and the colour coding represent the phylogenetic hypothesis to be tested: blue to species currently assigned to Cheloniidae, red to Dermochelyidae, green to Protostegidae and purple to Ctenochelyidae.

2.2. Geometric Morphometrics

To each osteological structure, anatomical loci of interest were geometrically defined in the form of landmarks. Thus, a configuration of LMs should represent the overall shape of that structure and help to track morphological differences across species with much more accuracy and less subjectivity than discrete characters. The definition of shape herein follows Dryden &Mardia (45), in which the shape of a LM configuration consists of all its geometric information, except for its size, position in space and orientation (46).

For each configuration of LM's (carapace, coracoid, humerus, ilium, ischium, jaw, plastron, pubis, and skull – dorsal, ventral, and lateral), were defined as many LM's as possible. Then these LM's were digitised using tpsDig of the TPS series version 2.22.0.0 by James Rohlf (47). In consonance with Cardini& O'Higgins (48), LM were digitized only on the right size in all symmetrical structures, to avoid redundancy.

Table 1. This table describes the sample used in the phylogenetic analysis, the source of the images for Geometric Morphometrics, taxonomic, locality and geostratigraphic information, as well as the availability of data for each configuration of landmarks.

Species	Source	Family	Data												Geoestratigraphy	Locality
			Skull			MD	CAD	P	II	IS	PU	UM	CO	Matrix of traditional ch.		
			CD	CV	CL											
† *Allopleuron hofmanni* Gray 1831	Hirayama, 1994/ Mulder, 2003/ Jansen *et al.*, 2011/ Hans-Volker *et al.*, 2012	Pancheloniidae		X			X					X		X	Maastrichtian	Belgium; Netherlands; France; Germany; Spain
† *Ashleychelys palmeri* Weems & Sanders 2014	Weems & Brown, 2017	Pancheloniidae	X	X			X	X							Oligocene	Charleston, South Carolina, USA
Caretta caretta Linnaeus 1758	LAPOC: MZUFV0074, MZUFV0111, MZUFV0118/ UNIVALI: MOVI16405, MOVI01919, MOVI15068/ Smith, 1989/ Gaffney, 1979/ Wyneken, 2001	Pancheloniidae	X	X	X	X		X	X		X	X	X	X	Lower Calabrian - present	Atlantic, Pacific and Indian Oceans, in tropical and temperate waters
† *Carolinochelys wilsoni* Hay 1923	Weems & Brown, 2017	Pancheloniidae	X	X		X	X	X							Oligocene	Charleston, South Carolina, USA
Chelonia mydas Linnaeus 1758	LAPOC: MZUFV0068, MZUFV0113, MZUFV0114, MZUFV0115, MZUFV0116, MZUFV0117 / Smith, 1989/ Wyneken, 2001	Pancheloniidae	X	X	X	X	X	X	X	X	X		X	X	Upper Pleistocene - present	Cosmopolitan; tropical and temperate waters
† *Eochelone brabantica* Dollo 1903	Gaffney, 1979/ Smith, 1989/ Casier, 1968	Pancheloniidae	X	X	X	X								X	Lutetian	Belgium
Eretmochelys imbricata Linnaeus 1766	UNIVALI: MOVI27799/ Gaffney, 1979/ Smith, 1989/ Cadena et al, 2018/ S. Evers, personal visual collection: FMNH22241, MNHNPal1934-563, ZMB46556, ZMB53493	Pancheloniidae	X	X	X	X			X	X	X	X	X	X	Upper Pleistocene - present	Cosmopolitan; tropical waters; pelagic; shallow waters; coral reefs
Lepidochelys kempii Garman 1880	Brinkman, 2009/ Gaffney, 1979/ Smith, 1989/ Wyneken, 2001/ Wilson & Zug, 1991	Pancheloniidae	X	X	X	X	X							X	Lower Pliocene - present	North Atlantic Ocean; Gulf of Mexico
Lepidochelys olivacea Eschscholtz 1829	LAPOC: MZUFV0112/ Smith, 1989/ Gaffney, 1979/ UNIVALI: MOVI05815/ S. Evers, personal visual collection: QMJ85545, SMNS11070, ZMB51999/ Wilson & Zug, 1991	Pancheloniidae	X	X	X	X	X	X	X		X	X	X	X	Present	Epipelagic; Pacific, Indian, and south Atlantic Oceans

Table 1 (continued)

Species	Source	Family	Data												Geoestratigraphy	Locality
			Skull			MD	CAD	P	II	IS	PU	UM	CO	Matrix of traditional ch.		
			CD	CV	CL											
Natator depressus Garman 1880	Brinkman, 2009/ Gaffney, 1979/ Smith, 1989/ S. Evers, personal visual collection: QMJ4058, QMJ14463, QMJ56891, QMJ9457	Pancheloniidae	X	X	X	X	X	X	X	X	X	X	X	X	Present	Northern Oceania; continental shelf
† *Euclastes wielandi* Hay 1908	Hirayama, 1994/ Smith, 1989/ Schwimmer *et al.*, 2015	Pancheloniidae		X								X			Upper Campanian - Lower Selandian	United States; Morocco
† *Procolpochelys charlestonensis* Weems and Sanders 2014	Weems & Brown, 2017	Pancheloniidae	X	X		X	X	X							Upper Rupelian - Upper Chattian	Charleston, South Carolina, USA
† *Procolpochelys grandaeva* Leidy 1861	Weems & Brown, 2017	Pancheloniidae	X	X			X	X							Middle Burdigalian - Tortonian	Charleston, South Carolina, USA
† *Puppigerus camperi* Gray 1831	Gaffney, 1979/ Tong, 2012/ Moody, 1974/ Smith, 1989/ Weems & Brown, 2017	Pancheloniidae	X	X	X									X	Ypresian - Lutetian	Austria; Belgium; Morocco; USA; UK
† *Erquelinnesia gosseleti* Dollo 1886	Gaffney, 1979/ Smith, 1989/ Zangerl, 1971/ Weems & Brown, 2017	former "Toxochelyidae" †	X	X		X									Thanetian	Belgium
† *Erquelinnesia planimentum* Owen 1842	Karl, 1998	former "Toxochelyidae" †		X											Ypresian - Lutetian	Belgium, France
Dermochelys coriacea Vandelli 1761	UNIVALI: MOVI00574, MOVI01917, MOVI0575/ Gaffney, 1979/ Hirayama, 1994/ Wyneken, 2001/ S. Evers, personal visual collection: AMNH7160, AMNH7161, AMNH46845, MNHNPal1870-101, FMNH171756, QMJ47453	Dermochelyidae	X	X	X	X			X	X	X	X	X	X	Upper Pleistocene - present	Cosmopolitan
† *Eosphargis breineri* Nielsen 1959	Gaffney, 1979/ Smith, 1989/ Nielsen, 1959/ Hirayama, 1997	Dermochelyidae					X							X	Ypresian	Denmark
† Eo sphargis gigas Owen 1880	Smith, 1989	Dermochelyidae	X			X									Middle Ypresian	Belgium; UK; USA
† *Mesodermochelys undulatus* Hirayama and Chitoku 1996	Hirayama 1996	Dermochelyidae				X			X		X	X	X		Upper Campanian - Upper Maastrichtian	North Japan

Table 1 (continued)

Species	Source	Family	Data												Geoestratigraphy	Locality
			Skull			MD	CAD	P	II	IS	PU	UM	CO	Matrix of traditional ch.		
			CD	CV	CL											
† *Ocepechelon bouyai* Bardet *et al.* 2013	Bardet et al, 2013	Dermochelyidae					X				X			X	Upper Campanian - Upper Maastrichtian	Morocco
† *Archelon ischyros* Wieland 1896	Gaffney, 1979/ Hirayama, 1997	Protostegidae †		X			X					X		X	Upper Santonian - Upper Maastrichtian	South Dakota, USA
†*Bouliachelys suteri* Kear and Lee 2006	Kear & Lee, 2006/ Evers & Benson, 2018	Protostegidae †		X		X								X	Upper Albian - Lower Cenomanian	Dunraven Station, Austrália
† *Desmatochelys lowii* Williston 1894	Gaffney, 1979/ Smith, 1989 / Hirayama, 1997/ Sato *et al.*, 2012	Protostegidae †	X			X	X	X				X		X	Upper Cenomanian - Lower Maastrichtian	USA; Canada; Japan; Mexico
† *Protostega gigas* Cope 1871	Zangerl, 1953a/ Hirayama, 1997	Protostegidae †		X										X	Middle Santonian - Middle Campanian	USA; Canada; Japan
† *Santanachelys gaffneyi* Hirayama 1998	Hirayama, 1998/ Evers & Benson, 2018	Protostegidae †	X		X									X	Albian	Ceará, Brazil
† *Ctenochelys acris* Zangerl 1953	Gentry *et al.*, 2016/ Gentry, 2018	Ctenochelyidae †		X			X		X	X	X		X	X	Upper Santonian - Lower Maastrichtian	Greene County, Alabama, USA
† *Ctenochelys procax* Hay 1905	Hay, 1905/Hirayama, 1997, Gaffney, 1979	Ctenochelyidae †		X											Conician - Campanian	USA; UK
† *Prionochelys matutina* Zangerl 1953	Gentry, 2018	Ctenochelyidae †		X				X	X	X	X	X		X	Upper Conician - Middle Campanian	Alabama, USA
† *Ctenochelys stenoporus* Hay 1905	Hay, 1905/ Hirayama, 1997/ Gentry, 2018/ Zangerl 1953b/ Gentry, 2016	Ctenochelyidae †		X		X	X	X	X	X	X		X		Middle Santonian - Middle Thanetian	Denmark; Germany; USA
† *Toxochelys latiremis* Cope 1873	Hirayama, 1994/ Nicholls, 1998/ Kauffman *et al.*, 1993/ Gentry *et al.*, 2018	former "Toxochelyidae" †	X	X										X	Middle Santonian - Middle Maastrichtian	USA; Canada
Chelydra serpentina Linnaeus 1758	S. Evers, personal visual collection: FMNH8717, FMNH2256, SMNS14375, USNM246935	Chelydridae	X	X	X	X	X	X	X	X	X			X	Lower Calabrian - present	Eastern North America; freshwater

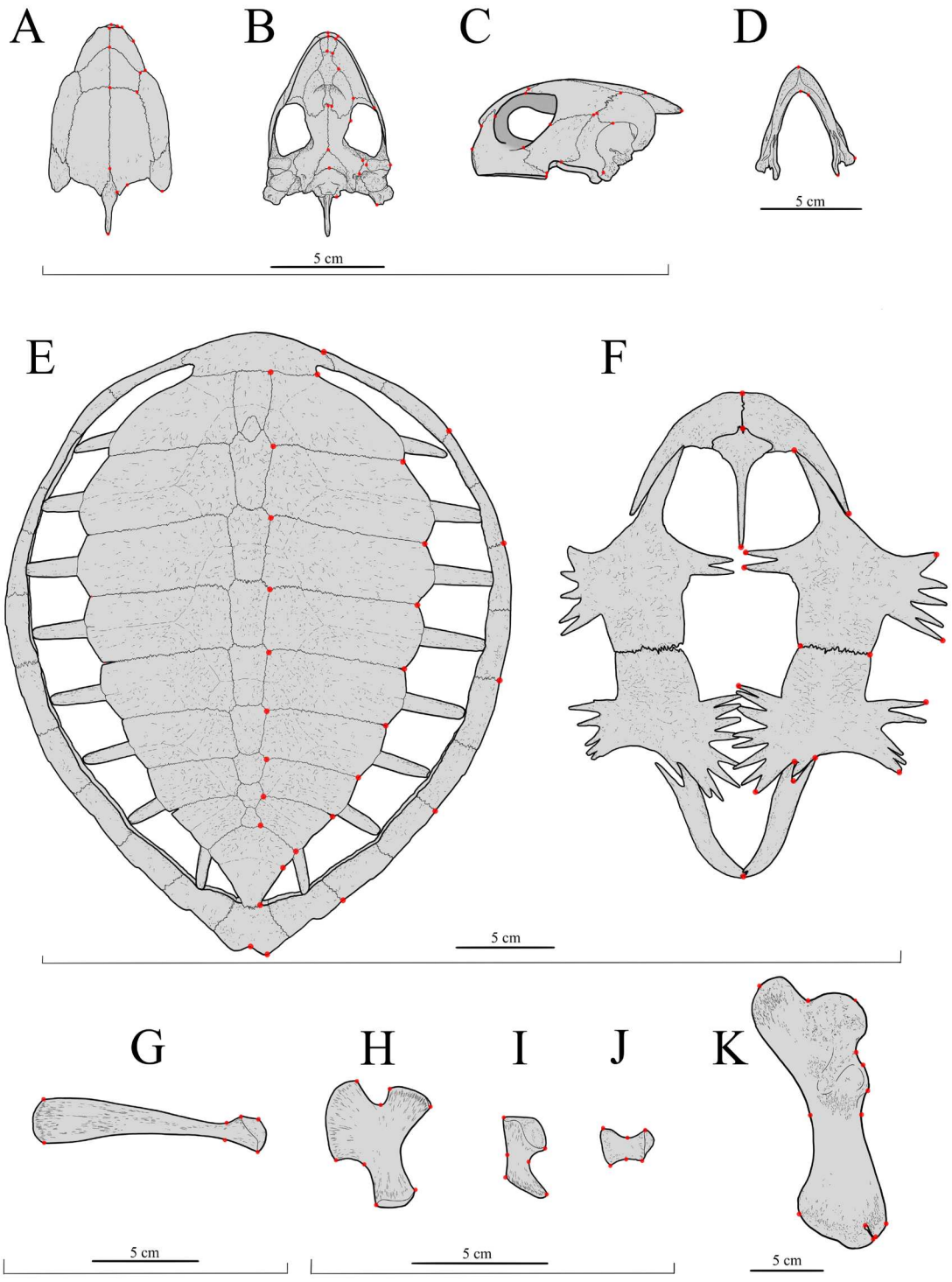

Figure 1. Schematic reference of landmark configurations shown in *Chelonia mydas* (humerus based on MOVI27799 and all the other bones based on MZUFV0068-C). Descriptions of all landmarks illustrated in here are presented in Appendix A. Legend: A: skull in dorsal view, B: skull in ventral view, C: skull in lateral view, D: jaw in dorsal view, E: carapace in dorsal view, F: plastron in ventral view, G: right coracoid in dorsal view, H: right pubis in dorsal view, I: right ilium in dorsal view, J: right ischium in dorsal view, K: left humerus in ventral view. Scale 5 cm.

Succeeding the initial digitisation of LM, we assessed the missing data and made an error test in order to refine both LM and species choice and reach the final configurations and sample group (Figure 1). Error testing is fundamental for refining LM choice. For this phase of the analysis, we submitted a representative portion of our raw data (i.e., straight from tpsDig; matrices of original coordinates; Matrix_X) to error testing in tpsSmall according to Adriaens, 2007 protocol. The aim was to verify if the data allows the analysis to be reproducible without embedding significant error. All LMs causing abnormal distribution of species in the plot were excluded until all LM sets were optimized – through this process, we were able to remove uninformative and ambiguous LM's.

After the final matrices of original coordinates (Matrix_X.tps) were obtained for all configurations, the data was superimposed by Generalized Procrustes Analysis (GPA) (49,50) using tpsRelw, then the TPS files (Matrix_Y.tps) were merged into a TNT file (Matrix_Z.tnt). An index of the matrices used can be found in the Supplementary Material along with all the original data.

Finally, we assessed the patterns of change in shape with Relative Warps (refer to Bookstein (51), 7.6: 339-358), a non-parametrical statistical analysis (in this case, a PCA) that allows geometrical comparison and quantification of shape variation between specimens (52). The Relative Warps (RW) correlate changes in shape in the two axes and apply it to decrease the relative bending energy of the successive relative eigenvectors (51). The RW's of each of configuration were obtained using the software PAST 4.03 (53) with RW1 x RW2 – the two Principal Components corresponding to the highest variability. The deformation grids (i.e., thin-plate splines; TPS) were obtained in tpsRelw, for means of comparing the variation in shape – these are illustrated in Figures 14-24.

2.3. Phylogenetic Morphometrics

Phylogenetic analyses were conducted in TNT 1.5 (54,55) under phylogenetic morphometrics (40) with optimization algorithms (41) to approximate optimal positions for ancestral LM's heuristically, using a system of grids and iterative calculation of Fermat points for the internal nodes of the tree (55). Each configuration was accounted as a single character.

In the phylogenetic study conducted by Perrard, Lopez-Osorio and Carpenter (56), tree resolution was significantly improved by the conjunction of landmark and traditional morphological characters. Thus, we combined the eleven configurations (matrixes with Procrustes residuals coordinates) with Gentry *et al.* (13) traditional morphological data. Characters 7, 14, 18, 58, 67, 74, 76, 79, 93, 94, 98, 103, 130, 145, 147, 157, 206, 218, 254, 293, 306, 327, 341, 342, 249 and 346 were treated as additives. LM characters were

upweighted from 1 to 31, so that the sum of the LM configurations change costs equals the sum of the traditional characters weights, otherwise the contribution of 11 LM configuration characters would be underestimated compared to the 347 discrete characters from Gentry *et al.* (13). This discrete dataset was chosen because it is the most extensive set of morphological characters used recently for phylogenetic studies of fossil turtles. Gentry *et al.* (13)'s matrix is modified from Evers & Benson (2)'s, which is a revised compilation of three other datasets (10,31,57).

No constraints were used, and zero-length branches were collapsed after branch swapping.

As abovementioned, all configurations of LM were imported to TNT already superimposed via GPA, which minimises the sum of the squared distances between corresponding LMs and a consensus configuration (43,50). This method is excellent for removing undesirable variance of the data, leaving only differences in shape between individuals. However, it doesn't mean that these changes in shape can be accounted to common ancestry, because the consensus configuration is an average configuration, not an ancestral configuration. An ancestral configuration, according to the principles of cladistic inference, should be the one that minimises the sum of the Euclidean distances between the nodes of a given tree (42) – this also helps to keep evolutionary features localised in the nodes in which they appeared, and not spread along the tree (40).

Resistant-fit theta-rho analysis (RFTRA) (59,60) was used to realign the LM configurations, since it's based on repeated medians and less sensitive to outliers (i.e., it keeps the change within the set of LM where the change in shape was observed, as opposed to GPA, which spread the change along the entire configuration in order to approximate all configurations to an average position (40)). In this study, the RFTRA alignment of the configurations was made by pairwise comparisons with *Natator depressus* because it does not have any missing character, then making possible for all configurations to be aligned with the same species.

The method proposed by Catalano *et al.* (40–42,55,58) calculates ancestral positions to each LM in a configuration that minimizes the linear distance between ancestors and descendants, much like the estimation of character states in traditional parsimony (37) and optimizes the data as multivariate characters so the correlation of landmark displacements in different taxa can be attributed to common ancestry, which is consistent to a parsimony framework. The score of the tree is calculated by summing up the Euclidean distance between the displacement of each landmark to its ancestral correspondent in each landmark of each configuration on the entire tree (42).

Even though the trees generated with the input of all geometrical structures are the best option to hypothesize the phylogeny of the group, preliminary analysis taking into account one LM configuration at a time can shine light on the evolution of structures individually and how they relate to each other. Preliminary analyses were conducted also with sets of configurations, structures that most likely coevolved, such as girdles and shell. Those sets were combined, forming more complex sets of structures, as post-cranium, cranium and then all studied configurations together. The list of matrices, combinations of sets of configurations and the parenthetical trees resulting of these preliminary searches are found in appendices C-J. All preliminary analyses were performed as the following: alignment by pairwise comparison with *Natator depressus* using RFTRA and adjusting size; optimization initially approximating LM positions with a 6x6 grid; nesting Sankoff 3 times, with a window of 2000 cells; using iterative-pass for landmark optimization; shaking grid 1 time; using term points in addition to grid points; shrinking frame when approximating landmark positions and not rescaling moves within each landmark character; branch swapping with 20% maximum error, branching up to 10 nodes from the union, with up to 5 iterations ((41); S. Catalano, personal communication). This 6x6 grid gives 36 possible positions for the ancestral position of a landmark; when an optimal position is found, a new grid is "nested" within the chosen position, refining even more the ancestral position; and this nesting process was repeated 3 times. In the study conducted by Ascarrunz *et al.* (37), two levels of nesting were more effective improving tree score than increasing the number of subdivisions of the original grid.

Then a traditional search was run, with 50 random additional sequences (RAS) followed by tree bisection-reconnection (TBR), with random seed 1 and holding 100 trees per replicate. The trees stored in RAM from this run were submitted to New Technology Ratchet (61) with random seed 1 and default configurations.

In order to compare the results of this analysis with a reference topology, we run a reanalysis of Gentry *et al.*, (13) matrix. In this analysis were used only the species present in our sample and *Chelydra serpentina* as outgroup. Characters 7, 14, 18, 58, 67, 74, 76, 79, 93, 94, 98, 103, 130, 145, 147, 157, 206, 218, 254, 293, 306, 327, 341, 342, 249 and 346 were treated as additives. We were able to run an exact search (Implicit Enumeration).

To evaluate the efficiency of the phylogenetic reconstructions, four search strategies were performed with the complete dataset. I: Using all configurations of landmarks plus the pruned matrix of Gentry *et al.* (13). The optimization, branch swapping and alignment were the same as in the preliminary searches, the same characters were marked additive and the geometric characters were also weighted up to 31. Then a traditional search was run with 50 RAS+TBR, other traditional search was run with the most parsimonious trees from the first search as a starting point and subsequently New Technology with the Ratchet algorithm using the trees from the second traditional search stored in RAM. II: Then,

a second analysis were performed using the same settings as the first, but with no character weighting. III: A third analysis were performed excluding the palatal view of the skull LM configuration. Morphological specializations in the skull of turtles often show a strong correlation with feeding strategies (62) and such adaptations (e.g., durophagy) have evolved multiple times on marine turtles (63,64). Since the LMs seen in palatal view have ecological influence in their development, this character could reduce reliability in the data by inputting homoplasy. IV: The fourth global preliminary analysis utilizes the same settings as the first one, but this time aligning with *L. olivacea* instead of *N. depressus*. This was performed in order to test if the re-alignment of configurations prior to tree search were biasing the results. *L. olivacea* was chosen because, despite missing one configuration, it is often recovered in the RW's close to the average shape configuration. Once these four searches were completed, two more were run in order to test the rooting of Pancheloniidae: V: The fifth analysis was performed excluding all species with less than three configurations sampled, once these species, due to lack of information, could result in wildcards. VI: The sixth was divided in two parts – one with Pancheloniidae + Dermochelyoidea species and the other with earlier diverging taxa (according to the results of the previous searches.

Additionally, Relative Bremmer Supports (65) were calculated in order to estimate the degree to which the optimal solution is preferred to the alternatives (66–68); as an heuristic solution, it indicates poorly supported groups – with suboptimal by 31 steps and RFD (i.e., Relative Fit Difference) of 0.8, following Goloboff & Farris (69).

All specifications about the searches can be found on Table 10. Figure 10 is a flowchart that sums up all the steps of the methodology used in the present work.

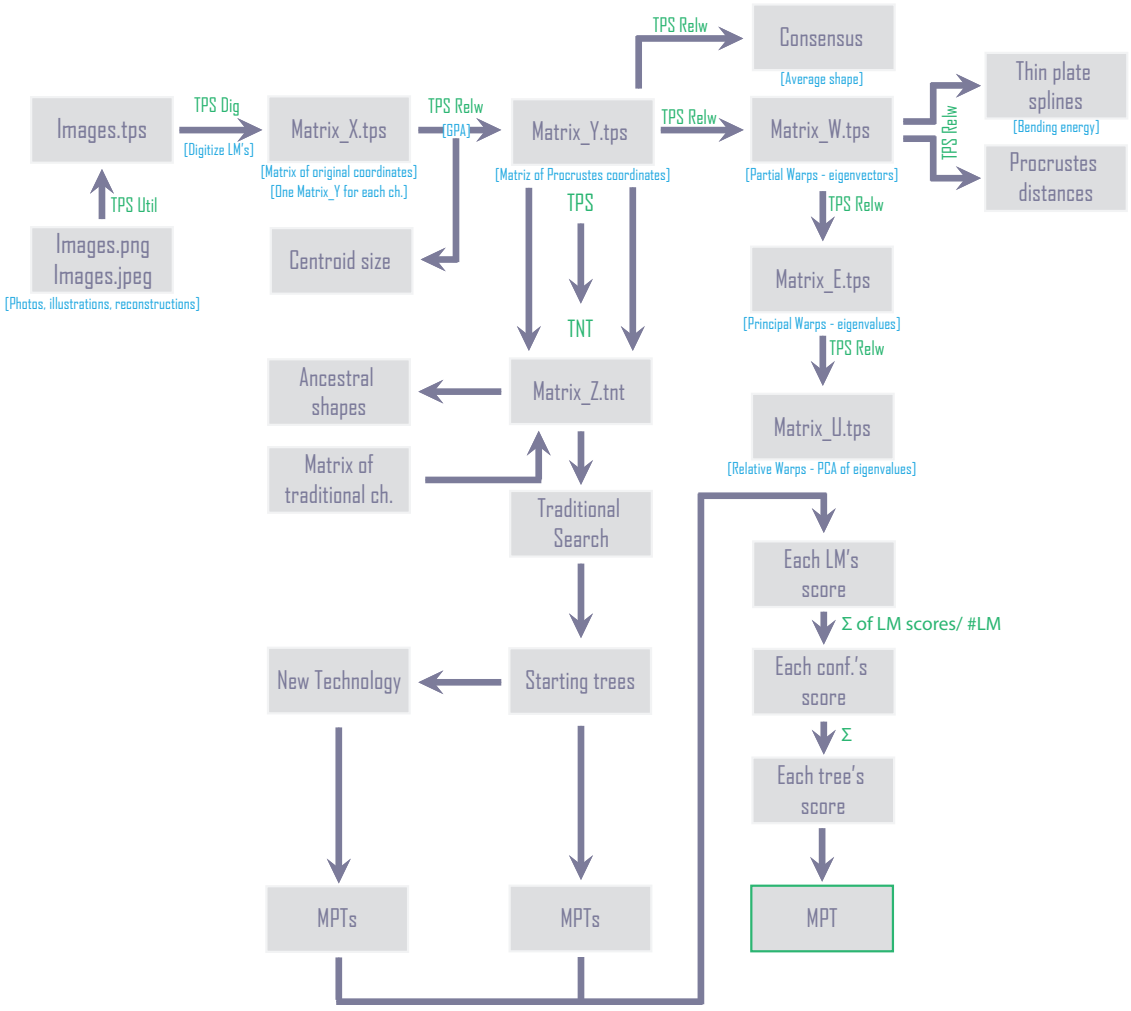

Figure 13. Flowchart summarizing the steps taken in this analysis from raw data to the most parsimonious tree (MPT). LM's – landmarks; ch. – characters; conf. – configurations.

Table 13. Compilation of settings, computational specifications and results of every phylogenetic search in this paper. All matrices and trees (figures and parenthetic notations) can be found in the Supplementary Material. Legend: BIOMETRIA is a cluster run by the Laboratory of Biometrical Processing in Federal University of Viçosa to which we were granted access during the execution of this research; the operational system is Windows Server 2008 R2 enterprise 64 bit, with two processors Intel Xeon CPU E5-2643 0 3.30GHz, memory of 96GB and 4 HD's totalizing 4.6 TB storage. PC Fernando is a personal computer Dell 64bit with processor Intel Core i7-4700MQ CPU 2.4GHz, memory of 16GB, operating with a Windows 10 Home 2020 and 1TB storage. PC Dell is a personal computer Dell 64bit with processor Intel Core i7-6700HQ CPU 2.6GHz, memory of 16GB, operating with a Windows 10 Home 2018 and 1TB storage. PC HP is a personal computer HP Pavilion Sleekbook 14 RW 64bit, with processor Intel Core i3-32171 CPU 1.8GHz, memory of 4GB, operating with a Windows 10 Home version 10.1018363 and 500GB storage.

		Single configurations			**Sets of configurations**		
		Jaw			**Head**		
		settings	**results**		**settings**	**results**	
Dataset		MATRIX_Z_partial_md.tnt			MATRIX_Z_partial_HE.tnt		
Outgroup		*Chelydra serpentina*			*Chelydra serpentina*		
Alignment	with	*Natator depressus*			*Natator depressus*		
	using	RFTRA			RFTRA		
Optimization		cmd - "lmark cell 6 nest 3 2 iter shake 1 term-points shrink noinscale"			cmd - "lmark cell 6 nest 3 2 iter shake 1 term-points shrink noinscale"		
Branch swapping		20% max error; branching up to 10 nodes from union; with up to 5 iterations			20% max error; branching up to 10 nodes from union; with up to 5 iterations		
Traditional search	RAS	50	Best score	1,95821	50	Best score	11,45118
	Random Seed	1	Time	00:00:58	1	Time	07:45:41
	trees/rep	100	Rearrang.	212909	100	Rearrang.	3352355
	swappping algorithm	TBR	Trees retained	1	TBR	Trees retained	1
	Analysis code	analysis_par026_MD_trad			analysis_par034_HE_trad		
New Technology		Ratchet from RAM (default settings)	Best score	1,95821	Ratchet from RAM (default settings)	Best score	11,45118
			Time	00:00:07		Time	01:21:32
			Rearrang.	24140		Rearrang.	318615
			Trees retained	1		Trees retained	1
	Analysis code	analysis_par027_MD_NT			analysis_par035_HE_NT		
Server/hardware		BIOMETRIA			BIOMETRIA		

Table 13 (continued)

		Single configurations								
		Skull								
		Dorsal			Lateral			Ventral		
		settings	results		settings	results		settings	results	
Dataset		MATRIX_Z_partial_cd.tnt			MATRIX_Z_partial_cl.tnt			MATRIX_Z_partial_cv.tnt		
Outgroup		*Chelydra serpentina*			*Chelydra serpentina*			*Chelydra serpentina*		
Alignment	with	*Natator depressus*			*Natator depressus*			*Natator depressus*		
	using	RFTRA			RFTRA			RFTRA		
Optimization		cmd - "lmark cell 6 nest 3 2 iter shake 1 termpoints shrink noinscale"			cmd - "lmark cell 6 nest 3 2 iter shake 1 termpoints shrink noinscale"			cmd - "lmark cell 6 nest 3 2 iter shake 1 termpoints shrink noinscale"		
Branch swapping		20% max error; branching up to 10 nodes from union; with up to 5 iterations			20% max error; branching up to 10 nodes from union; with up to 5 iterations			20% max error; branching up to 10 nodes from union; with up to 5 iterations		
Traditional search	RAS	50	Best score	2,82011	50	Best score	2,237178	50	Best score	3,66786
	Random Seed	1	Time	00:04:10	1	Time	00:00:33	1	Time	00:20:24
	trees/rep	100	Rearrang.	303425	100	Rearrang.	27439	100	Rearrang.	1203400
	swapping algorithm	TBR	Trees retained	1	TBR	Trees retained	1	TBR	Trees retained	1
	Analysis code	analysis_par014_CD_trad			analysis_par016_CL_trad			analysis_par020_CV_trad		
New Technology		Ratchet from RAM (default settings)	Best score	2,82011	Ratchet from RAM (default settings)	Best score	2,37178	Ratchet from RAM (default settings)	Best score	3,66786
			Time	00:01:30		Time	00:00:30		Time	00:05:29
			Rearrang.	59550		Rearrang.	8948		Rearrang.	154575
			Trees retained	1		Trees retained	1		Trees retained	1
	Analysis code	analysis_par015_CD_NT			analysis_par017_CL_NT			analysis_par021_CV_NT		
Server/hardware		BIOMETRIA			BIOMETRIA			BIOMETRIA		

Table 13 (continued)

		Single configurations								
		Ilium			Ischium			Pubis		
		settings	results		settings	results		settings	results	
Dataset		MATRIX_Z_partial_ii.tnt			MATRIX_Z_partial_is.tnt			MATRIX_Z_partial_pu.tnt		
Outgroup		*Chelydra serpentina*			*Chelydra serpentina*			*Chelydra serpentina*		
Alignment (pairwise comp.)	with	*Natator depressus*			*Natator depressus*			*Natator depressus*		
	using	RFTRA			RFTRA			RFTRA		
Optimization		cmd - "lmark cell 6 nest 3 2 iter shake 1 termpoints shrink noinscale"			cmd - "lmark cell 6 nest 3 2 iter shake 1 termpoints shrink noinscale"			cmd - "lmark cell 6 nest 3 2 iter shake 1 termpoints shrink noinscale"		
Branch swapping		20% max error; branching up to 10 nodes from union; with up to 5 iterations			20% max error; branching up to 10 nodes from union; with up to 5 iterations			20% max error; branching up to 10 nodes from union; with up to 5 iterations		
Traditional search	RAS	50	Best score	2,07047	50	Best score	1,74523	50	Best score	2,23168
	Random Seed	1	Time	00:00:10	1	Time	00:00:02	1	Time	00:00:22
	trees/rep	100	Rear-rang.	24005	100	Rear-rang.	3848	100	Rearrang.	39155
	swappping algorithm	TBR	Trees retained	1	TBR	Trees retained	1	TBR	Trees retained	1
	Analysis code	analysis_par022_II_trad			analysis_par024_IS_trad			analysis_par030_PU_trad		
New Tech-nology		Ratchet from RAM (default settings)	Best score	2,07047	Ratchet from RAM (default settings)	Best score	1,74523	Ratchet from RAM (default settings)	Best score	2,23168
			Time	00:00:04		Time	00:00:00		Time	00:00:10
			Rear-rang.	7410		Rear-rang.	1820		Rearrang.	9887
			Trees retained	1		Trees retained	1		Trees retained	1
	Analysis code	analysis_par023_II_NT			analysis_par025_IS_NT			analysis_par031_PU_NT		
Server/hardware		BIOMETRIA			BIOMETRIA			BIOMETRIA		

Table 13 (continued)

		Single configurations						Sets of configurations		
		Carapace			Plastron			Shell		
		settings	results		settings	results		settings	results	
Dataset		MATRIX_Z_partial_cad.tnt			MATRIX_Z_partial_p.tnt			MATRIX_Z_partial_SH.tnt		
Outgroup		*Chelydra serpentina*			*Chelydra serpentina*			*Chelydra serpentina*		
Alignment (pairwise comp.)	with	*Natator depressus*			*Natator depressus*			*Natator depressus*		
	using	RFTRA			RFTRA			RFTRA		
Optimization		cmd - "lmark cell 6 nest 3 2 iter shake 1 termpoints shrink noinscale"			cmd - "lmark cell 6 nest 3 2 iter shake 1 termpoints shrink noinscale"			cmd - "lmark cell 6 nest 3 2 iter shake 1 termpoints shrink noinscale"		
Branch swapping		20% max error; branching up to 10 nodes from union; with up to 5 iterations			20% max error; branching up to 10 nodes from union; with up to 5 iterations			20% max error; branching up to 10 nodes from union; with up to 5 iterations		
Traditional search	RAS	50	Best score	2,75207	50	Best score	2,34313	50	Best score	5,24795
	Random Seed	1	Time	00:06:48	1	Time	00:00:43	1	Time	00:26:04
	trees/rep	100	Rearrang.	271586	100	Rearrang.	42237	100	Rearrang.	368460
	swappping algorithm	TBR	Trees retained	1	TBR	Trees retained	1	TBR	Trees retained	1
	Analysis code	analysis_par012_CAD_trad			analysis_par028_P_trad			analysis_par036_SH_trad		
New Technology		Ratchet from RAM (default settings)	Best score	2,75207	Ratchet from RAM (default settings)	Best score	2,34313	Ratchet from RAM (default settings)	Best score	5,24795
			Time	00:01:05		Time	00:00:21		Time	00:04:45
			Rearrang.	31389		Rearrang.	10382		Rearrang.	43943
			Trees retained	1		Trees retained	1		Trees retained	1
	Analysis code	analysis_par013_CAD_NT			analysis_par029_P_NT			analysis_par037_SH_NT		
Server/hardware		BIOMETRIA			BIOMETRIA			PC Fernando		

Table 13 (continued)

		Sets of configurations											
		Pelvic girdle			Appendices			Post-cranium			Turtle		
		settings	results		settings	results		settings	results		settings	results	
Dataset		MATRIX_Z_partial_PEG.tnt			MATRIX_Z_partial_AP.tnt			MATRIX_Z_partial_PC.tnt			MATRIX_Z_partial_TU.tnt		
Outgroup		*Chelydra serpentina*			*Chelydra serpentina*			*Chelydra serpentina*			*Chelydra serpentina*		
Alignment	with	*Natator depressus*			*Natator depressus*			*Natator depressus*			*Natator depressus*		
	using	RFTRA			RFTRA			RFTRA			RFTRA		
Optimization		cmd - "lmark cell 6 nest 3 2 iter shake 1 termpoints shrink noinscale"			cmd - "lmark cell 6 nest 3 2 iter shake 1 termpoints shrink noinscale"			cmd - "lmark cell 6 nest 3 2 iter shake 1 termpoints shrink noinscale"			cmd - "lmark cell 6 nest 3 2 iter shake 1 termpoints shrink noinscale"		
Branch swapping		20% max error; branching up to 10 nodes from union; with up to 5 iterations			20% max error; branching up to 10 nodes from union; with up to 5 iterations			20% max error; branching up to 10 nodes from union; with up to 5 iterations			20% max error; branching up to 10 nodes from union; with up to 5 iterations		
Traditional search	RAS	50	Best score	6,52218	50	Best score	10,57823	50	Best score	15,97272	50	Best score	28,03367
	Random Seed	1	Time	00:01:33	1	Time	00:16:04	1	Time	02:24:53	1	Time	21:25:17
	trees/rep	100	Rearrang.	40370	100	Rearrang.	171853	100	Rearrang.	755648	100	Rearrang.	3919864
	swappping algorithm	TBR	Trees retained	1	TBR	Trees retained	1	TBR	Trees retained	1	TBR	Trees retained	1
	Analysis code	analysis_par038_PEG_trad			analysis_par042_AP_trad			analysis_par044_PC_trad			analysis_par046_TU_trad		
New Technology		Ratchet from RAM (default settings)	Best score	6,52218	Ratchet from RAM (default settings)	Best score	10,57823	Ratchet from RAM (default settings)	Best score	15,97272	Ratchet from RAM (default settings)	Best score	28,03367
			Time	00:00:39		Time	00:04:25		Time	00:41:23		Time	03:51:45
			Rearrang.	8944		Rearrang.	20370		Rearrang.	101076		Rearrang.	423152
			Trees retained	1		Trees retained	1		Trees retained	1		Trees retained	1
	Analysis code	analysis_par039_PEG_NT			analysis_par043_AP_NT			analysis_par045_PC_NT			analysis_par047_TU_NT		
Server/hardware		PC HP			BIOMETRIA			PC Fernando			PC Fernando		

Table 13 (continued)

		LM + traditional characters					
		1			2		
		settings	results		settings	results	
Dataset		MATRIX_Z_2.tnt			MATRIX_Z_2.tnt		
Outgroup		*Chelydra serpentina*			*Chelydra serpentina*		
Alignment (pairwise comp.)	with	*Natator depressus*			*Natator depressus*		
	using	RFTRA			RFTRA		
Character settings		Ordered characters: 7 14 18 58 67 74 76 79 93 94 98 103 130 145 147 157 206 218 249 254 293 306 327 341 342 346			Ordered characters: 7 14 18 58 67 74 76 79 93 94 98 103 130 145 147 157 206 218 249 254 293 306 327 341 342 346		
Optimization		cmd - "lmark cell 6 nest 3 2 iter shake 1 term-points shrink noinscale"			cmd - "lmark cell 6 nest 3 2 iter shake 1 term-points shrink noinscale"		
Character weighting		cmd - "lmark wts = 31 [347-357]"			none		
Branch swapping		20% max error; branching up to 10 nodes from union; with up to 5 iterations			20% max error; branching up to 10 nodes from union; with up to 5 iterations		
Traditional search	RAS	50	Best score	1277,58082	50	Best score	403,74897
	Random Seed	1	Time	12:46:21	1	Time	04:03:18
	trees/rep	100	Rearrang.	3090807	100	Rearrang.	2777574
	swappping algo-rithm	TBR	Trees retai-ned	1	TBR	Trees retained	1
	Analysis code	analysis_tot003_trad			analysis_tot006_trad		
Traditional search (2nd round)		RAM	Best score	1277,58082	RAM	Best score	403,74897
			Time	00:04:24		Time	00:01:22
			Rearrang.	14919		Rearrang.	11631
			Trees retai-ned	1		Trees retained	1
		analysis_tot004_trad			analysis_tot007_trad		
New Tech		Ratchet from RAM (default settings)	Best score	1277,58082	Ratchet from RAM (default settings)	Best score	403,74897
			Time	00:41:23		Time	02:15:41
			Rearrang.	101076		Rearrang.	1200266
			Trees retai-ned	1		Trees retained	1
	Analysis code	analysis_tot005_NT			analysis_tot008_NT		
Server/hardware		BIOMETRIA			PC Dell		
Branch support		suboptimal by 31 steps; RFD 0.8			suboptimal by 31 steps; RFD 0.8		

Table 13 (continued)

		LM + traditional characters					
		3			4		
		settings	results		settings	results	
Dataset		MATRIX_Z_3.tnt			MATRIX_Z_2.tnt		
Outgroup		*Chelydra serpentina*			*Chelydra serpentina*		
Alignment (pairwise comp.)	with	*Natator depressus*			*Lepidochelys olivacea*		
	using	RFTRA			RFTRA		
Character settings		Ordered characters: 7 14 18 58 67 74 76 79 93 94 98 103 130 145 147 157 206 218 249 254 293 306 327 341 342 346			Ordered characters: 7 14 18 58 67 74 76 79 93 94 98 103 130 145 147 157 206 218 249 254 293 306 327 341 342 346		
Optimization		cmd - "lmark cell 6 nest 3 2 iter shake 1 term-points shrink noinscale"			cmd - "lmark cell 6 nest 3 2 iter shake 1 term-points shrink noinscale"		
Character weighting		cmd - "lmark wts = 31 [347-357]"			cmd - "lmark wts = 31 [347-357]"		
Branch swapping		20% max error; branching up to 10 nodes from union; with up to 5 iterations			20% max error; branching up to 10 nodes from union; with up to 5 iterations		
Traditional search	RAS	50	Best score	115.309.347	50	Best score	1257,28319
	Random Seed	1	Time	08:06:29	1	Time	11:03:36
	trees/rep	100	Rearrang.	2492702	100	Rearrang.	3155176
	swappping algorithm	TBR	Trees retai-ned	1	TBR	Trees retained	1
	Analysis code	analysis_tot009_1_trad			analysis_tot012_trad		
Traditional search (2nd round)		RAM	Best score	115.309.347	RAM	Best score	1257,28319
			Time	00:02:50		Time	00:04:29
			Rearrang.	11537		Rearrang.	12559
			Trees retai-ned	1		Trees retained	1
		analysis_tot010_trad			analysis_tot013_trad		
New Tech		Ratchet from RAM (default settings)	Best score	115.309.347	Ratchet from RAM (default settings)	Best score	1257,28319
			Time	00:39:58		Time	01:48:49
			Rearrang.	142620		Rearrang.	287942
			Trees retai-ned	1		Trees retained	1
	Analysis code	analysis_tot011_NT			analysis_tot014_NT		
Server/hardware		BIOMETRIA			PC Dell		
Branch support		suboptimal by 31 steps; RFD 0.8			suboptimal by 31 steps; RFD 0.8		

Table 13 (continued)

		LM + traditional characters					
		5			6.1		
		settings	results		settings	results	
Dataset		MATRIX_Z_4.tnt			MATRIX_Z_5.tnt		
Outgroup		*Chelydra serpentina*			*Chelydra serpentina*		
Alignment (pairwise comp.)	with	*Natator depressus*			*Chelydra serpentina*		
	using	RFTRA			RFTRA		
Character settings		Ordered characters: 7 14 18 58 67 74 76 79 93 94 98 103 130 145 147 157 206 218 249 254 293 306 327 341 342 346			Ordered characters: 7 14 18 58 67 74 76 79 93 94 98 103 130 145 147 157 206 218 249 254 293 306 327 341 342 346		
Optimization		cmd - "lmark cell 6 nest 3 2 iter shake 1 term-points shrink noinscale"			cmd - "lmark cell 6 nest 3 2 iter shake 1 term-points shrink noinscale"		
Character weighting		cmd - "lmark wts = 31 [347-357]"			cmd - "lmark wts = 31 [347-357]"		
Branch swapping		20% max error; branching up to 10 nodes from union; with up to 5 iterations			20% max error; branching up to 10 nodes from union; with up to 5 iterations		
Traditional search	RAS	50	Best score	1044.29858	50	Best score	494.09740
	Random Seed	1	Time	01:42:35	1	Time	00:03:17
	trees/rep	100	Rearrang.	252499	100	Rearrang.	6376
	swappping algorithm	TBR	Trees retained	1	TBR	Trees retained	1
	Analysis code	analysis_tot019_trad			analysis_tot022_trad		
Traditional search (2nd round)		RAM	Best score	1044.29858	RAM	Best score	494.09740
			Time	00:01:58		Time	00:00:10
			Rearrang.	2189		Rearrang.	189
			Trees retained	1		Trees retained	1
		analysis_tot020_trad			analysis_tot023_trad		
New Tech		Ratchet from RAM (default settings)	Best score	1044.29858	Ratchet from RAM (default settings)	Best score	494.09740
			Time	00:21:11		Time	00:02:11
			Rearrang.	27530		Rearrang.	2506
			Trees retained	1		Trees retained	1
	Analysis code	analysis_tot021_NT			analysis_tot024_NT		
Server/hardware		BIOMETRIA			BIOMETRIA		
Branch support		suboptimal by 31 steps; RFD 0.8			suboptimal by 31 steps; RFD 0.8		

Table 13 (continued)

		LM + traditional characters		
		6.2		
		settings	results	
Dataset		MATRIX_Z_6.tnt		
Outgroup		*Chelydra serpentina*		
Alignment (pairwise comp.)	with	*Natator depressus*		
	using	RFTRA		
Character settings		Ordered characters: 7 14 18 58 67 74 76 79 93 94 98 103 130 145 147 157 206 218 249 254 293 306 327 341 342 346		
Optimization		cmd - "lmark cell 6 nest 3 2 iter shake 1 termpoints shrink noinscale"		
Character weighting		cmd - "lmark wts = 31 [347-357]"		
Branch swapping		20% max error; branching up to 10 nodes from union; with up to 5 iterations		
Traditional search	RAS	50	Best score	1095.69293
	Random Seed	1	Time	04:17:20
	trees/rep	100	Rearrang.	796154
	swappping algorithm	TBR	Trees retained	1
	Analysis code	analysis_tot025_trad		
Traditional search (2nd round)		RAM	Best score	1095.69293
			Time	00:03:15
			Rearrang.	5869
			Trees retained	1
		analysis_tot026_trad		
New Tech		Ratchet from RAM (default settings)	Best score	1095.69293
			Time	00:33:48
			Rearrang.	68030
			Trees retained	1
	Analysis code	analysis_tot027_NT		
Server/hardware		BIOMETRIA		
Branch support		suboptimal by 31 steps; RFD 0.8		

Table 13 (continued)

		Reanalysis Gentry *et al.*, 2019 settings	results	
Dataset		Gentry_et_al_2019_prunned.tnt		
Outgroup		*Chelydra serpentina*		
Character settings		Ordered characters: 7 14 18 58 67 74 76 79 93 94 98 103 130 145 147 157 206 218 249 254 293 306 327 341 342 346		
Traditional search		Implicit Enumeration	Best score	386
			Time	19:17:57
			CI: 0.526; RI: 0.596	
			Trees retained	2
	Analysis code	analysis_tot015_implicitenumeration		
Server/hardware		PC Dell		

3. RESULTS

3.1. Relative Warps

In the dorsal view of the skull, the RW_1 (Figure 14) shows mainly the variation in the temporal emargination, with most of the species of Panchelonioidea concentrated in the positive scores. *Toxochelys latiremis* was the species closer to the outgroup, *Chelydra serpentina*, a notorious durophage turtle. *P. camperi* is found very distant from the rest of the cheloniids, in the negative scores of the RW_2, indicating a rather shallow temporal emargination. In the ventral view of the skull, Protostegidae is restricted to the fourth quadrant, characterized by a small secondary palate and narrow skull. The two species of *Erquelinnesia* are also separated from the rest, with the broader secondary palate, followed by *Euclastes wielandi*. The remaining Pancheloniidae concentrate close to the average.

The RW of the jaw (Figure 17) exhibits the development of the triturating surface, from a high development in the negative scores to a very low development in the positive scores of the RW_1; and the angle between the mandibular rami on RW_2, from broader jaws in the higher values to relatively narrower jaws in the lower. *Eochelone brabantica* is at the extreme of the second quadrant, with a broad jaw and a larger triturating surface. *Erquelinnesia gosseleti* also has a large secondary palate, but a much narrower jaw. Also in the quadrant of large palate triturating surfaces are *Caretta caretta*, *Procolpochelys charlestonensis* and *Lepidochelys olivacea*. In the opposite quadrant, are all representatives of Dermochelyidae and Protostegidae, being the dermochelyids the ones with the smallest triturating surfaces of the palate. Pancheloniidae is wildly spread across the shape space, showing a considerable variety in jaw morphology.

RW_1 of the carapace in dorsal view (Figure 18) demonstrates a reduction of the costals from the lower to the higher scores. Pancheloniidae concentrates on the negative scores, except for *Allopleuron hofmanni*. In the positive scores, are Ctenochelyidae, Protostegidae, and in the extreme, *Eosphargis breineri*. Lower scores of RW_2 concentrate species with a more elongated shape of the carapace and higher scores, a rounder shape. The most significative aspect of the plastron RW is its broadening from positive to negative scores, especially in the hyo and hypoplastron – it can be observed a lateral expansion of the plastron in the RW_1 and cranio-caudal expansion in the RW_2.

On the humerus (Figure 21), most of the variance concentrates on the X axis, with the lower scores of RW_1 displaying shorter, broader humeri with larger lateral processes. Most Pancheloniidae concentrate on the higher scores, while Dermochelyidae and Protostegidae remain in the lower scores. The higher scores of RW_1 and the lower scores of RW_2 show an almost closed ectepicondylar groove.

The RW of highest variation in the ilium (Figure 23) mainly illustrates the shape of the posterior process – from a very prominent one in the negative scores, with *Mesodermochelys undulatus* and Ctenochelyidae, to a nearly absent one in the positive, with crown-Cheloniidae.

In the pubis RW (Figure 22), the RW_2 differentiates Panchelonioidea from the outgroup primarily in respect to the size of the blade – narrow in Chelydridae and broader in sea turtles, being intermediate in *Dermochelys coriacea*.

It's also in the blade the main variation of shape in the coracoid (Figure 20), with Dermochelyidae and Pancheloniidae in the centre and of the negative scores, and Ctenochelyidae in the positive scores of the RW_1.

3.2. Preliminary trees

The searches for MPTs using each configuration alone and for subsets of configurations were performed in order to evaluate the phylogenetic signal of each set of LMs. All partitioned searches resulted each in one tree (Figures 25-38), as expected for continuous data for supporting continuous variables with variation in decimal scale. All the details of the searches as well as best scores and processing time for all searches are compiled in Table 13.

The dorsal view of the carapace (Figure 25) resulted in Chelonioidea including all the ingroup. *Allopleuron hofmanni* is recovered among Protostegidae + *Eosphargis breineri*; but when the plastron information is included, the cladogram of the shell (Figure 31) no longer recovers all the representatives of Protostegidae as close relatives.

The dorsal view of the skull (Figure 25) does not recover any of the major families in a monophyletic group; both *Toxochelys* and *Santanachelys* can be found at the basis of the tree and the crown-group seems to bring together all the species that were concentrated next to the origin in the RWA (Figure 14). The ventral view of the skull (Figure 26) shows little congruence with reference phylogenies and the only structured group is Protostegidae, that is also assembled in an isolated group in the shape space of the RW (Figure 15). Protostegidae along with *Eretmochelys* and *Allopleuron* are the chelonioids with the narrower skull and the smallest palate triturating surface, according to the RW (Figure 15). Two clades of wide headed turtles can be highlighted, one with *N. depressus*, *C. caretta*, *E. wielandi*and *Erquelinnesia* spp., and the other with broad but more round shaped skulls including *D. coriacea*, *C. acris*, *T. latiremis*, *C. stenoporus*, *C. procax* and *P. matutina*. *Chelonia mydas* is found at the basis of the tree. The topology of the jaw (Figure 28) configuration finds the species with higher angles between the mandibular rami like *Dermochelys coriacea* (70) to be at the first divergency nodes, and all the species

structured in the negative scores of RW_1 (Figure 17) in the RW are grouped in the same clade (*C. stenoporus* (*L. olivacea* (*C. caretta* (*P. charlestonensis* (*E. gosseleti*, *E. brabantica*))))). In the preliminary analysis containing the three views of the skull plus the jaw (Figure 30), the clade containing the narrow-headed turtles (*E. imbricata*, *A. hofmanni*, *B. suteri*, *A. ischyros* and *P. gigas*) is still structured, but the wide-headed are now dispersed along the tree and none of the families form a monophyletic group.

The pelvic girdle (Figure 31) recovers all extant species in a monophyletic group, which is sister-group to a clade containing Ctenochelyidae and fossil Dermochelyidae; and the tree using only the ischium configuration (Figure 28) groups together all ctenochelyids in its sample with an exclusive common ancestor. The same group can be seen in the appendices cladogram (Figure 32), obtained by the combination of pelvic and pectoral girdles data, with a crown-group putting together highly pelagic turtles. Lastly is the "turtle" cladogram (Figure 33), compiling all landmark data, without the adding of discrete characters nor weighting. All protostegids share a close but not exclusive common ancestor. *Ctenochelys procax* is recovered at the first divergence node, followed by a clade containing more ctenochelyids, *Mesodermochelys* + *Ocepechelon* and *Euclastes wielandi*. Dermochelyidae is recovered as a polyphyletic group.

3.3. Reanalysis

The Implicit Enumeration yielded two trees with a best score of 386, CI=0.526 and RI=0.596 and a strict consensus was made (Figure 34). The nodes in which there was change are marked with a purple dot in the Figure 34. *Eochelone brabantica* was present in the dataset, but not figured in the paper's phylogeny (Gentry *et al.* (13), fig 2). This species is mentioned in Gentry *et al.,* (13) only as being part of a large polytomy along with *Puppigerus* and *Argillochelys* in the Bayesian analysis. The position of *Euclastes wielandi* changed between diverging earlier or later than *Toxochelys* + Ctenochelydae at the two MPT's, so the strict consensus produced a polytomy. In the reanalysis, *Toxochelys latiremis* was recovered as sister to Ctenochelyidae, instead of a stem-clade to Chelonioidea + Ctenochelyidae lineage. The stem-cheloniid *Puppigerus camperi* is recovered as *Euclastes wielandi*'s sister-taxon. With the exception of *E. imbricata* being sister-taxon to Carettini, all internal relationships of crown-Cheloniidae changed if compared to original search performed by Gentry *et al.* (13). Dermochelyoidea (Protostegidae + Dermochelyidae) was recovered in this reanalysis, while in the original search Protostegidae is the first diverging clade and Dermochelyidae is recovered among pancheloniids. The internal relationships of Dermochelyidae, Ctenochelyidae and Protostegidae remained unchanged.

3.4. Landmark plus traditional characters analysis

The time-calibrated tree in Figure 39 is the result of the first global preliminary search (Figure 35), run with all landmark data plus the matrix of discrete characters - Gentry *et al.* (13). The landmark characters were weighted up so their total contribution would be the same as the total weight of the traditional morphological characters matrix. The position of *Ctenochelys procax* marks the divergence node of Panchelonioidea. The Cretaceous stem-cheloniids, *Euclastes wielandi* and *Allopleuron hofmanni*, are separated from the remainder cheloniids, showing more affinity with Upper Cretaceous clades than with Cenozoic sea turtles. As for Cretaceous panchelonioids, there are Cteochelyidae and Protostegidae, the latter dating back to the Aptian, with a well-supported clade containing the oldest sea turtles in the sample: *Santanachelys gaffneyi* and *Bouliachelys suteri*. This group is sister to *Desmatochelys lowii* and those are sister to *Ocepechelon bouyai*, an Upper Cretaceous dermochelyoid with a unique morphology, which will be discussed in the section below. Those groups are followed by *Archelon ischyros* + *Protostega gigas*, a clade consistent in all global preliminary trees (Fugures 35-38), in the preliminary trees of ventral view of the skull (Figure 26) and in the one containing all three views of the skull plus the dorsal view of the jaw (Figure 30). The same assemblage of protostegids recovered in this topology is found in all global preliminary trees (Figures 35-38). The other Upper Cretaceous dermochelyid – *Mesodermochelys undulatus* – is recovered at the stem of Ctenochelyidae. There can also be noticed two relatively well supported clades of Paleogene turtles, one containing *Eochelone brabantica* + Procolpochelys spp., and other with (*Carolinochelys wilsoni* (*Puppigerus camperi*, *Erquelinnesia* spp.)). The first diverging crown-Chelonioidea is a group known as Carettini Zangerl 1958 (*sensu* Parham &Fastovsky (22)), comprising the genera *Caretta* and *Lepidochelys*. *Chelonia mydas*, *Natator depressus* and *Allopleuron hofmanni* are recovered at the stem of Dermochelyoidea *sensu* Evers & Benson (2). The colour coding in this cladogram shows the conclusions about phylogenetic positioning that could be made after testing the hypothesis.

The global preliminary search 2 (Figure 36) was run with all characters weighting 1. It means that each of the 11 morphogeometrical characters weighted the same as each of the 347 discrete ones. It should be expected that this result would be the most similar to Gentry *et al.* (13)'s topology among all our trees. Protostegidae has the exact same topology as theirs in our results, even regarding its early radiation (earlier than *Toxochelys latiremis* and all Pancheloniidae), but in global preliminary tree 2 it is not associated with Dermochelyidae + *Allopleuron hofmanni* – this clade is herein nested among panchelonioids and *Euclastes* is recovered among ctenochelyids. There were some species (marked with an asterisk of Figure 36) present in our sample, but not in Gentry *et al.* (13)'s. With the available information, they could not be coded for most of the charac-

ters in the discrete dataset, hence the LM data herein contribute to suggest a hypothesis of their positioning within the established topology: *Mesodermochelys undulatus* was recovered as sister-taxon to all Protostegidae (including *Ocepechelon*, which will be discussed below). The other dermochelyids are recovered associated with *Allopleuron hofmanni* (also to be discussed below). *Euclastes wielandi* is placed among ctenochelyids, such as *Ctenochelys stenoporus* and *Ctenochelys procax*. *Procolpochelys charlestonensis* is associated with *Eochelone brabantica* in an early-diverging clade and *Procolpochelys grandaeva* is found as sister-group to ((*E. gigas*, *A. hofmanni*) (*E. breineri*, *D. coriacea*)). The remaining cheloniids not present in Gentry *et al.*, (13)'s matrix are grouped in a clade containing other stem-Cheloniidae. All extant cheloniids form a monophyletic group, however *Chelonia mydas* and *Natator depressus* do not form a clade.

The global preliminary tree 3 (Figure 37) – the one without the palatal view of the skull (CV) – is expected to have less ecological influence due to feeding specialization (63,71), which could lead to convergence; but in the other hand, it has significantly less geometrical information, since the CV configuration is the one with the least missing data. With that said, the only major change in relation to the preferred topology is *Procolpochelys grandaeva*, that falls at the stem of the group containing *Mesodermochelys*, *Euclastes* and Ctenochelyidae. Carettini is comparatively very well supported (Bremer decay index of ~2) and notably *Lepidochelys olivacea* shows a greater affinity with *Caretta caretta* (Bremer support of ~3) than with *L. kempii*.

The global preliminary tree 4 (Figure 38) features the result of a phylogenetic search aligning the landmark characters against *Lepidochelys olivacea*, instead of *Natator depressus*. As a reference, *L. olivacea* can even be considered a better choice than *N. depressus*, once it has a shape closer to the average shape in the sample – noticeable in all RWA's, except in skull (ventral view), carapace and humerus –, however it has one missing configuration (ischium), making *N. depressus* more appropriate as a reference taxon, since it has landmarks digitized for all configurations. The three differences in this tree in relation to the preferred topology are remarkable though: *Euclastes wielandi*, *Eretmochelys imbricata* and *Mesodermochelys undulatus* have fallen in much more "expectable" positions, (according to the hypothesis considered): *Euclastes* associated with other durophagous stem-cheloniids, such as *Erquelinnesia* spp. and *P. camperi*; *Eretmochelys* along with other extant cheloniids – *C. caretta* and *Lepidochelys* spp. – and *Mesodermochelys* inside Dermochelyioidea.

The fifth global preliminary tree (Figure 39) contains only the species with four or more than four configurations sampled. It was possible to notice a clade with all extant species, but there is no noticeable structure within neither of the families – except Ctenochelyidae.

The sixth global preliminary analysis yielded two trees (Figures 40 and 41). In tree 6.1 (Figure 40) it can be noticed that, once separated from the other clades, *Mesodermochelys undulatus* is not grouped with *Ctenochelys acris*, *Ctenochelys stenoporus* and *Euclastes wielandi*. Whereas in tree 6.2 (Figure 41), the withdraw of Ctenochelyidae and early diverging taxa do not alter the structure of Pancheloniidae and Dermochelyioidea.

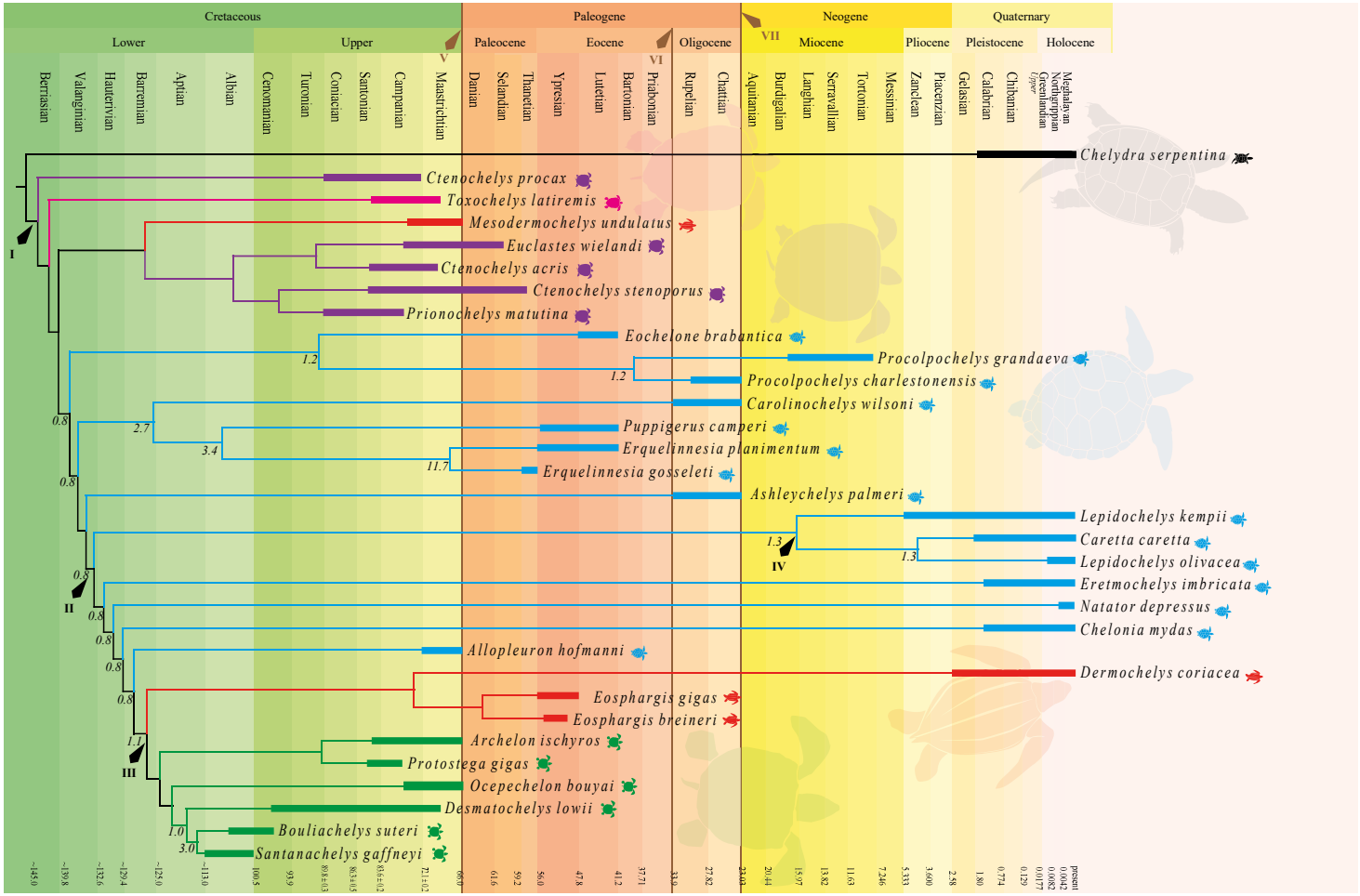

Figure 39. Time-calibrated phylogeny combining all landmark data with Gentry *et al.*, 2019's pruned dataset of discrete morphological characters, aligned to *Natator depressus*. Relative Bremer Supports (above 0.5) are indicated under the nodes, rounded to one decimal place. Legend: I: divergence node of Pancheloniodea; II: crown-Chelonioidea; III: Dermochelyoidea; IV: Carettini; V: K-Pg mass extinction; VI: Eocene-Oligocene cooling event; VII: Pg-N brief glacial event; blue – Pancheloniidae; red – Dermochelyidae; black – Chelydridae; purple – Ctenochelyidae; pink – *Toxochelys latiremis*. The numerical ages are in Ma. Chart from the International Commission on Stratigraphy (1), accessed on December 11, 2020.

4. DISCUSSION

The time-calibrated preferred topology (Figure 39) allows the conclusion that Pan--Cheloniidae diversified following the extinction of Protostegidae and most of the Ctenochelyidae species after K-Pg mass extinction (72) (marked as V in Figure 39), which also coincides with the evolution of sea grass (63). The Eocene marks the end of the fossil record of *Eochelone brabantica, Puppigerus camperi* and *Erquelinnesia planimentum*. There was a major cooling event in the Eocene-Oligocene boundary (marked as VII in Figure 39), resulting in the extinction of ~35% of marine species (73,74). Similarly, still in the same chain of events, we can correlate the apparent extinction of P*rocolpochelys charlestonensis, Carolinochelys wilsoni* and *Ashleychelys palmeri* with a brief glacial event at the end of the Oligocene (marked as VII in Figure 39), characterized by the reversal of trans-Atlantic flow caused by the inflow of Antartic circumpolar circulation (75).

Ctenochelys procax was recovered as the first diverging taxa in Panchelonioidea. In 1953, Zangerl (26) revised the "Toxochelyidae" family and identified *Toxochelys procax* Hay 1905 – a skull + jaw from the Cretaceous deposits of Niobara Chalk (Kansas) found in 1901 – as *Ctenochelys procax* (Hay, 1905). He references to the images from the original publication (76), and the fig. 13 from page 181 was the one used in this analysis for LM digitisation. Hirayama (3) synonymizes *Toxochelys procax* Hay, 1905 and many others (*Toxochelys serrifer* Cope, 1875 [part]; *T. elkader* Hay, 1908; *Lophochelys natarix* Zangerl, 1953 and *Ctenochelys acris* Zangerl, 1953) with *C. stenoporus* (Hay, 1905). The RWA of the skull in ventral view (Figure 15) illustrates that *Ctenochelys procax* has the closest shape to the consensus configuration of Panchelonioidea, both in RW_1 and RW_2. In the preliminary analyses, *C. procax* was recovered inside Ctenochelyidae using only the configuration of skull in ventral view (Figure 26); using the 3 views of the skull and the jaw (Figure 30) and in the global preliminary analysis 2 (with no character weighting) (Figure 36). In the preliminary analysis using all LM configurations (Figure 33), in global preliminary analysis 4 (aligning with *L. olivacea*) (Figure 38) and in the preferred topology (Figure 39), *C. procax* was recovered at the first divergence node of Panchelonioidea. Our results (based solely on the configuration of the skull in palatal view for this species) refute the inclusion of *C. procax* in any previously established genera, but since its diagnosis relies solely on vague morphological features of the skull, we think it is premature to draw a conclusion and suggest a new genus. Hence, *Ctenochelys procax* should be considered an *insertae sedis* and the identification as a *Ctenochelys* taken as provisory.

We agree that *Toxochelys latiremis* is one of the first diverging branches inside Panchelonioidea (2,5,6,19,20,72,77); this species has movable articulations of the first and second digits and dorsally faced orbits, indicating a similarity with chelydrids and trionichlyds regarding swimming habits (6).

Karl *et al.* (25) already presumed that "Osteopygidae" would consist on a polyphyletic group, once the main differentiating criterion was the presence of the nasal bone (25). Pritchard & Trebbau (78) suggested that *Erquelinnesia gosseleti* is a specialization extreme in terms of secondary palate and "probably derived" (sic) from "Osteopygis". Our data places the former members of "Osteopygidae" – *Erquelinnesia* spp, *Euclastes wielandi (Osteopygis emarginatus)* and *Ctenochelys* spp. – with distinct origins (Figure 39). The main morphological resemblance between them is having a wide caudal portion of the skull composed by the parietal and post orbital, with dorsal plates and vomer almost entirely covered by the extensive secondary palate (64). However, the significance of the secondary palate development in turtle evolution is most likely associated to specific feeding habits (25,79). Lynch & Parham (80) assigned all species of osteopygines (hyper-durophagous stem cheloniids) to the genus *Euclastes* Cope 1867 (63). Seven years later, Parham & Pyenson (63) included those species in their phylogenetic analysis and revised their taxonomy, concluding that *Erquelinnesia* Dollo 1887 should be used only to *Erquelinnesia gosseleti* (Dollo 1886) (type species) and *Erquelinnesia meridionalis* (de la Fuente & Casadío, 2000), and changed *Erquelinnesia planimentum* to *Glossochelys planimentum* (Owen, 1842) claiming that even though it is a durophagous pancheloniid, it lacks the dorsally directed orbits of *Euclastes* and the elongated secondary palate of *Erquelinnesia*. Our data strongly support the use of the name *Erquelinnesia planimentum*, since both species (*E. planimentum* and *E. gosseleti*) were consistently recovered as sister groups (with 11.65581 Bremer Support on global preliminary tree 1 – Figure 35 – and 9.55014 on global preliminary tree 4 – Figure 38).

In the literature, we found 4 phylogenetic studies including both *Euclastes* and Ctenochelyidae: Scavezzoni & Fisher (19), in which they are inside a polytomy inside Cheloniidae; Hirayama (6), with a clade containing *Toxochelys, Ctenochelys,* "Osteopygis", *Puppigerus* and *Chelonia mydas*; Kear & Lee (9), that recovered *Euclastes* associated with *Puppigerus* and "advanced cheloniids" (sic) and Weems & Brown (72), with *Euclastes* as an early-diverging pancheloniid. All of those analysis (except the one from Scavezzoni & Fisher (19)) figure *Euclastes*, instead of *Euclastes wielandi* specifically. In the present work, *Euclastes wielandi* was recovered among ctenochelyids in several analysis (Figures 29, 32, 33, 36, 37, 39), so we herein defend the placement of this species inside Ctenochelyidae.

Two well supported groups represent all Paleogene pancheloniids (Figure 39). Without a molecular backbone, the less structured group in the final topology was the one with extant Cheloniidae, and maybe for that same reason, there was not possible to recover Cheloniidae sensu Evers & Benson (2) on a monophyletic group. On the other hand, it is possible to notice that in the global preliminary tree 2 (Figure 36), where there is no character weighting, the extant Cheloniidae constitute a topology very similar to previous ones (16,18,29,81).

Although the data supports the hypothesis of a tribe comprising the carnivorous extant cheloniids *Caretta caretta* and *Lepidochelys* spp., (i.e., Carettini), it does not recover Chelonini Burmeister 1835. Chelonini (allegedly *Chelonia mydas* + *Natator depressus*) is recovered only in molecular phylogenies (81,82) and consequentially in morphological ones using molecular backbone (2,13,18,20,29). We opted for not using a molecular backbone for this analysis because this means that the phylogenetic hypothesis of the internal relationships of living species is not being tested with morphological data. It is possible that molecular constraints are forcing a "false" monophyleticism in Pancheloniidae, a group that can be polyphyletic and far more complex than expected. Likewise, instead of being sister taxa in "Chelonini", the extant *Natator depressus* and *Chelonia mydas* can represent very distinct lineages, which may even impact our conservation efforts. This can possibly be explained by long-branch attraction, a common phenomenon in molecular data in which long branches of taxa not closely related to each other acquire by chance identical bases independently and that is accounted as synapomorphy in a parsimony analysis (83). Morphological characters are not "immune" to long-branch attraction, however, since there are much more possible morphological character states than 4 nucleotides or 20 amino acids, this kind of convergent evolution can be avoided with more efficiency (83,84). The goal of the fourth and fifth global preliminary analysis was to verify if the scattered rooting of Pancheloniidae taxa was due to lack of information or due to influence of early diverging clades - in both tests, the removal of terminals did not improve the resolution of Pancheloniidae as a monpophyletic clade. Naturally it is necessary to conduct further research specifically on the origins and internal relationships of Pancheloniidae in order to refute the hypothesis of an exclusive common ancestor to all pancheloniids.

Allopleuron hofmanni appears to have a close affinity to Dermochelyoidea, as in Gentry et al., (13) (Figure 39). Hirayama (3) explains that the similarity between the carapaces of *Allopleuron* and *Eosphargis* can be considered extreme convergence, due to pelagic habits. In our carapace RWA (Figure 18), *Allopleuron* is the only crown-Cheloniidae in the high positive scores of RW_1, alongside all Protostegids in the sample (more notably *Archelon* and *Protostega*) and *Eosphargis breineri*, which can indicate similar pelagic

lifestyles. That is also consistent stratigraphically, because *Allopleuron* is one of the only two pancheloniid species originated in the Cretaceous. Extant sea turtles, especially *C. caretta* and *D. coriacea,* are known to migrate great distances between foraging and nesting grounds (85) – both have very different shell anatomies; one highly ossified and the other hardly ossified at all (86). This can indicate at least two distinct shell morphologies adapted to a pelagic way of life in cryptodiran sea turtles.

The placing of Protostegidae inside crown-Chelonioidea is controversial (see discussion in Evers & Benson (2) and Cadena & Parham (29)) and implies at least 54 million years of ghost-lineage for most cheloniids. This placement has been considered a result of convergence of pelagic specializations (11,13,29); However, Protostegidae was still recovered as chelonioids after the exclusion of characters related to a pelagic lifestyle in Evers & Benson (2). *Santanachelys gaffneyi*, often used as sole representative of its family (11,14,15), was recovered deep nested in Protostegidae in all analysis using LM + discrete characters (Figures 35-38).

The tested dermochelyids from the Upper Cretaceous, *Mesodermochelys undulatus* and *Ocepechelon bouyai* were recovered out of *Dermochelys* and *Eosphargis* group (i.e., crown-Dermochelyidae). In Bardet *et al.* (87), in which the species is first described, *Ocepechelon bouyai* is identified as a stem-Dermochelyoidae *sensu* Bour & Dubois (88). As found by Evers & Benson (2), in this work *Ocepechelon bouyai* was nested into Protostegidae as sister group to *(Desmatochelys lowii (Bouliachelys suteri, Santanachelys gaffney))*. Evers *et al.* (18) and Gentry *et al.* (13) also recovered this species as a protostegid, associated with *Archelon, Protostega* and *Desmatochelys*. So, in our final tree, *Ocepechelon bouyai* is established as a protostegid (Figure 39). *Mesodermochelys undulatus* is already well established as a stem-Dermochelyidae (6,16,19,20,29,64,89). Herein, this Upper Cretaceous dermochelyid was not recovered associated with D*ermochelys coriacea*, but with mesozoic turtles (Ctenochelyidae + *Euclastes wielandi*). There is also a chronostratigraphic correlation between *Euclastes wielandi* and *Allopleuron hofmanni*, stem-cheloniids associated with Cretaceous turtles and not with their Paleogene clade – *Allopleuron* as sister-taxon to Protostegidae and *Euclastes* among ctenochelyids

The reanalysis of Gentry et al., (13) pruned dataset (Figure 34) recovered Dermochelyoidea (Protostegidae + Dermochelyidae) instead of Protostegidae being the first diverging clade and Dermochelyidae among pancheloniids. The exclusion of non-chelonioid cryptodires – in particular Angolachelonia –, can have influenced the resolution at the base of the tree. These clades could not be included in this phylogenetic morphometric analysis due to computational limits – this method increases drastically the processing effort and the time consumed in each analysis with the number of terminals, because the heuristic spatial optimization is performed to each landmark of each terminal taxon. But

this “limitation” is a matter of time. In the 90’s, analysis that today are made in seconds in personal computers used to take months to complete (61,90). The internal relationships of Dermochelyidae, Ctenochelyidae and Protostegidae remained unchanged in this reanalysis. Internal relationships of Pancheloniidae presented several incongruences, though; which can be attributed to the decision not to include a molecular backbone to the extant species, as already commented above.

5. CONCLUSION

In this study, we proposed – to our knowledge –, for the first time in the literature, a phylogenetic hypothesis for Panchelonioidea based on morphogeometric data. It was possible to increment the resolution of some problematic clades, such as the former "Osteopygidae", *Allopleuron hofmanni* and *Ocepechelon bouyai.* Our data also supports the placement of Protostegidae and Dermochelyidae as sister-groups nested within crown-Chelonioidea, however, this brings about an extensive ghost-lineage to Cenozoic cheloniids standing back at least 54 Ma. Pan-Cheloniidae was not recovered as a monophyletic group, however, some affinities could be clarified and explained with phylogenetic morphometrics data. Two relatively well supported clades congregate all Paleocene stem cheloniids except *Ashleychelys palmeri*, and it was possible to recover the Quaternary clade of extant cheloniids Carettini, yet separating the *Lepidochelys* genus in two rami. It was possible to recover an exclusive common ancestor to the following Upper Cretaceous fossil taxa: "*(Mesodermochelys undulatus ((Euclastes wielandi, Ctenochelys acris) (Ctenochelys stenoporus, Prionochelys matutina)))*", and *Euclastes wielandi* was reallocated to Ctenochelyidae. We agree that "Osteopygidae" and "Toxochelyidae" are polyphyletic and invalid taxa.

6. ACKNOWLEDGMENTS

The authors thank Santiago Catalano for counselling and revision along the process, and for being a member of the evaluating committee for the present dissertation. We also thank Gustavo Oliveira for being part of the evaluating committee and help improve this project. Thanks to Leonardo Bherig, for allowing the use of the Laboratory of Biometrical Processing's cluster for performing the phylogenetic analysis; F. James Rohlf and Stony Brook Morphometrics for making the TPS series of software freely available, and Willy Hennig Society for making possible the free access to the software TNT. We appreciate the help of Serjoscha Evers for providing skeletal pictures of several specimens added to this sample; and we are grateful for the access to the chelonian collection of UNIVALI and the help of the curators Jules, Bibiana and Gerson. Also, to CAPES, for MSc student grant. And finally, but most important, thanks to the team of our lab – LAPOC – for tips, suggestions and for always being willing to share their knowledge.

7. AUTHOR CONTRIBUTIONS

I. Goulart carried out data acquisition and analysis, participated in the design of the study and drafted the manuscript, conceived of the study, designed the study, coordinated the study and helped draft the manuscript. P. Romano participated in the design of the study, conceived of the study, designed the study, coordinated the study and helped draft the manuscript. All authors gave final approval for publication.

8. DATA ACCESSIBILITY

all TNT and TPS files, as well as trees topologies used in this study have been made available for the judging committee. These files will be made publicly available at open official repositories after the publication of the results presented here.

9. FUNDING

This study was financed in part by the Coordenação de Aperfeiçoamento de Pessoal de Nível Superior – Brasil (CAPES) – Finance Code 001.

10. COMPETING INTERESTS

The authors have no competing interests

11. ETHICAL STATEMENT

No specific permits were required for the described procedures.

12. REFERENCES

1. Cohen KM, Finney SC, Gibbard PL, Fan J-X. The ICS International Chronostratigraphic Chart. 36:199–204. Available from: http://www.stratigraphy.org/ICSchart/ChronostratChart2020-03.pdf
2. Evers SW, Benson RB. A new phylogenetic hypothesis of turtles with implications for the timing and number of evolutionary transitions to marine lifestyles in the group. Palaeontology. 2019;62(1):93–134.
3. Hirayama R. Distribution and Diversity of Cretaceous Chelonioids. In: Ancient Marine Reptiles. Academic Press; 1997. p. 225–41.
4. Zangerl R. Patterns of phylogenetic differentiation in the toxochelyid and cheloniid sea turtles. Integr Comp Biol. 1980;20(3):585–96.
5. Hirayama R. Phylogenetic systematics of chelonioid sea turtles. Isl Arc. 1994;3:270–84.
6. Hirayama R. Oldest known sea turtle. Nature. 1998;392(April):2259–62.
7. Lehman TM, Tomlinson SL. Terlinguachelys fischbecki, a new genus and species of sea turtle (Chelonioidea: Protostegidae) from the Upper Cretaceous of Texas. J Paleontol. 2004;78:1163–1178.
8. Brinkman DB, Hart M, Jamniczky H, Colbert M. Nichollsemys baieri gen. et sp. nov., a primitive chelonioid turtle from the Late Campanian of North America. Paludicola. 2006;5(4):111–24.
9. Kear BP, Lee MSY. A primitive protostegid from Australia and early sea turtle evolution. Biol Lett. 2006;2:116–9.
10. Cadena EA. The first South American sandownid turtle fromthe Lower Cretaceous of Colombia. PeerJ. 2015;1–24.
11. Joyce WG. Phylogenetic Relationships of Mesozoic Turtles. Bull Peabody Museum Nat Hist. 2007;48(1):3–102.
12. Gentry AD, Ebersole JA. The first report of Toxochelys latiremis Cope, 1873 (Testudines: Panchelonioidea) from the early Campanian of Alabama, USA. PaleoBios. 2018;35:1–10.
13. Gentry AD, Ebersole JA, Kiernan CR. Asmodochelys parhami , a new fossil marine turtle from the Campanian Demopolis Chalk and the stratigraphic congruence of competing marine turtle phylogenies. R Soc open sci. 2019;6(191950):12.
14. Sterli J. Phylogenetic relationships among extinct and extant turtles: The position of Pleurodira and the effects of the fossils on rooting crown-group turtles. Contrib to Zool. 2010;79:93–106.
15. Anquentin J. Reassessment of the phylogenetic interrelationships of basal turtles (Testudinata). J Syst Palaeontol. 2012;10(1):3–45.
16. Gentry AD, Parham JF, Ehret DJ, Ebersole JA. A new species of Peritresius Leidy , 1856 (Testudines : Pan-Cheloniidae) from the Late Cretaceous (Campanian) of Alabama , USA , and the occurrence of the genus within the Mississippi Embayment of North America. PLoS One [Internet]. 2018;13(4):1–24. Available from: https://doi.org/10.1371/journal. pone.0195651
17. Joyce WG, Parham JF, Lyson TR, Warnock RC, Philip CJ. A Divergence Dating Analysis of Turtles Using Fossil Calibrations: An Example of Best Practices. BioOne. 2013;87(4):612–34.
18. Evers SW, Barrett PM, Benson RB. Anatomy of Rhinochelys pulchriceps (Protostegidae) and marine adaptation during the early evolution of chelonioids. PeerJ. 2019;1–94.
19. Scavezzoni I, Fischer V. Rhinochelys amaberti Moret (1935), a protostegid turtle from the Early Cretaceous of France. PeerJ. 2018;
20. Gentry AD. Prionochelys matutina Zangerl , 1953 (Testudines : Pan-Cheloniidae) from the Late Cretaceous of the United States and the evolution of epithecal ossifications in marine turtles. PeerJ. 2018;1–34.
21. Gentry AD. New material of the Late Cretaceous marine turtle Ctenochelys acris Zangerl , 1953 and a phylogenetic reassessment of the ‘toxochelyid’-grade taxa. J Syst Palaeontol. 2016;(September 2016):22.
22. Parham JF, Fastovsky DE. The phylogeny of cheloniid marine turtles revisited. Chel Cons Biol. 1997;2:548–554.
23. Parham JF, Hutchison JH. A New Eucryptodiran Turtle From the Late Cretaceous of North America (Dinosaur Parovincial Park, Alberta, Canada). J Vertebr Paleontol. 2003;23(4):783–98.
24. Parham JF. A reassessment of the referral of sea turtle skulls to the genus Osteopygis (Late Cretaceous, New Jersey, USA). J Vertebr Paleontol. 2005;25(1):71–7.

25. Karl H, Tichy G, Ruschak H. Osteopygoides priscus n. gen. n. sp. und die Taxonomie und Evolution der Osteopygidae (Testudines: Chelonioidea). Mitt Geol und Paläont Landesmuseum Joanneum. 1998;56(1981):329–50.
26. Zangerl R. The vertebrate fauna of the Selma Formation of Alabama. Part IV. the turtles of the family Toxochelyidae. Fieldiana Geol Mem [Internet]. 1953;3(4):1–306. Available from: http://www.biodiversitylibrary.org/bibliography/5224
27. Gaffney ES. A Phylogeny and Classification of the Higher Categories ofTurtles. Vols. 155–5. New York: Bulletin of the American Museum of Natural History; 1975. 387–436 p.
28. Zangerl R, Sloan RE. A new specimen of Desmatochelys lowii Williston: A primitive sea turtle from the Cretaceous of South Dakota. Fieldiana, Geol. 1960;14:7–40.
29. Cadena EA, Parham JF. Oldest known marine turtle? A new protostegid from the Lower Cretaceous of Colombia. PaleoBios. 2015;32(1):42.
30. Danilov LG, Parham JF. A reassessment of some poorly known turtles from the Middle Jurassic of China, with comments on the antiquity of extant turtles. J Vertebr Paleontol. 2008;28:306–318.
31. Zhou C-F, Rabi M. A sinemydid turtle from the Jehol Biota provides insights into the basal divergence of crown turtles. Sci Rep [Internet]. 2015 Dec 10;5(1):16299. Available from: http://www.nature.com/articles/srep16299
32. Klingenberg CP, Gidaszewski NA. Society of Systematic Biologists Testing and Quantifying Phylogenetic Signals and Homoplasy in Morphometric Data. Syst Biol. 2010;59(3):245–61.
33. Gonzáles-José R, Escapa I, Neves WA, Cúneo R, Puccia-relli HM. Cladistic analysis of continuous modularized traits provides phylogenetic signals in Homo evolution. Nature. 2008;453:775–8.
34. Lockwood C, Kimbel W, Lynch J. No Morphometrics and hominoid phylogeny: support for a chimpanzee–human clade and differentiation among great ape subspecies. Proc Natl Acad Sci U S A. 2004;101:4356–4360.
35. Rohlf FJ. Geometric morphometrics and phylogeny. In: Macleod N, Forey P, editors. Morphology, Shape, and Phylogeny. London: Taylor & Francis; 2002. p. 175–93.
36. Catalano SA, Ercoli M, Prevosti F. The more, the better: the use of multiple landmark configurations to solve the phylogenetic relationships in Musteloids. Syst Biol. 2015;64:294–306.
37. Ascarrunz E, Claude J, Joyce WG. Estimating the phylogeny of geoemydid turtles (Cryptodira) from landmark data: An assessment of different methods. PeerJ. 2019;1–38.
38. Catalano SA, Torres A. Phylogenetic inference based on landmark data in 41 empirical data sets. Zool Scr. 2017;46(1):1–11.
39. Oxnard CE. Morphometrics of the primate skeleton and the functional and developmental underpinnings of species diversity. In: O'Higgins P, Cohn MJ, editors. Development, Growth and Evolution. London: Academic Press; 2000. p. 235–63.
40. Catalano SA, Goloboff PA, Giannini NP. Phylogenetic morphometrics (I): the use of landmark data in a phylogenetic framework Santiago. Cladistics. 2010;26:539–49.
41. Goloboff PA, Catalano SA. Phylogenetic morphometrics (II): algorithms for landmark optimization Pablo. Cladistics. 2011;27:42–51.
42. Catalano SA, Goloboff PA. Simultaneously mapping and superimposing landmark configurations with parsimony as optimality criterion. Syst Biol. 2012;61(3):392–400.
43. Rohlf FJ. Morphometrics. Annu Rev Ecol Syst. 1990;21:299–316.
44. Viscosi V, Cardini A. Leaf morphology, taxonomy and geometric morphometrics: A simplified protocol for beginners. PLoS One. 2011;6(10).
45. Dryden IL, Mardia K V. Statistical shape analysis, with applications in R. 2nd ed. Chichester: Wiley; 2016.
46. Klingenberg CP. Walking on Kendall's Shape Space : Understanding Shape Spaces and Their Coordinate Systems. Evol Biol [Internet]. 2020; Available from: https://doi.org/10.1007/s11692-020-09513-x
47. Rohlf FJ. The tps series of software. Hystrix, Ital J Mammal. 2015;26(1):9–12.
48. Cardini A, O'Higgins P. Patterns of morphological evolution in Marmota (Rodentia , Sciuridae): geometric morphometrics of the cranium in the context of marmot phylogeny, ecology and conservation. Biol J Linn Soc. 2004;82:385–407.
49. Gower JC. Generalized procrustes analysis. Psychometrika. 1975;40(1):33–51.
50. Rohlf FJ, Slice D. Extensions of the procrustes method for the optimal superimposition of landmarks. Syst Zool. 1990;39(1):40–59.

51. Bookstein FL. Morphometric Tools for Landmark Data. Cambridge: Cambridge University Press; 1991. 435 p.
52. Mandarim de Lacerda CA. Métodos Quantitativos em Morfometria. Rio de Janeiro: edUERJ; 1995. 124 p.
53. Hammer Ø. PAST 4.03: Reference manual. 2020;(1999).
54. Goloboff PA, Farris JS, Nixon KC. TNT , a free program for phylogenetic analysis. Cladistics. 2008;24:774–86.
55. Goloboff PA, Catalano SA. TNT version 1.5, including a full implementation of phylogenetic morphometrics Pablo. Cladistics. 2016;32:221–38.
56. Perrard A, Lopez-Osorio F, Carpenter JM. Phylogeny, landmark analysis and the use of wing venation to study the evolution of social wasps (Hymenoptera: Vespidae: Vespinae). Cladistics. 2016;32(4):406–25.
57. Anquentin J, Püntener C, Billon-Bruyat J-P. Portlandemys gracilis n. sp. a new coastal marine Turtle from the Late Jurassic of Porrentruy (Switzer- land) and a reconsideration of Plesiochelyid cranial anatomy. PLoS One. 2015;10.
58. Catalano SA, Goloboff PA. A guide for the analysis of continuous and landmark characters in TNT (Tree Analysis using New Technologies). Tech Rep [Internet]. 2018;(September):1–36. Available from: https://www.researchgate.net/publication/323615953
59. Siegel AF, Benson RH. A Robust Comparison of Biological Shapes. Biometrics. 1982;38(2):341–50.
60. Benson RH, Chapman RE, Siegel AF. On the Measurement of Morphology and its Change. Princet Univ Press. 1982;(2):1–35.
61. Nixon KC. The Parsimony Ratchet, a New Method for Rapid Parsimony Analysis. Cladistics. 1999;15:407–14.
62. Claude J, Pritchard PC, Tong H, Paradis E, Auffray JC. Ecological correlates and evolutionary divergence in the skull of turtles: A geometric morphometric assessment. Syst Biol. 2004;53(6):933–48.
63. Parham JF, Pyenson ND. New Sea Turtle From The Miocene of Peru And The Iterative Evolution of Feeding Ecomorphologies Since the Cretaceous. J Paleont. 2010;84(2):231–47.
64. Myers TS, Polcyn MJ, Avio OC, Vineyard DP, Onio AN, Jacobs LL. A New Durophagous Stem Cheloniid Turtle From the Lower Paleocene of Cabinda, Angola. Pap Palaeontol. 2017;1–16.
65. Bremer K. Branch Support and Tree Stability. Vol. 10, Cladistics. 1994. p. 295–304.
66. Kim J. Improving the accuracy of phylogenetic estimation by combining different methods. Syst Biol. 1993;42:331–40.
67. Sidall ME. Measures of support. In: DeSalle R, Giribet G, Wheeler W, editors. Techniques in Molecular Systematics and Evolution. Switzerland: Bir-khaüser, Verlag; 2002. p. 80–101.
68. Aagesen L, Petersen G, Seberg O. Sequence length variation, indel costs, and congruence in sensitivity analysis. Cladistics. 2005;21:15–30.
69. Goloboff PA, Farris JS. Methods for Quick Consensus Estimation. Cladistics. 2001;17:26–34.
70. Falbo AD, Agnolin FL. First record of a chelonioid sea turtle (Testudines, Pan-Cheloniidae) from the late Miocene of Argentina. Alcheringa [Internet]. 2020;44(3):475–80. Available from: https://doi.org/10.1080/03115518.2020.1814411
71. Foth C, Joyce WG. Skull shape variation in extant and extinct Testudinata and its relation to habitat and feeding ecology. Acta Zool. 2016;0:1–16.
72. Weems RE, Brown KM. More-complete remains of Procolpochelys charlestonensis (Oligocene , South Carolina), an occurrence of Euclastes (upper Eocene , South Carolina), and their bearing on Cenozoic pancheloniid sea turtle distribution and phylogeny. J Paleontol. 2017;1–16.
73. Raup DM. Large-body impact and extinction in the Phanerozoic. Paleobiology. 1992;18:80–8.
74. Rampino MR. Chapter 4 - Catastrophe: impact of comets and asteroids. In: Henderson-Sellers ABT--WS of C, editor. Future climates of the world: a modelling perspective [Internet]. Elsevier; 1995. p. 95–147. Available from: http://www.sciencedirect.com/science/article/pii/S0168632106800271
75. Pfuhl HA, Mccave IN. The Oligocene–Miocene boundary – cause and consequence from a Southern Ocean perspective. In: Williams M, Haywood AM, Gregory FJ, Schmidt DN, editors. Deep-Time Perspectives on Climate Change: Marrying the Signal from Computer Models and Biological Proxies [Internet]. Geological Society of London; 2007. Available from: https://doi.org/10.1144/TMS002.17
76. Hay OP. A revision of the species of the family of fossil turtles called Toxochelyidae: with descriptions of two new species of Toxochelys and a new species of Porthochelys. Order Trust Am Museum Nat Hist. 1905;21.

77. Raselli I. Comparative cranial morphology of the Late Cretaceous protostegid sea turtle Desmatochelys lowii. PeerJ. 2018;1–87.

78. Pritchard PC, Trebbau P. The Turtles of Venezuela. Athens, Ohio: Society for the Study of Amphibians and Reptiles; 1984.

79. Moody RTL. The relative importance of cranial - post cranial characters in the classification of sea turtles. Stud Palaeochelonio- Log I. 1984;1:205–13.

80. Lynch SC, Parham JF. The first report of hard-shelled sea turtles (Cheloniidae sensu lato) from the Miocene of California, including a new species (Euclastes hutchisoni) with unusually plesiomorphic characters. PaleoBios. 2003;23(3):21–35.

81. Naro-maciel E, Le M, Fitzsimmons NN, Amato G. Molecular Phylogenetics and Evolution Evolutionary relationships of marine turtles : A molecular phylogeny based on nuclear and mitochondrial genes. Mol Phylogenet Evol [Internet]. 2008;49(2):659–62. Available from: http://dx.doi.org/10.1016/j.ympev.2008.08.004

82. Pereira AG, Sterli J, Moreira FRR, Schrago CG. Multilocus phylogeny and statistical biogeography clarify the evolutionary history of major lineages of turtles. Mol Phylogenet Evol [Internet]. 2017;113:59–66. Available from: http://dx.doi.org/10.1016/j.ympev.2017.05.008

83. Bergsten J. A review of long-branch attraction. Cladistics. 2005;21:163–93.

84. Jenner RA. Accepting partnership by submission? Morphological phylogenetics in a molecular millennium. Syst Biol. 2004;53(2):333–42.

85. SEE Turtles. Sea Turtle Migration [Internet]. Available from: www.seeturtles.org/sea-turtle-migration

86. Wyneken J. The Anatomy of Sea Turtles. Miami, FL: U. S. Department of Commerce NOAA Technical Memorandum NMFS-SEEFSC-470; 2001. 172 p.

87. Bardet N, Jalil N, Lapparent de Broin F, Germain D, Lambert O, Amaghzaz M. A Giant Chelonioid Turtle from the Late Cretaceous of Morocco with a Suction Feeding Apparatus Unique among Tetrapods. PLoS One. 2013;8(7):1–10.

88. Bour R, Dubois A. Nomenclature ordinale et familiale des Tortues (Reptilia). Note complèmentaire. Bull mens Soc Lin Lyon. 1986;55(3):87–90.

89. Hirayama R, Chitoku T. Family Dermochelyidae (Superfamily Chelonioidea) from the Upper Cretaceous of North Japan. Trans Proc Paleont Soc Japan. 1996;184:597–622.

90. Rice KA, Donoghue MJ, Olmstead RG. Analyzing large data sets: rbcL 500 revisited. Syst Biol. 1997;46:554–63.

APPENDIX A. LM descritions and schematic reference for digitisation

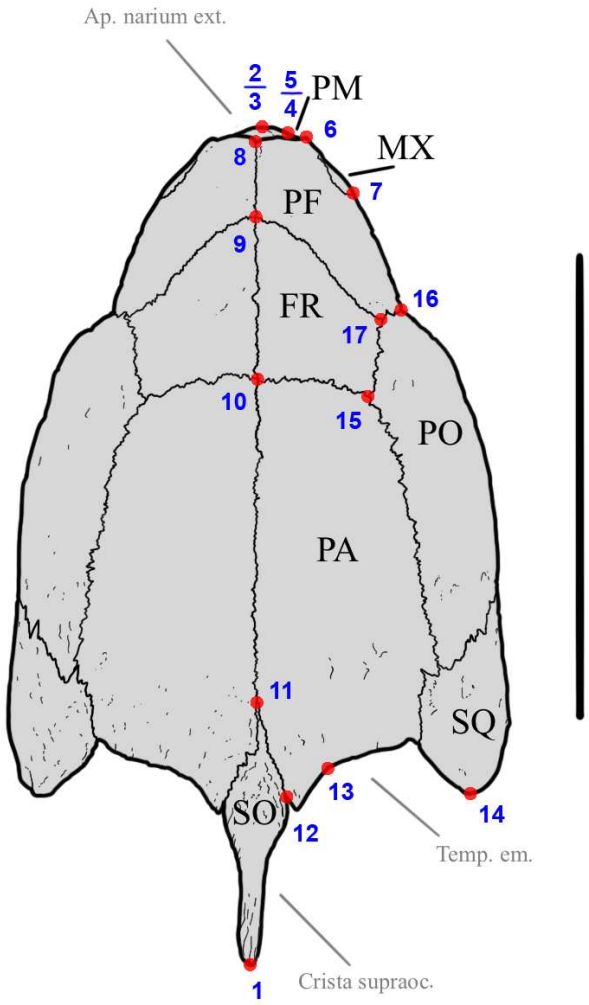

Figure 2. Cutout of the dorsal view of the skull from Figure 1, detailing osteological structures and anatomical reference for landmark digitisation. Scale 5 cm.

Table 2. This table contains anatomical descriptions of each landmark in Figure 2 and its classification by type, according to Bookstein, 1991: 1 – contact of 3 structures/tissues; 2 – maximum or minimal curvature of a structure; 3 – points located in boundaries, limits or edges.

	SKULL (dorsal view)	
Number	**Type**	**Description**
1	2	Caudal tip of crista supraoccipitalis
2	2	Junction of the two premaxillas at apertura narium externa
3	2	Junction of the two premaxillas at the labial ridge
4	2	Junction of premaxilla/maxilla at apertura narium externa
5	2	Junction of premaxilla/maxilla at the labial ridge
6	2	Dorsal tip pf maxilla/prefrontal suture
7	2	Junction of maxilla/prefrontal along orbit
8	2	Dorsal tip pf frontal/prefrontal suture
9	1	Mediorostral edge of the frontals junction
10	1	Junction of the prefrontal/frontal along midline
11	1	Junction of the parietals with the supraoccipital
12	2	Caudal tip of parietal/supraoccipital suture
13	2	Minimum curvature of temporal emargination of the parietal
14	2	Caudal tip of squamosal
15	1	Junction of parietal/postorbital/frontal
16	1	Lateral edge of prefrontal/postorbital suture
17	1	Lateral edge of prefrontal/frontal suture

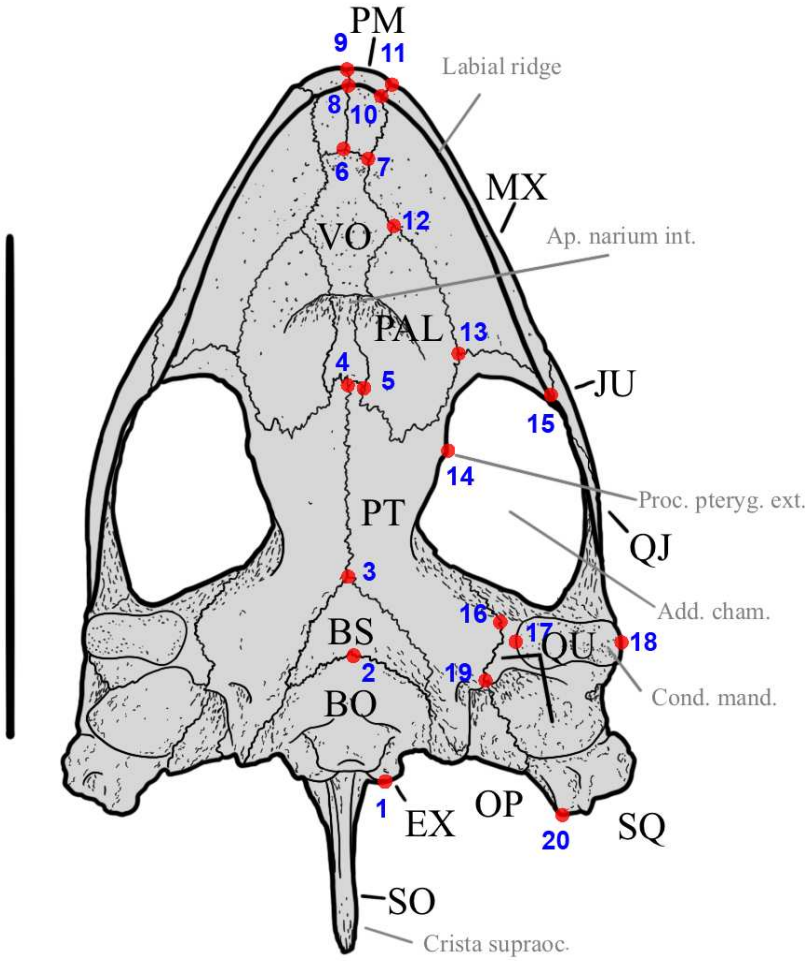

Figure 3. Cutout of the ventral view of the skull from Figure 1, detailing osteological structures and anatomical reference for landmark digitisation. Scale 5 cm.

Table 3. This table contains anatomical descriptions of each landmark in Figure 3 and its classification by type, according to Bookstein, 1991: 1 – contact of 3 structures/tissues; 2 – maximum or minimal curvature of a structure; 3 – points located in boundaries, limits or edges.

SKULL (ventral view)		
Number	**Type**	**Description**
1	2	Maximum curvature of from condylus occipitalis at the exoccipital
2	2	Caudal tip of basisphenoid at midline
3	2	Rostral tip of basisphenoid at midline
4	1	Contact between the two pterygoids and vomer
5	1	Junction of pterygoid/palatine/vomer
6	1	Junction of the two premaxillas and vomer
7	1	Junction of maxilla/premaxilla/vomer
8	1	Contact between the two premaxillas at the labial ridge
9	2	Rostral external edge of the suture between the two premaxillas
10	1	Contact between premaxilla/maxilla at the labial ridge
11	2	Rostral edge of the suture between premaxilla/maxilla outside the palate
12	1	Junction of vomer/maxilla/palatine
13	1	Caudal tip of palatine/maxilla suture
14	2	Maximum curvature of processus pterygoideus externus
15	1	Junction of maxilla/jugal at the labial ridge
16	2	Contact between pterygoid/quadrate at the edge of the adductor chamber
17	2	Maximum lateral curvature of condylus mandibularis of the quadrate
18	2	Maximum medial curvature of condylus mandibularis of the quadrate
19	2	Caudal edge of pterygoid/quarate suture
20	2	Caudal tip of squamosal

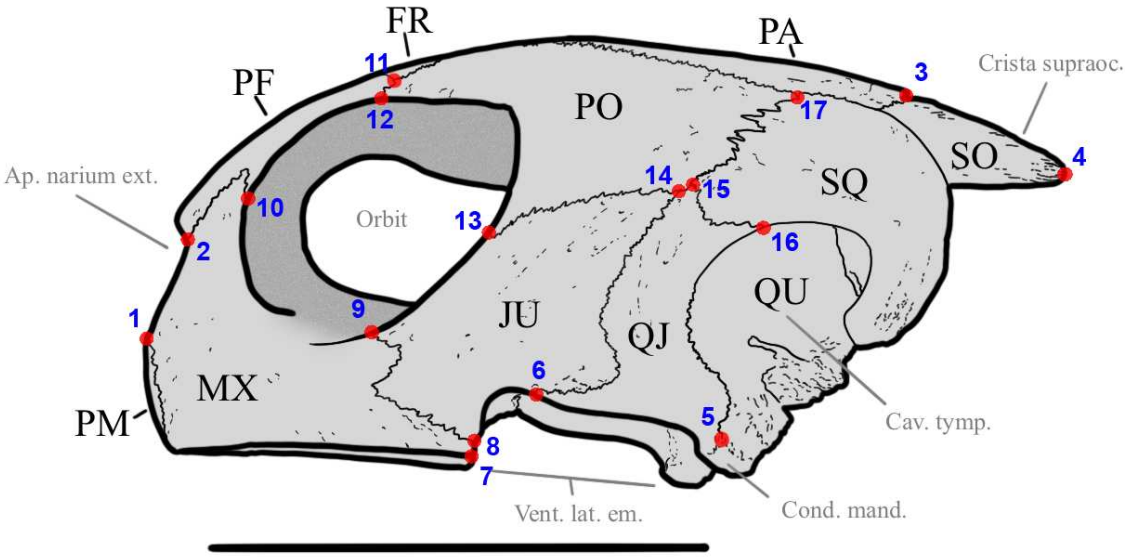

Figure 4. Cutout of the lateral view of the skull from Figure 1, detailing osteological structures and anatomical reference for landmark digitisation. Scale 5 cm.

Table 4. This table contains anatomical descriptions of each landmark in Figure 4 and its classification by type, according to Bookstein, 1991: 1 – contact of 3 structures/tissues; 2 – maximum or minimal curvature of a structure; 3 – points located in boundaries, limits or edges.

SKULL (lateral view)

Number	Type	Description
1	1	Edge of premaxilla/maxilla suture at apertura narium externa
2	1	Edge of prefrontal/maxilla suture at apertura narium externa
3	1	Junction of the parietals and supraoccipital along midline
4	2	Caudal tip of crista supraoccipitalis
5	2	Tip of quadratojugal/quadrate suture at the condylus mandibularis
6	1	Ventral edge of quadratojugal/jugal suture
7	2	Ventrocaudal edge of maxilla
8	1	Ventral tip of maxilla/jugal suture
9	2	Dorsal tip of maxilla/jugal suture
10	2	Edge of maxilla/prefrontal suture along orbit
11	1	Lateral edge of frontal/prefrontal suture
12	2	Edge of postorbital/frontal or postorbital/prefrontal suture along orbit
13	2	Edge of postorbital/jugal suture along orbit
14	1	Junction of jugal/quadratojugal/postorbital
15	1	Junction of squamosal/quadratojugal/postorbital
16	2	Junction of squamosal/quadratojugal/quadrate
17	1	Junction of squamosal/parietal/postorbital

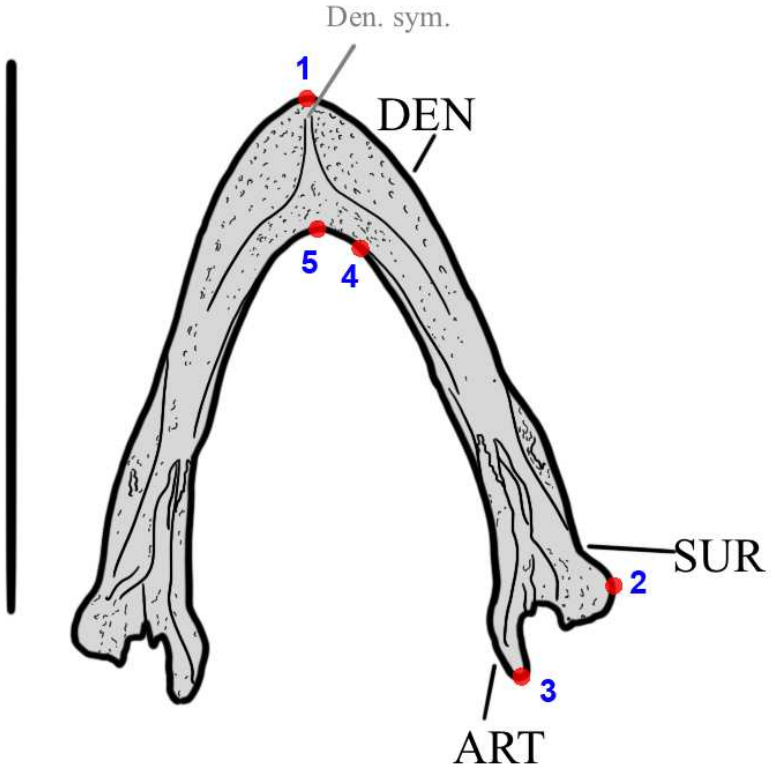

Figure 5. Cutout of the jaw from Figure 1, detailing osteological structures and anatomical reference for landmark digitisation. Scale 5 cm.

Table 5. This table contains anatomical descriptions of each landmark in Figure 5 and its classification by type, according to Bookstein, 1991: 1 – contact of 3 structures/tissues; 2 – maximum or minimal curvature of a structure; 3 – points located in boundaries, limits or edges.

JAW		
Number	**Type**	**Description**
1	2	Rostral tip of labial ridge at the dentary symphisis
2	2	Most lateral point of surangular (lateral tip of the angular process)
3	2	Most caudal point of articular
4	2	Minimum inner curvature of dentary appart from midline
5	2	Caudal tip of dentary symphisis

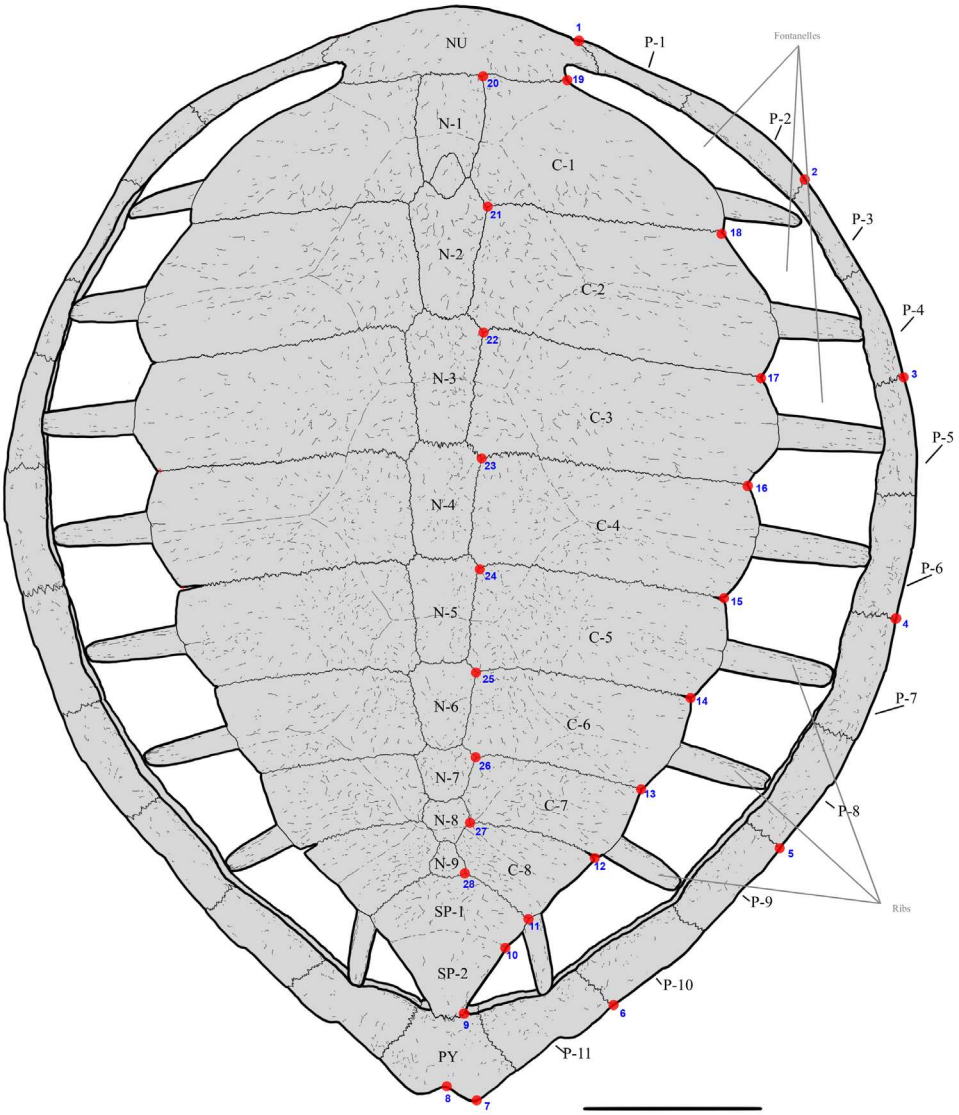

Figure 6. Cutout of the carapace from Figure 1, detailing osteological structures and anatomical reference for landmark digitisation. Scale 5 cm.

Table 6. This table contains anatomical descriptions of each landmark in Figure 6 and its classification by type, according to Bookstein, 1991: 1 – contact of 3 structures/tissues; 2 – maximum or minimal curvature of a structure; 3 – points located in boundaries, limits or edges.

CARAPACE		
Number	**Type**	**Description**
1	2	Lateral tip of nuchal/peripheral 1 suture
2	2	Lateral tip of peripheral 2/peripheral 3 suture
3	2	Lateral tip of peripheral 4/peripheral 5 suture
4	2	Lateral tip of peripheral 6/peripheral 7 suture
5	2	Lateral tip of peripheral 8/peripheral 9 suture
6	2	Lateral tip of peripheral 10/peripheral 11 suture
7	2	Caudal tip of the pygal indentation
8	2	Minimum curvature between the pygal indentations
9	1	Lateral tip of pygial/suprapygial 2 suture
10	1	Lateral tip of suprapygial 2/suprapygial 1 suture
11	1	Lateral tip of suprapygial 1/costal 8 suture
12	1	Lateral tip of costal 8/costal 7 suture
13	1	Lateral tip of costal 7/costal 6 suture
14	1	Lateral tip of costal 6/costal 5 suture

Table 6 (continued). This table contains anatomical descriptions of each landmark in Figure 6 and its classification by type, according to Bookstein, 1991: 1 – contact of 3 structures/tissues; 2 – maximum or minimal curvature of a structure; 3 – points located in boundaries, limits or edges.

CARAPACE		
Number	**Type**	**Description**
15	1	Lateral tip of costal 5/costal 4 suture
16	1	Lateral tip of costal 4/costal 3 suture
17	1	Lateral tip of costal 3/costal 2 suture
18	1	Lateral tip of costal 2/costal 1 suture
19	1	Lateral tip of costal 1/nuchal suture
20	1	Internal tip of costal 1/nuchal suture
21	1	Internal tip of costal 2/costal 1 suture
22	1	Internal tip of costal 3/costal 2 suture
23	1	Internal tip of costal 4/costal 3 suture
24	1	Internal tip of costal 5/costal 4 suture
25	1	Internal tip of costal 6/costal 5 suture
26	1	Internal tip of costal 7/costal 6 suture
27	1	Internal tip of costal 8/costal 7 suture
28	1	Internal tip of suprapygial 1/costal 8 suture

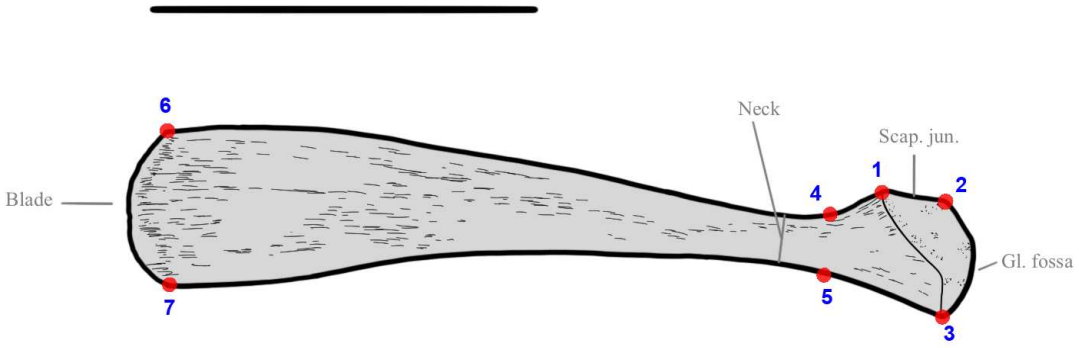

Figure 7. Cutout of the coracoid from Figure 1, detailing osteological structures and anatomical reference for landmark digitisation. Scale 5 cm.

Table 7. This table contains anatomical descriptions of each landmark in Figure 7 and its classification by type, according to Bookstein, 1991: 1 – contact of 3 structures/tissues; 2 – maximum or minimal curvature of a structure; 3 – points located in boundaries, limits or edges.

CORACOID		
Number	**Type**	**Description**
1	2	Medial edge of the scapula-coracoid junction
2	2	Lateral edge of the scapula-coracoid junction
3	2	Caudal tip of the glenoid fossa
4	2	Maximum curvature of the neck at the cranial side
5	2	Maximum curvature of the neck at the caudal side
6	2	Craniomedial tip of the coracoid blade
7	2	Caudomedial tip of the coracoid blade

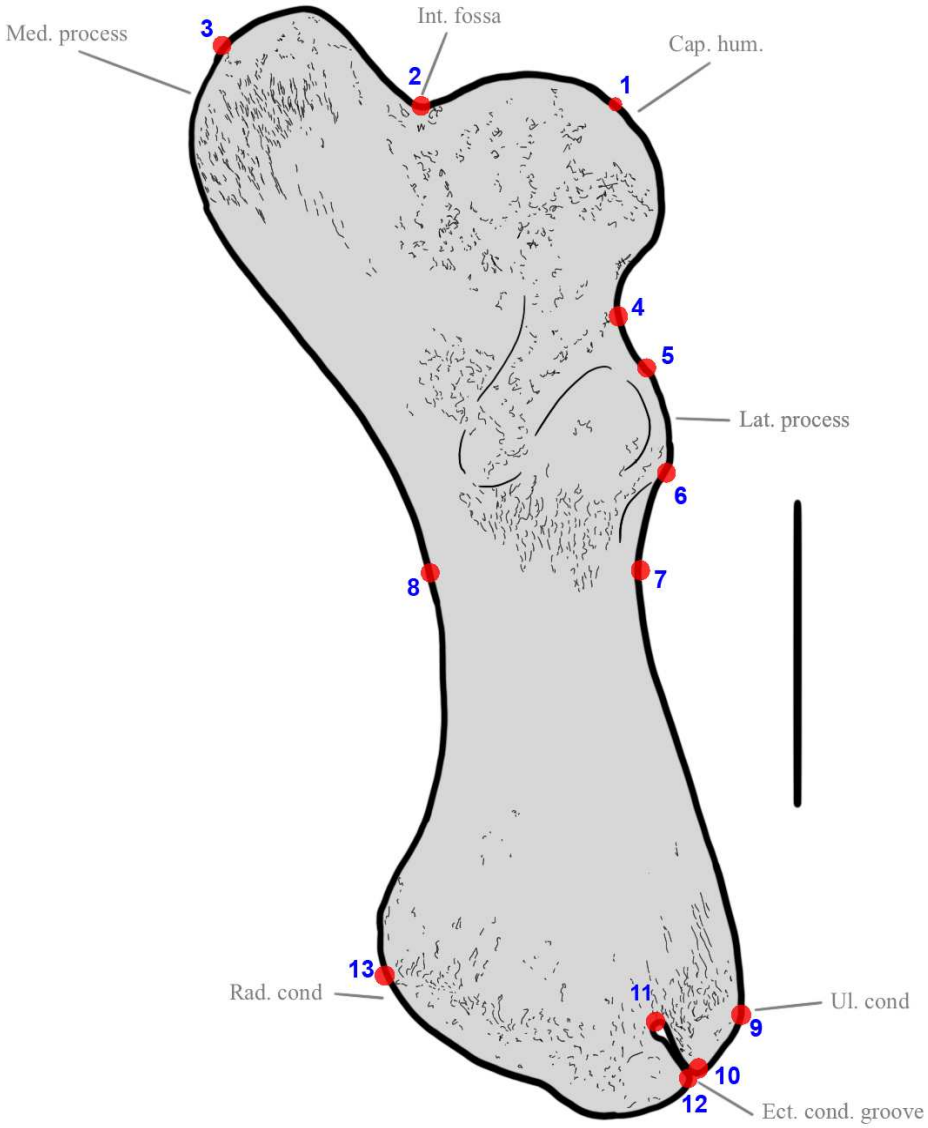

Figure 8. Cutout of the humerus from Figure 1, detailing osteological structures and anatomical reference for landmark digitisation. Scale 5 cm.

Table 8. This table contains anatomical descriptions of each landmark in Figure 8 and its classification by type, according to Bookstein, 1991: 1 – contact of 3 structures/tissues; 2 – maximum or minimal curvature of a structure; 3 – points located in boundaries, limits or edges.

UM Number	Type	Description
1	2	Maximum curvature of caput humeri
2	2	Minimum curvature of the intertubular fossa
3	2	Maximum curvature of the medial process
4	2	Minimum curvature between caput humeri and the lateral process
5	2	Proximal limit of the lateral process
6	2	Distal limit of the lateral process
7	2	Minimum curvature between the lateral process and the ulnar condyle
8	2	Minimum curvature between the medial process and the radial condyle
9	2	Maximum curvature of the ulnar condyle
10	2	Latero-distal limit of the ectepicondylar grooove
11	2	Proximal tip of the ectepicondylar grooove
12	2	Medio-distal limit of the ectepicondylar grooove
13	2	Maximum curvature of the radial condyle

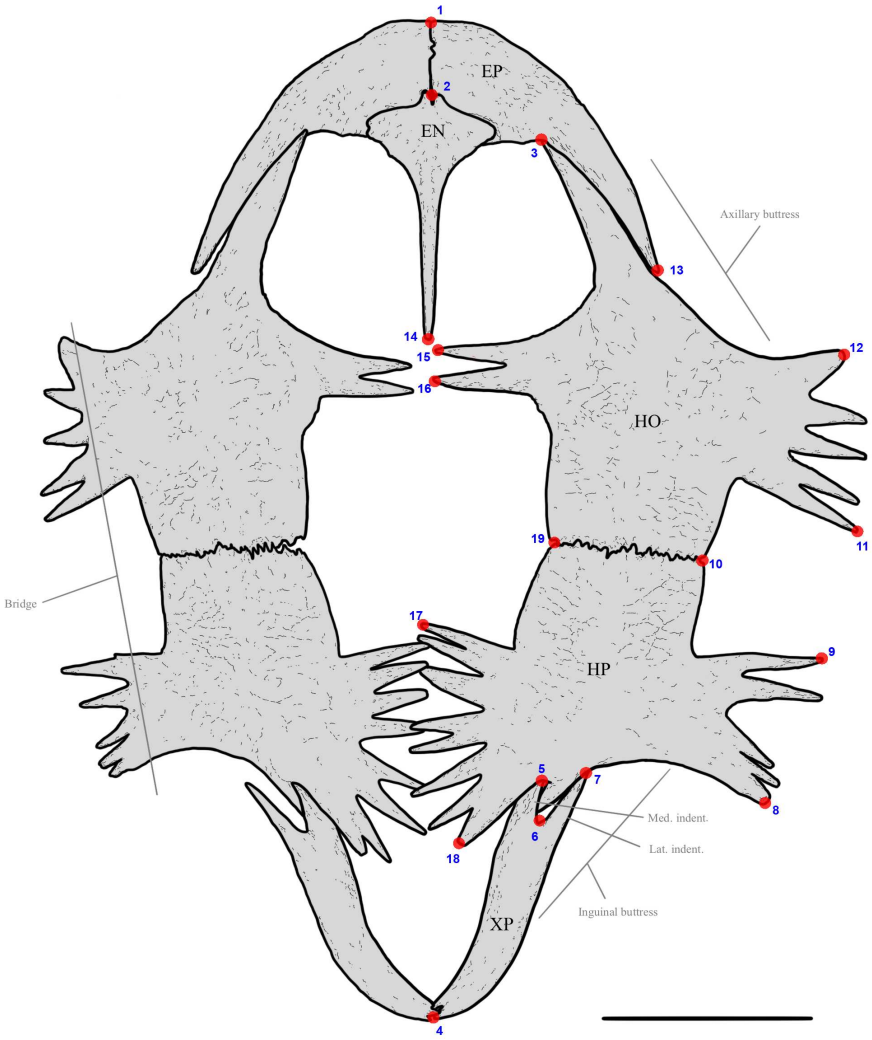

Figure 9. Cutout of the plastron from Figure 1, detailing osteological structures and anatomical reference for landmark digitisation. Scale 5 cm.

Table 9. This table contains anatomical descriptions of each landmark in Figure 9 and its classification by type, according to Bookstein, 1991: 1 – contact of 3 structures/tissues; 2 – maximum or minimal curvature of a structure; 3 – points located in boundaries, limits or edges.

PLASTRON		
Number	**Type**	**Description**
1	1	Cranial tip of midline epiplastra suture
2	1	Caudal tip of midline epiplastra suture
3	1	Caudal tip of ento/epiplastron suture
4	2	Caudal tip of xiphiplastra suture
5	2	Junction of medial xiphiplastron indentation with the hyoplastron
6	2	Most internal point between xiphiplastron medial and lateral indentations
7	2	Tip of lateral xiphiplastron indentation at the inguinal butress
8	2	Tip of the most caudal of the hypoplastron's bridge indentations
9	2	Tip of the most cranial of the hypoplastron's bridge indentations
10	1	Lateral tip of hyo/hypoplastra suture
11	2	Tip of the most caudal of the hyoplastron's bridge indentations
12	2	Tip of the most cranial of the hyoplastron's bridge indentations
13	2	Tip of eiplastron at the axillary butress
14	2	Caudal tip of entplastron along midline
15	2	Tip of the most cranial of the hyoplastron's medial indentations
16	2	Tip of the most caudal of the hyoplastron's medial indentations
17	2	Tip of the most cranial of the hypoplastron's medial indentations
18	2	Tip of the most caudal of the hypoplastron's medial indentations
19	1	Medial tip of hyo/hypoplastra suture

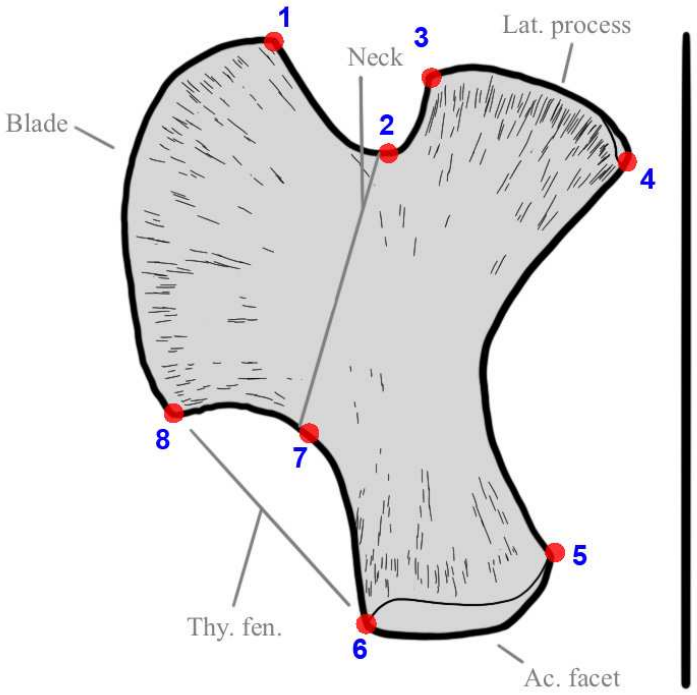

Figure 10. Cutout of the pubis from Figure 1, detailing osteological structures and anatomical reference for landmark digitisation. Scale 5 cm.

Table 10. This table contains anatomical descriptions of each landmark in Figure 10 and its classification by type, according to Bookstein, 1991: 1 – contact of 3 structures/tissues; 2 – maximum or minimal curvature of a structure; 3 – points located in boundaries, limits or edges.

PUBIS		
Number	**Type**	**Description**
1	2	Cranial tip of pubic blade at the medial end of the neck curvature
2	2	minimum curvature of the neck at the cranial side
3	2	Medial tip of the lateral process
4	2	Lateral tip of lateral process
5	2	Lateral tip of acetabular facet
6	2	Medial tip of acetabular facet
7	2	Minimum curvature of the thyroid fenestra
8	2	Tip of pubic blade at the thyroid fenestra

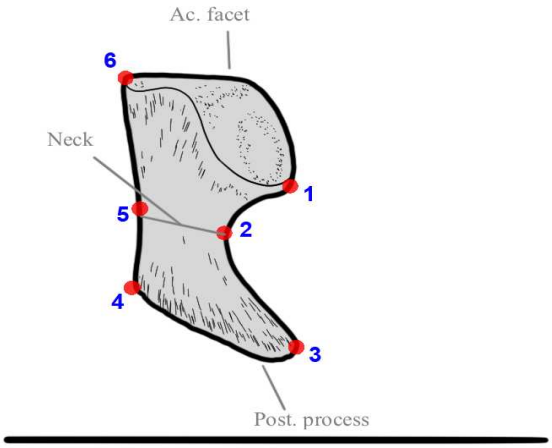

Figure 11. Cutout of the ischium from Figure 1, detailing osteological structures and anatomical reference for landmark digitisation. Scale 5 cm.

Table 11. This table contains anatomical descriptions of each landmark in Figure 11 and its classification by type, according to Bookstein, 1991: 1 – contact of 3 structures/tissues; 2 – maximum or minimal curvature of a structure; 3 – points located in boundaries, limits or edges.

ILIUM		
Number	**Type**	**Description**
1	2	Maximum curvature of the acetabular facet
2	2	Minimum curvature of iliac neck at the medial side
3	2	Maximum curvature of the tip of posterior iliac process
4	2	Medial curvature of the posterior process
5	2	Minimum curvature of iliac neck at the lateral side
6	2	Maximum curvature of the contact between ilium and pubis

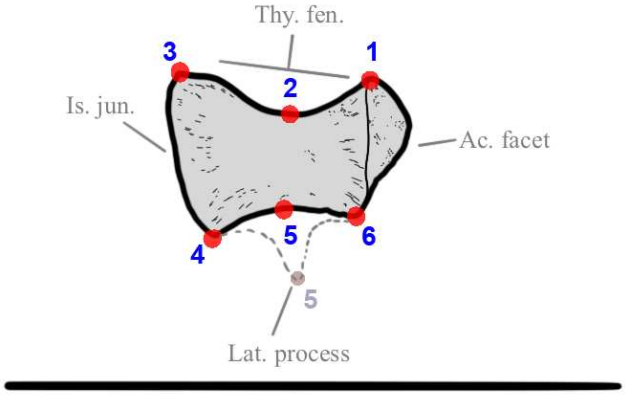

Figure 12. Cutout of the ischium from Figure 1, detailing osteological structures and anatomical reference for landmark digitisation. Scale 5 cm.

Table 12. This table contains anatomical descriptions of each landmark in Figure 12 and its classification by type, according to Bookstein, 1991: 1 – contact of 3 structures/tissues; 2 – maximum or minimal curvature of a structure; 3 – points located in boundaries, limits or edges.

ISCHIUM		
Number	**Type**	**Description**
1	2	Cranial tip of acetabular facet
2	2	Minimum curvature of ischium at the thyroid fenestra
3	2	Cranial tip the contact between left and right ischia
4	2	Caudal tip the contact between left and right ischia
5	2	Maximum curvature of the tip of lateral ischial process
6	2	Caudal tip of acetabular facet

SKULL (DORSAL VIEW)

MATRIX_Y_cd.tps

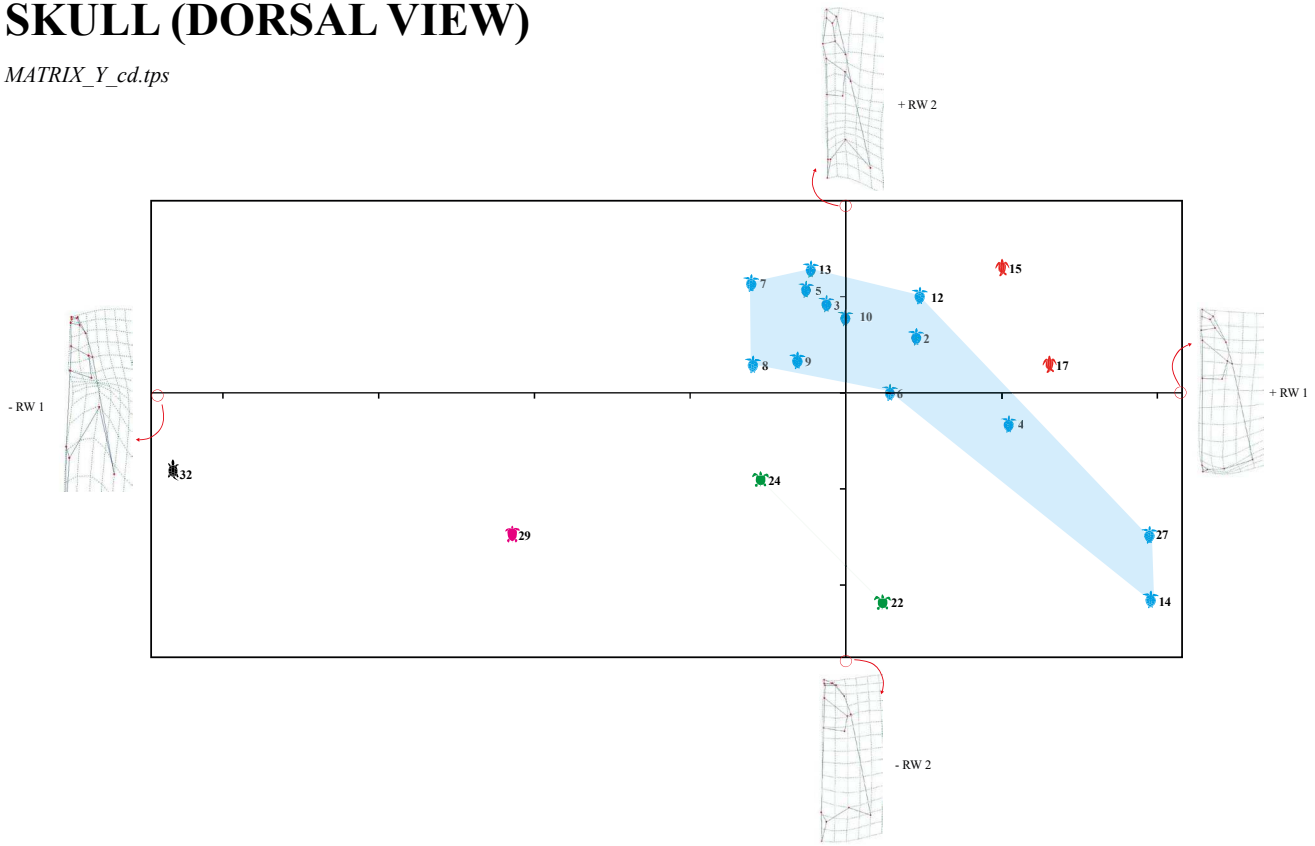

Figure 14. Relative Warps Analysis of the skull (dorsal view). The colors and icons represent the clades: green – Protostegidae; blue – Pancheloniidae; red – Dermochelyidae; black – Chelydridae; purple – Ctenochelyidae; pink – *Toxochelys latiremis.* The numbers represent the species: 2 – *Ashleychelys palmeri †,* 3 – *Caretta caretta,* 4 – *Carolinochelys wilsoni †,* 5 – *Chelonia mydas,* 6 – *Eochelone brabantica †,* 7 – *Eretmochelys imbricata,* 8 – *Lepidochelys kempii,* 9 – *Lepidochelys olivacea,* 10 – *Natator depressus,* 12 – *Procolpochelys charlestonensis †,* 13 – *Procolpochelys grandaeva †,* 14 – *Puppigerus camperi †,* 15 – *Dermochelys coriacea,* 17 – *Eosphargis gigas †,* 22 – *Desmatochelys lowii †,* 24 – *Santanachelys gaffneyi †,* 27 – *Erquelinnesia gosseleti †,* 29 – *Toxochelys latiremis †,* 32 – *Chelydra serpentina.* The polygons represent the shape range of each clade. Along the x and y axes, thin plate splines are placed indicating the shape represented by each extreme of that axis. RW_1 = 33,34% of the variance and RW_2 = 24,16%.

SKULL (LATERAL VIEW)

MATRIX_Y_cl.tps

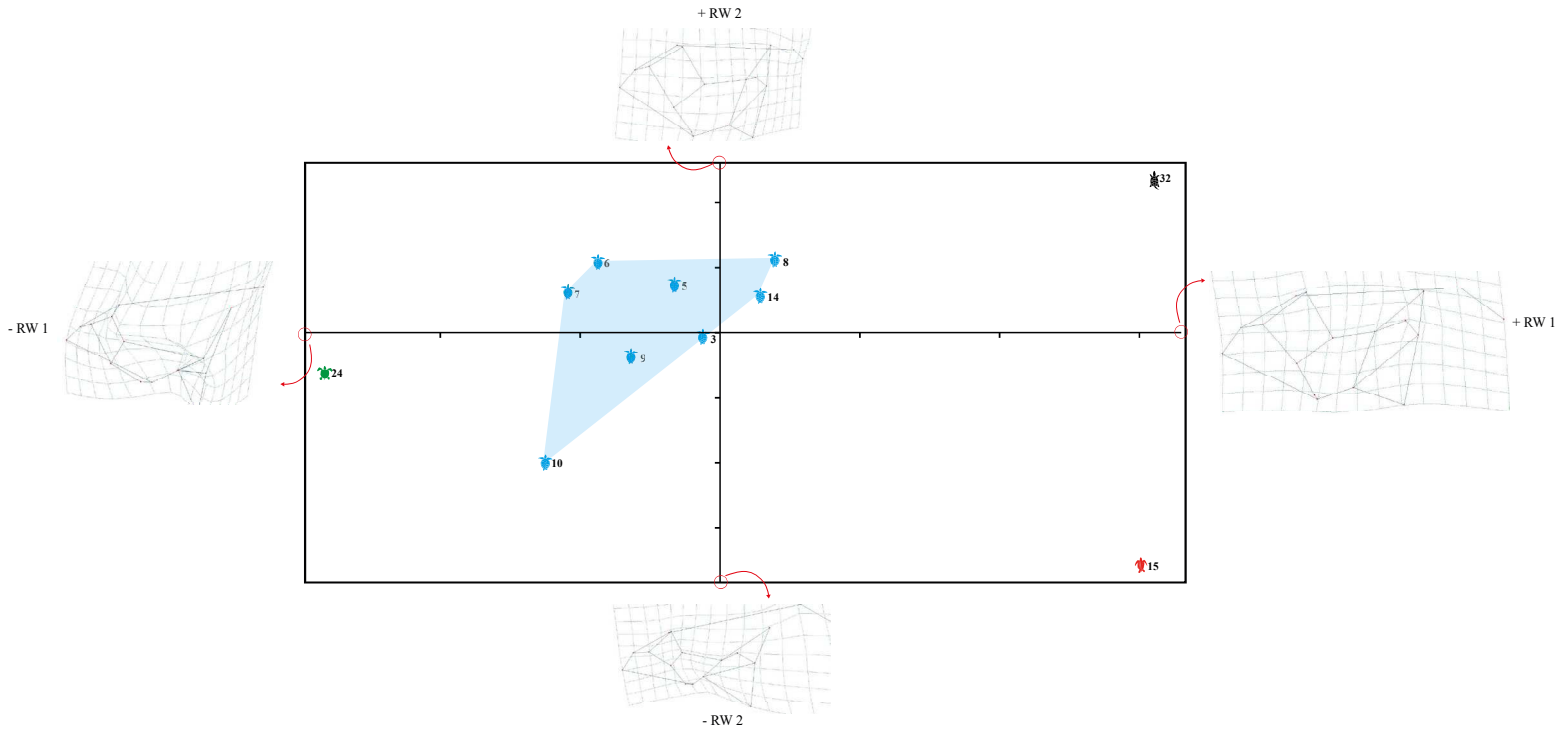

Figure 16. Relative Warps Analysis of the skull (lateral view). The colors and icons represent the clades: green – Protostegidae; blue – Pancheloniidae; red – Dermochelyidae; black – Chelydridae. The numbers represent the species: 3 – *Caretta caretta,* 5 – *Chelonia mydas,* 6 – *Eochelone brabantica †,* 7 – *Eretmochelys imbricata,* 8 – *Lepidochelys kempii,* 9 – *Lepidochelys olivacea,* 10 – *Natator depressus,* 14 – *Puppigerus camperi †,* 15 – *Dermochelys coriacea,* 24 – *Santanachelys gaffneyi †,* 32 – *Chelydra serpentina.* The polygons represent the shape range of each clade. Along the x and y axes, thin plate splines are placed indicating the shape represented by each extreme of that axis.RW_1 = 24,66% of the variance and RW_2 = 23,84%.

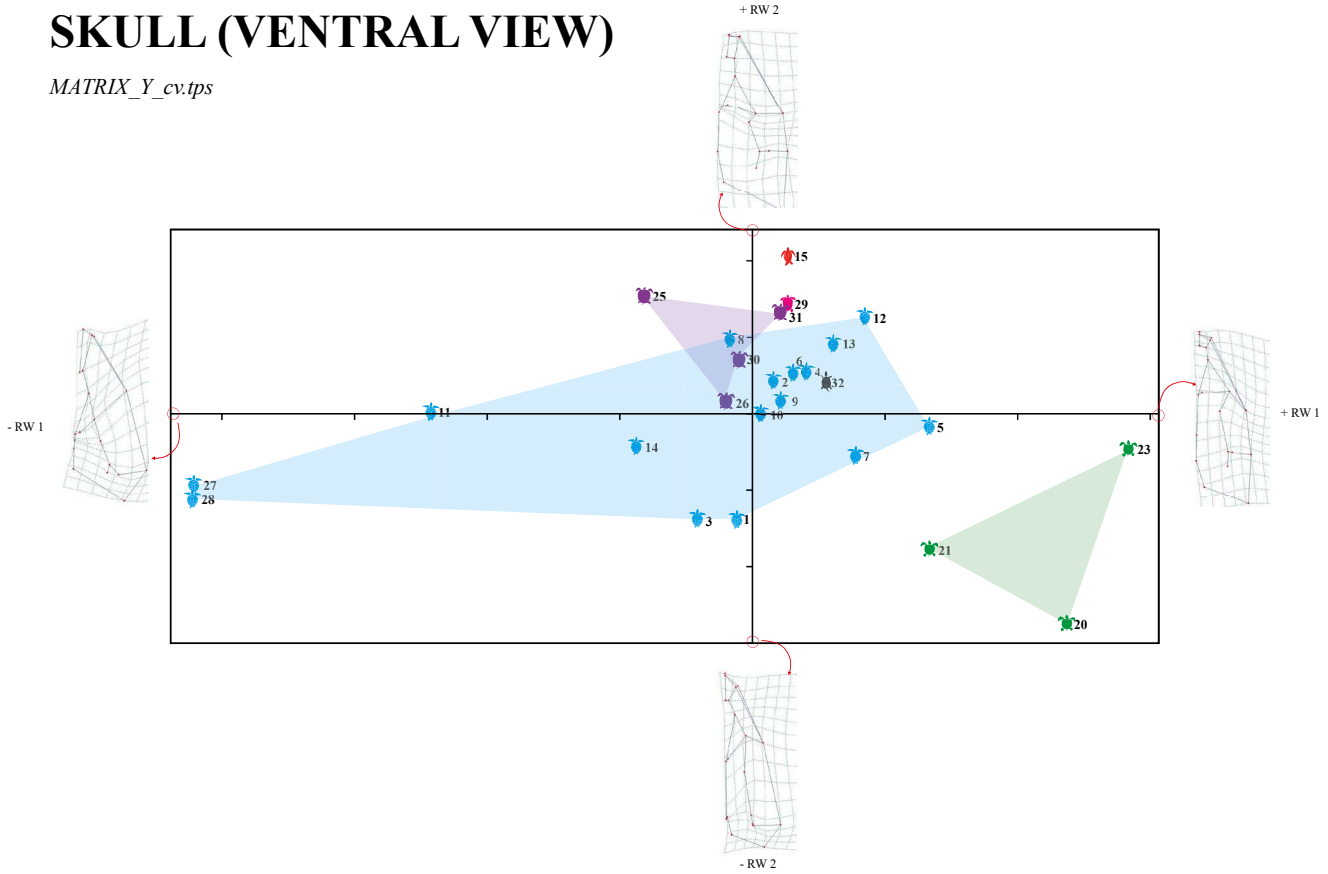

Figure 15. Relative Warps Analysis of the skull (ventral view). The colors and icons represent the clades: green – Protostegidae; blue – Pancheloniidae; red – Dermochelyidae; black – Chelydridae; purple – Ctenochelyidae; pink – *Toxochelys latiremis.* The numbers represent the species: 1 – *Allopleuron hofmanni †,* 2 – *Ashleychelys palmeri †,* 3 – *Caretta caretta,* 4 – *Carolinochelys wilsoni †,* 5 – *Chelonia mydas,* 6 – *Eochelone brabantica †,* 7 – *Eretmochelys imbricata,* 8 – *Lepidochelys kempii,* 9 – *Lepidochelys olivacea,* 10 – *Natator depressus,* 11 – *Euclastes wielandi †,* 12 – *Procolpochelys charlestonensis †,* 13 – *Procolpochelys grandaeva †,* 14 – *Puppigerus camperi †,* 15 – *Dermochelys coriacea,* 20 – *Archelon ischyros †,* 21 – *Bouliachelys suteri †,* 23 – *Protostega gigas †,* 25 – *Ctenochelys acris †,* 26 – *Ctenochelys procax †,* 27 – *Erquelinnesia gosseleti †,* 28 – *Erquelinnesia planimentum †,* 29 – *Toxochelys latiremis †,* 30 – *Prionochelys matutina †,* 31 – *Ctenochelys stenoporus †,* 32 – *Chelydra serpentina.* The polygons represent the shape range of each clade. Along the x and y axes, thin plate splines are placed indicating the shape represented by each extreme of that axis.RW_1 = 28,29% of the variance and RW_2 = 22,43%.

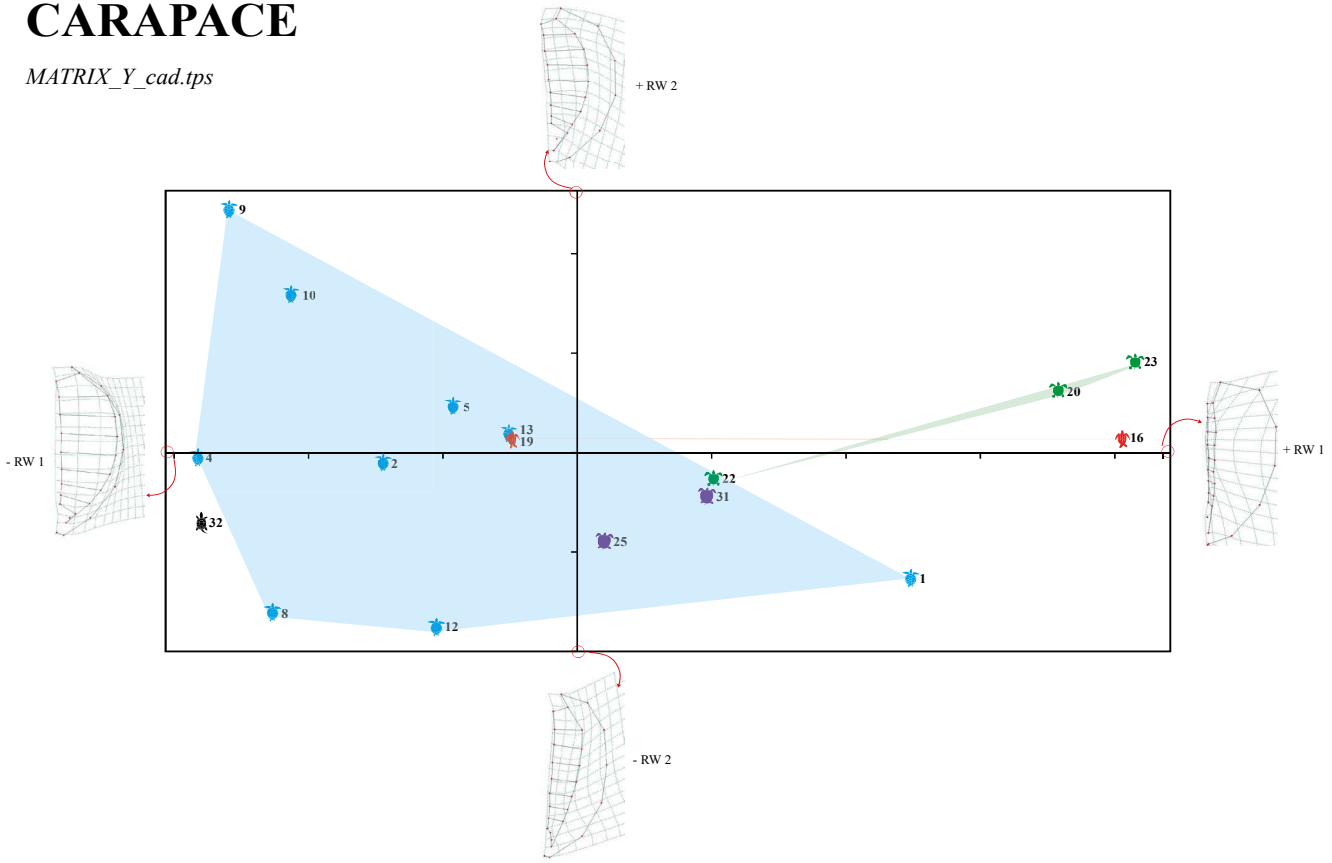

Figure 18. Relative Warps Analysis of the carapace. The colors and icons represent the clades: green – Protostegidae; blue – Pancheloniidae; red – Dermochelyidae; black – Chelydridae; purple – Ctenochelyidae. The numbers represent the species: 1 – *Allopleuron hofmanni †,* 2 – *Ashleychelys palmeri †,* 4 – *Carolinochelys wilsoni †,* 5 – *Chelonia mydas,* 8 – *Lepidochelys kempii,* 9 – *Lepidochelys olivacea,* 12 – *Procolpochelys charlestonensis †,* 13 – *Procolpochelys grandaeva †,* 16 – *Eosphargis breineri †,* 19 – *Ocepechelon bouyai †,* 20 – *Archelon ischyros †,* 22 – *Desmatochelys lowii †,* 23 – *Protostega gigas †,* 25 – *Ctenochelys acris †,* 31 – *Ctenochelys stenoporus †,* 32 – *Chelydra serpentina.* The polygons represent the shape range of each clade. Along the x and y axes, thin plate splines are placed indicating the shape represented by each extreme of that axis.RW_1 = 53,74% of the variance and RW_2 = 14,21%.

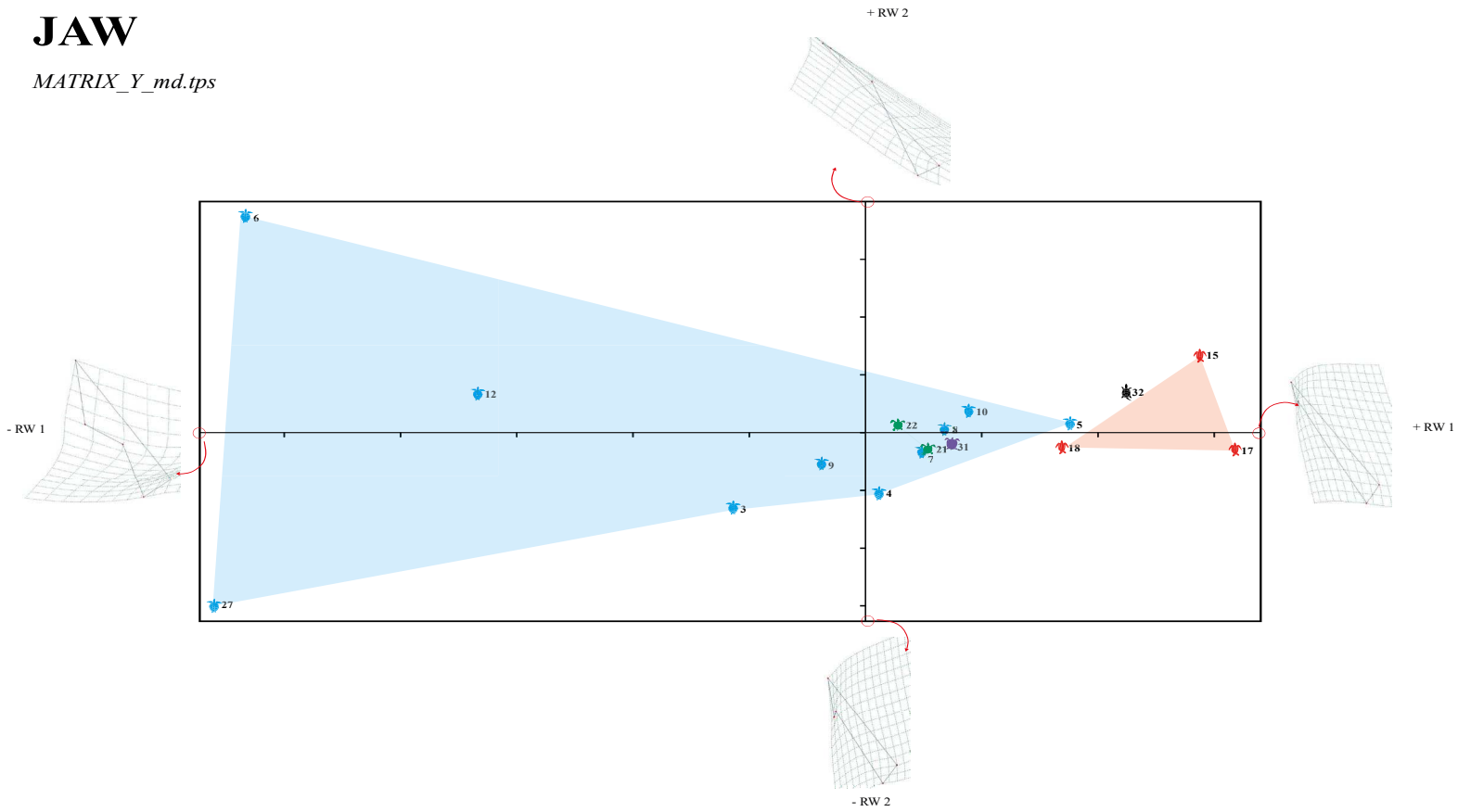

Figure 17. Relative Warps Analysis of the jaw. The colors and icons represent the clades: green – Protostegidae; blue – Pancheloniidae; red – Dermochelyidae; black – Chelydridae; purple – Ctenochelyidae. The numbers represent the species: 3 – *Caretta caretta,* 4 – *Carolinochelys wilsoni †,* 5 – *Chelonia mydas,* 6 – *Eochelone brabantica †,* 7 – *Eretmochelys imbricata,* 8 – *Lepidochelys kempii,* 9 – *Lepidochelys olivacea,* 10 – *Natator depressus,* 12 – *Procolpochelys charlestonensis †,* 15 – *Dermochelys coriacea,* 17 – *Eosphargis gigas †,* 18 – *Mesodermochelys undulatus †,* 21 – *Bouliachelys suteri †,* 22 – *Desmatochelys lowii †,* 27 – *Erquelinnesia gosseleti †,* 31 – *Ctenochelys stenoporus †,* 32 – *Chelydra serpentina.* The polygons represent the shape range of each clade. Along the x and y axes, thin plate splines are placed indicating the shape represented by each extreme of that axis.RW_1 = 66,93% of the variance and RW_2 = 18,14%.

CORACOID

MATRIX_Y_co.tps

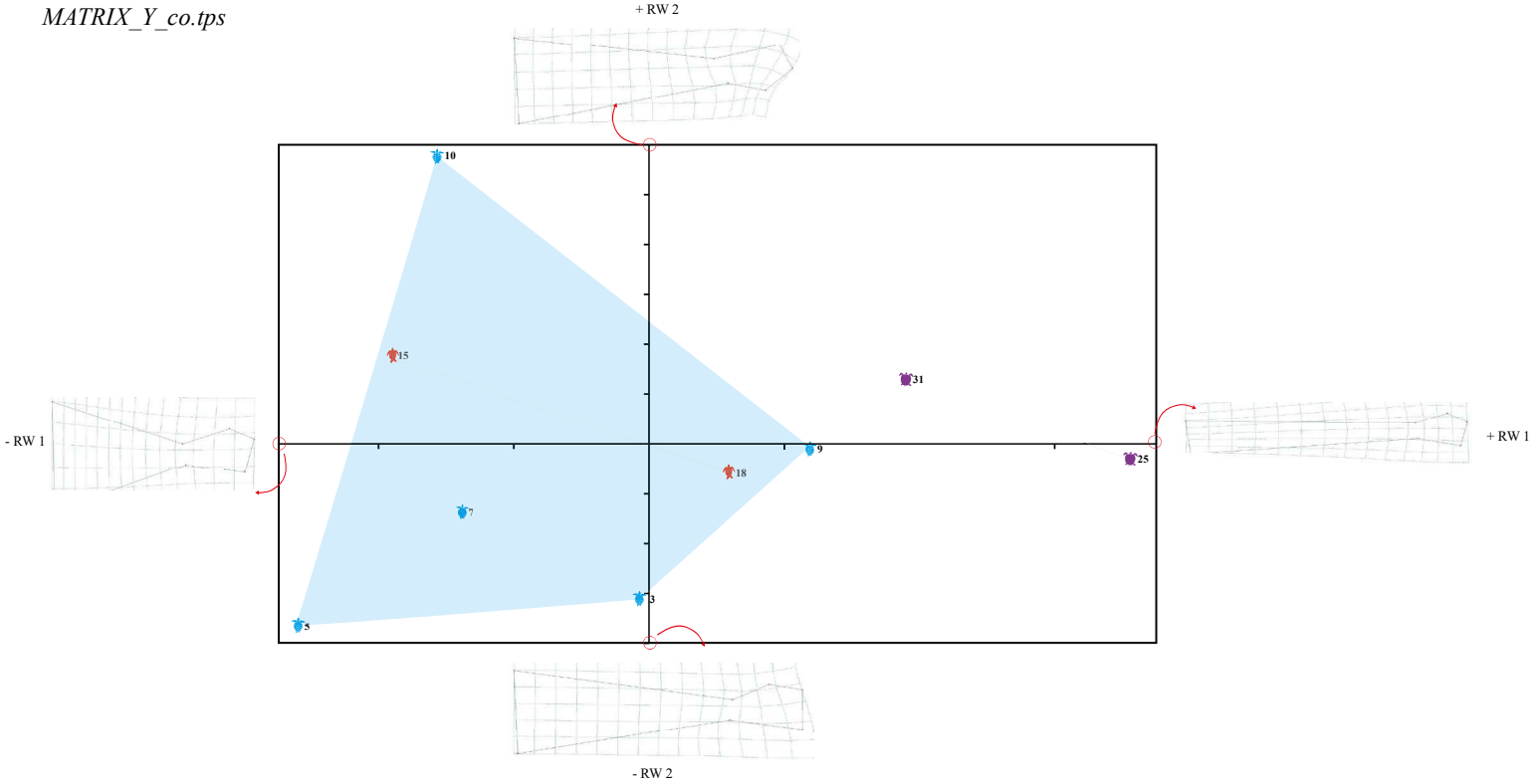

Figure 20. Relative Warps Analysis of the coracoid. The colors and icons represent the clades: blue – Pancheloniidae; red – Dermochelyidae; purple – Ctenochelyidae. The numbers represent the species: 3 – *Caretta caretta,* 5 – *Chelonia mydas,* 7 – *Eretmochelys imbricata,* 9 – *Lepidochelys olivacea,* 10 – *Natator depressus,* 15 – *Dermochelys coriacea,* 18 – *Mesodermochelys undulatus †,* 25 – *Ctenochelys acris †,* 31 – *Ctenochelys stenoporus †.* The polygons represent the shape range of each clade. Along the x and y axes, thin plate splines are placed indicating the shape represented by each extreme of that axis.RW_1 = 80,79% of the variance and RW_2 = 7,39%.

PLASTRON

MATRIX_Y_p.tps

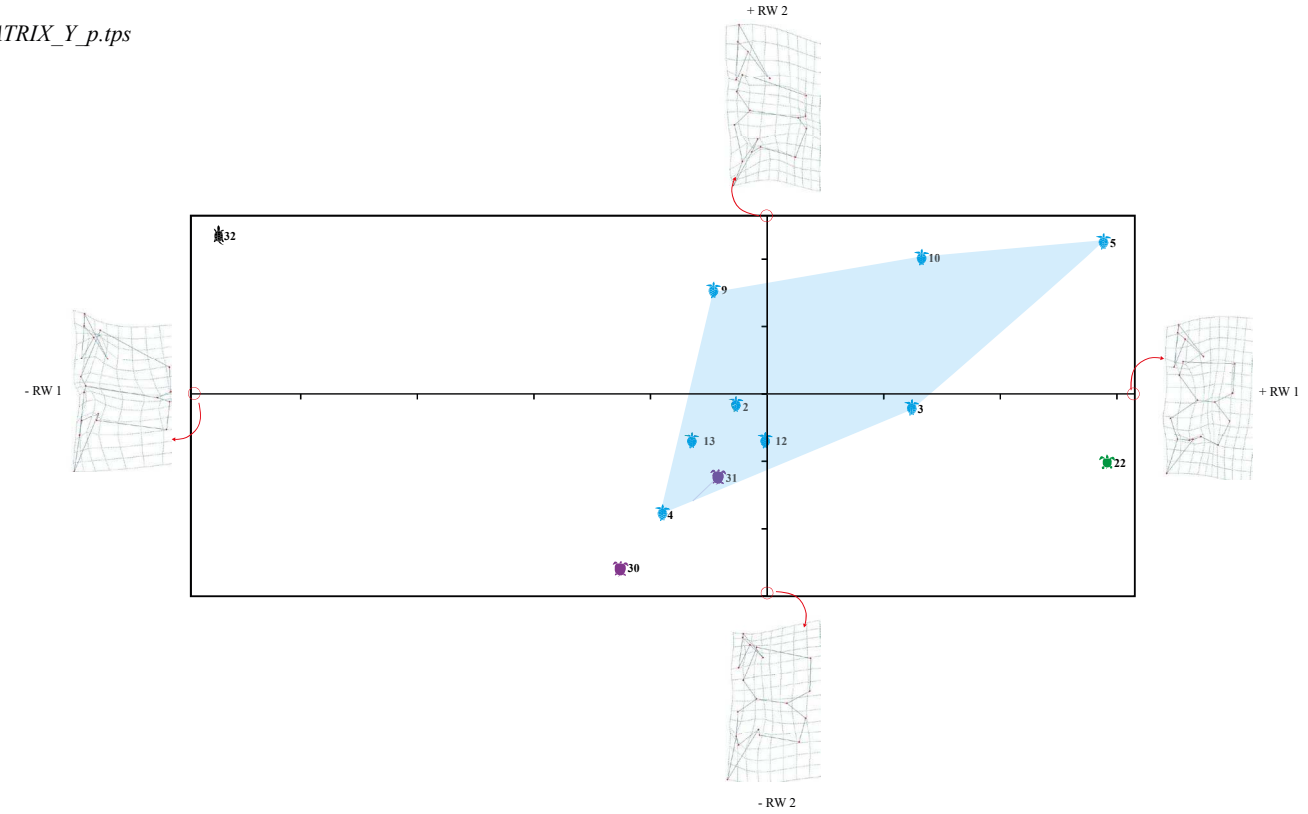

Figure 19. Relative Warps Analysis of the plastron. The colors and icons represent the clades: green – Protostegidae; from blue – Pancheloniidae; black – Chelydridae; purple – Ctenochelyidae. The numbers represent the species: 2 – *Ashleychelys palmeri †,* 3 – *Caretta caretta,* 5 – *Chelonia mydas,* 9 – *Lepidochelys olivacea,* 10 – *Natator depressus,* 12 – *Procolpochelys charlestonensis †,* 13 – *Procolpochelys grandaeva †,* 22 – *Desmatochelys lowii †,* 30 – *Prionochelys matutina †,* 31 – *Ctenochelys stenoporus †,* 32 – *Chelydra serpentina.* The polygons represent the shape range of each clade. Along the x and y axes, thin plate splines are placed indicating the shape represented by each extreme of that axis.RW_1 = 37,90% of the variance and RW_2 = 26,91%.

PUBIS

MATRIX_Y_pu.tps

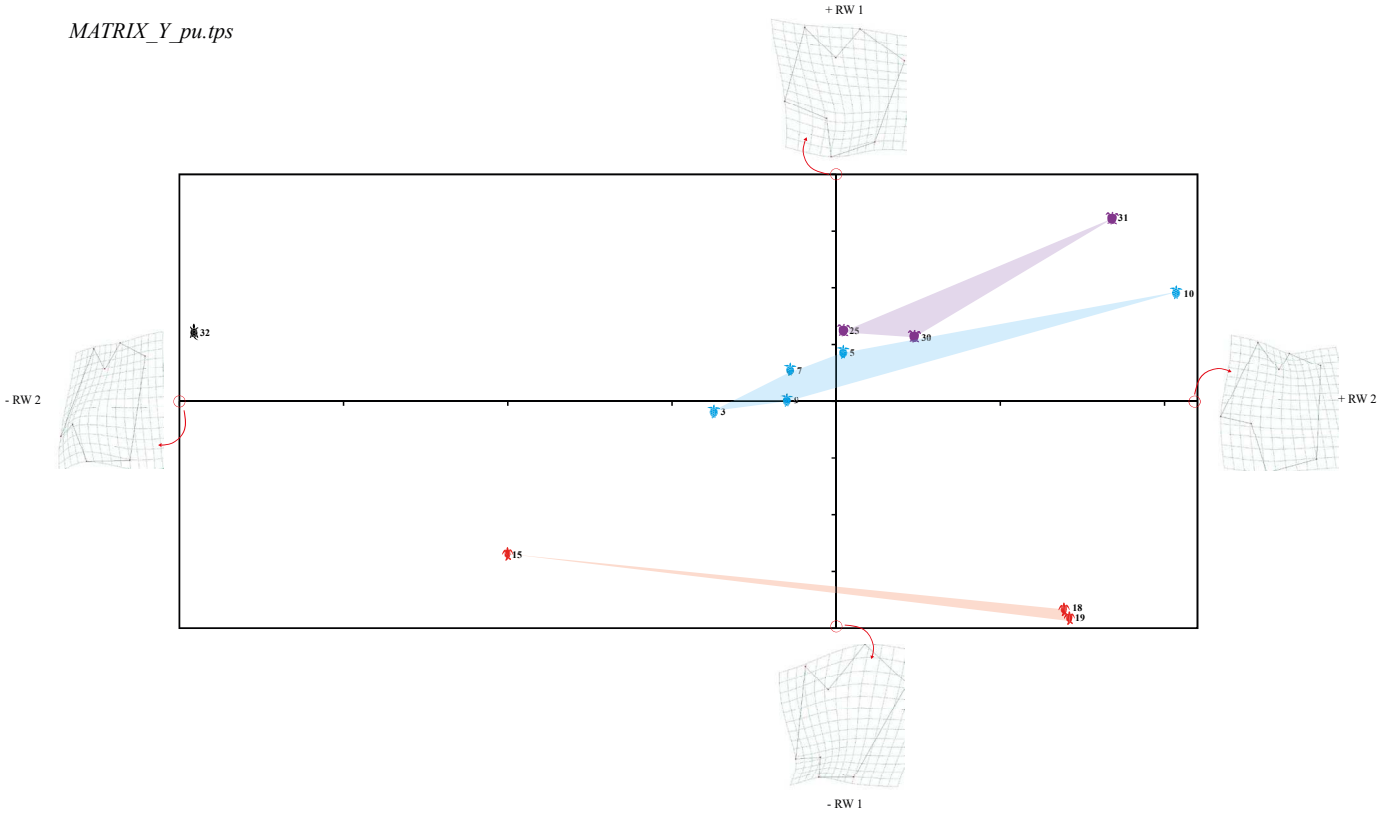

Figure 22. Relative Warps Analysis of the pubis. The colors and icons represent the clades: blue – Pancheloniidae; red – Dermochelyidae; black – Chelydridae; purple – Ctenochelyidae. The numbers represent the species: 3 – *Caretta caretta,* 5 – *Chelonia mydas,* 7 – *Eretmochelys imbricata,* 9 – *Lepidochelys olivacea,* 10 – *Natator depressus,* 15 – *Dermochelys coriacea,* 18 – *Mesodermochelys undulatus †,* 19 – *Ocepechelon bouyai †,* 25 – *Ctenochelys acris †,* 30 – *Prionochelys matutina †,* 31 – *Ctenochelys stenoporus †,* 32 – *Chelydra serpentina.* The polygons represent the shape range of each clade. Along the x and y axes, thin plate splines are placed indicating the shape represented by each extreme of that axis.RW_1 = 46,94% of the variance and RW_2 = 24,48%.

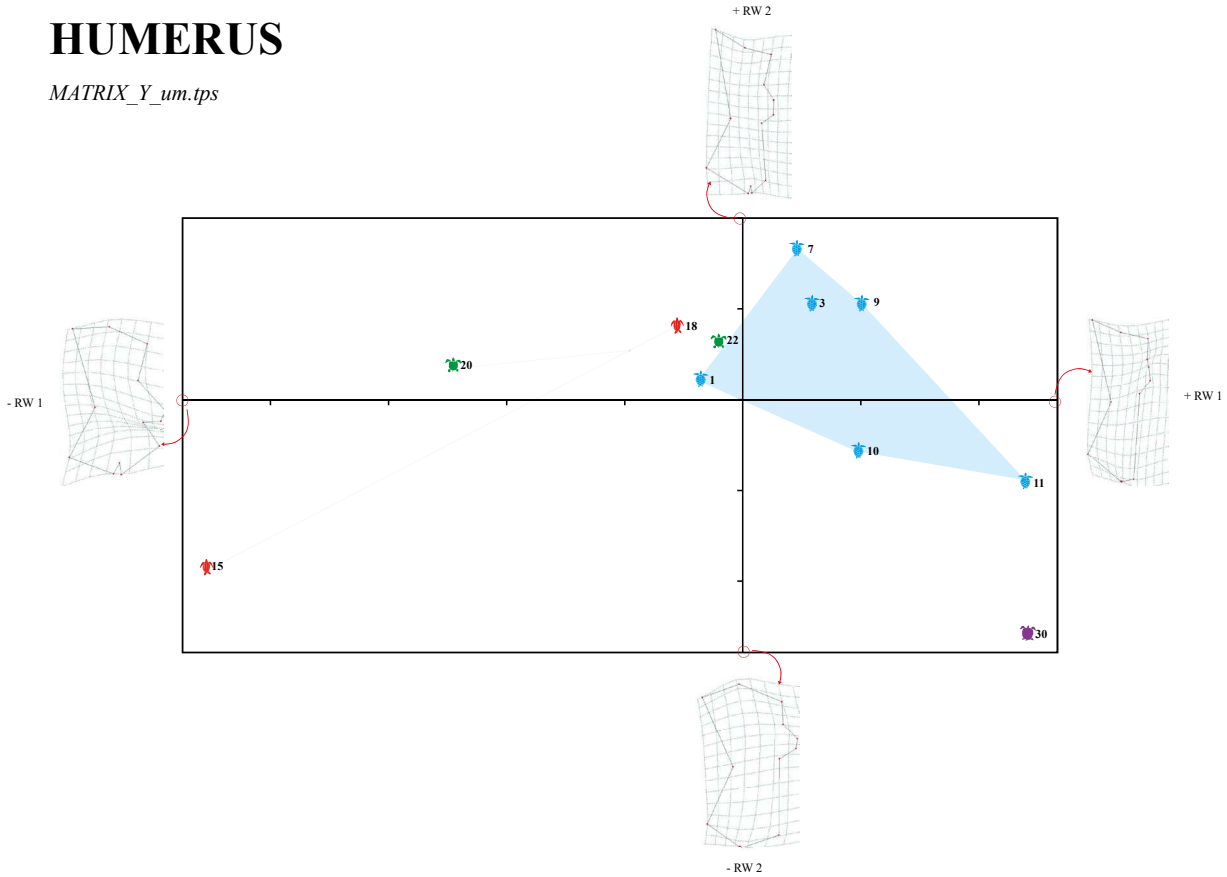

Figure 21. Relative Warps Analysis of the humerus. The colors and icons represent the clades: green – Protostegidae; blue – Pancheloniidae; red – Dermochelyidae; purple – Ctenochelyidae. The numbers represent the species: 1 – *Allopleuron hofmanni †,* 3 – *Caretta caretta,* 7 – *Eretmochelys imbricata,* 9 – *Lepidochelys olivacea,* 10 – *Natator depressus,* 11 – *Euclastes wielandi †,* 15 – *Dermochelys coriacea,* 18 – *Mesodermochelys undulatus †,* 20 – *Archelon ischyros †,* 22 – *Desmatochelys lowii †,* 30 – *Prionochelys matutina †.* The polygons represent the shape range of each clade. Along the x and y axes, thin plate splines are placed indicating the shape represented by each extreme of that axis.RW_1 = 58,37% of the variance and RW_2 = 14,17%.

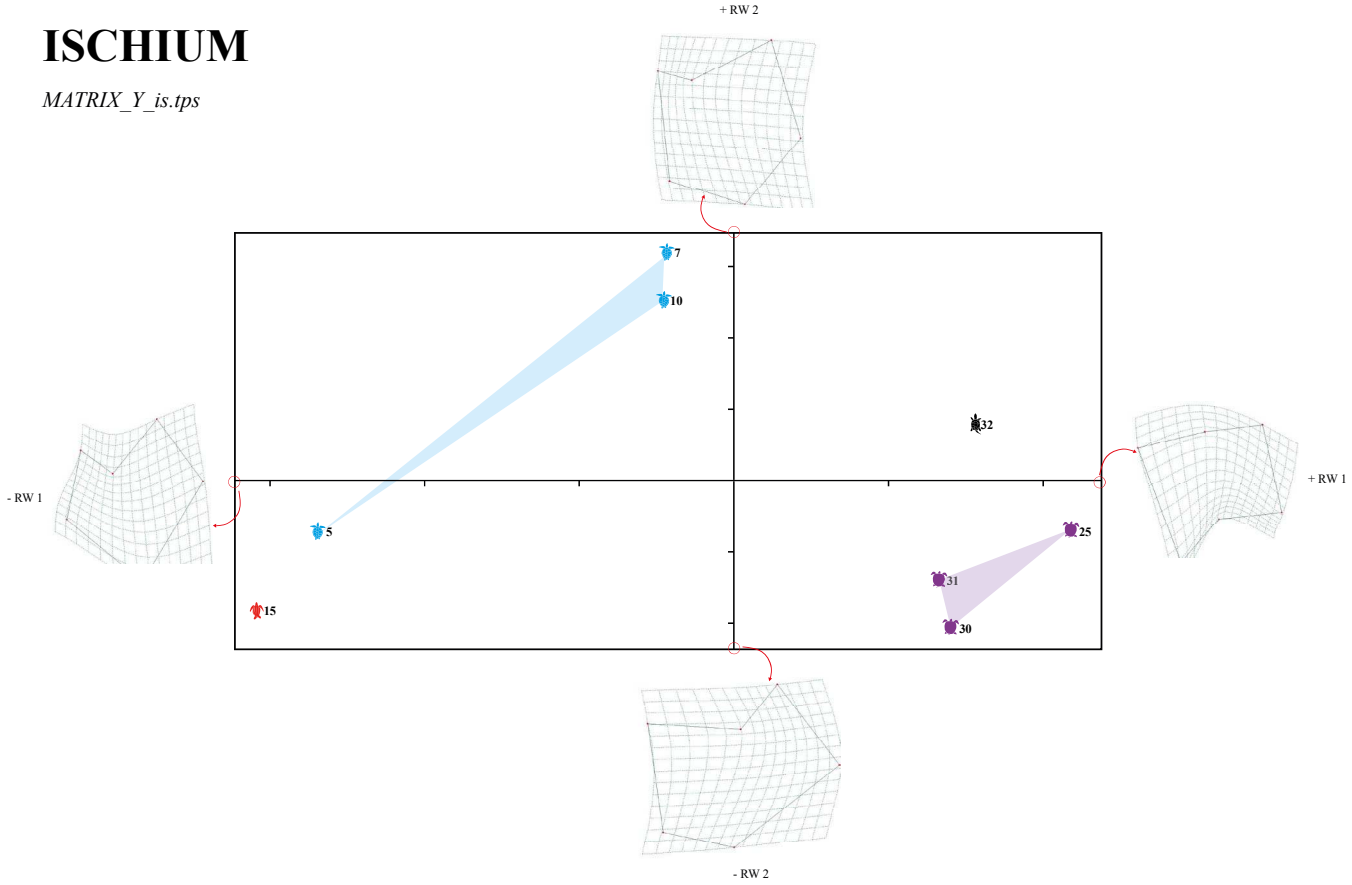

Figure 24. Relative Warps Analysis of the ischium. The colors and icons represent the clades: blue – Pancheloniidae; red – Dermochelyidae; black – Chelydridae; purple – Ctenochelyidae. The numbers represent the species: 5 – *Chelonia mydas,* 7 – *Eretmochelys imbricata,* 10 – *Natator depressus,* 15 – *Dermochelys coriacea,* 25 – *Ctenochelys acris †,* 30 – *Prionochelys matutina †,* 31 – *Ctenochelys stenoporus †,* 32 – *Chelydra serpentina.* The polygons represent the shape range of each clade. Along the x and y axes, thin plate splines are placed indicating the shape represented by each extreme of that axis.RW_1 = 69,28% of the variance and RW_2 = 10,45%.

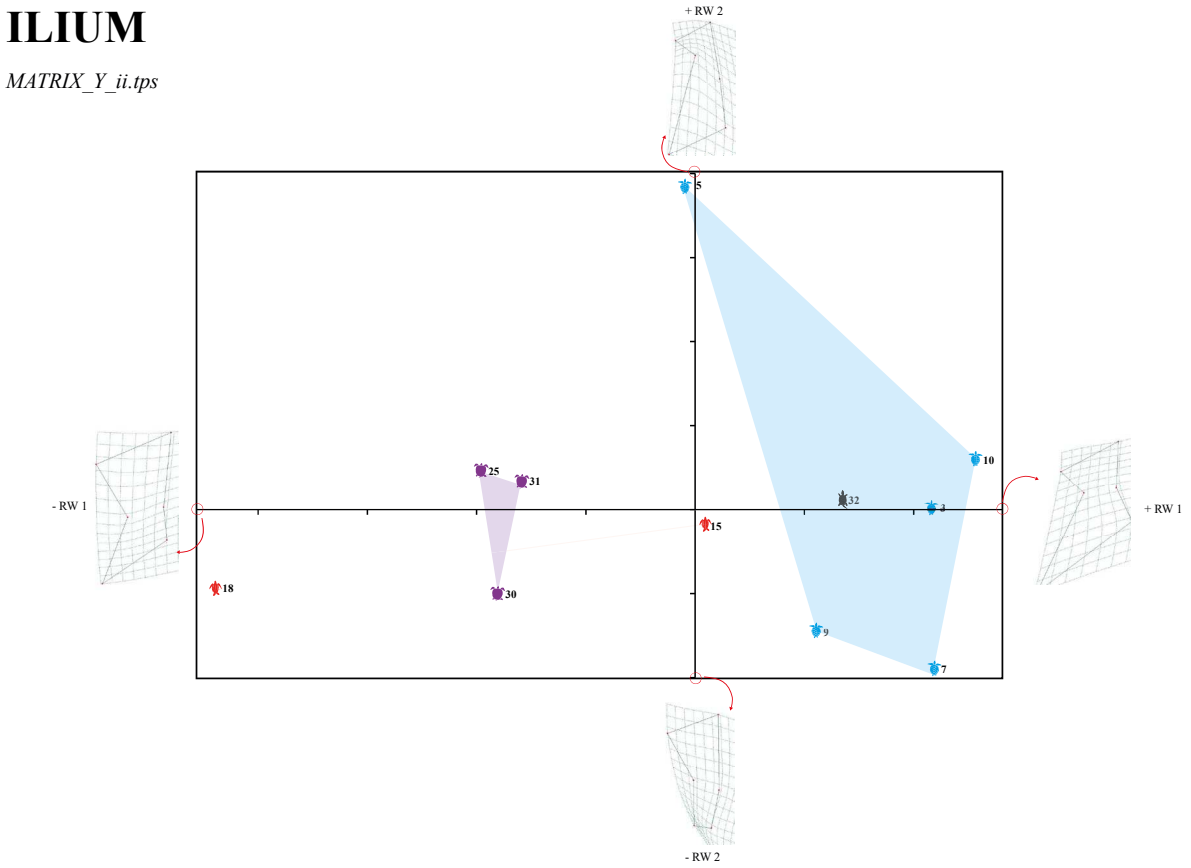

Figure 23. Relative Warps Analysis of the ilium. The colors and icons represent the clades: blue – Pancheloniidae; red – Dermochelyidae; black – Chelydridae; purple – Ctenochelyidae. The numbers represent the species: 3 – *Caretta caretta,* 5 – *Chelonia mydas,* 7 – *Eretmochelys imbricata,* 9 – *Lepidochelys olivacea,* 10 – *Natator depressus,* 15 – *Dermochelys coriacea,* 18 – *Mesodermochelys undulatus †,* 25 – *Ctenochelys acris †,* 30 – *Prionochelys matutina †,* 31 – *Ctenochelys stenoporus †,* 32 – *Chelydra serpentina.* The polygons represent the shape range of each clade. Along the x and y axes, thin plate splines are placed indicating the shape represented by each extreme of that axis.RW_1 = 58,70% of the variance and RW_2 = 23,70%.

APPENDIX C. Cladograms of the preliminary analises

CARAPACE (DORSAL VIEW)

analysys par13 CAD NT

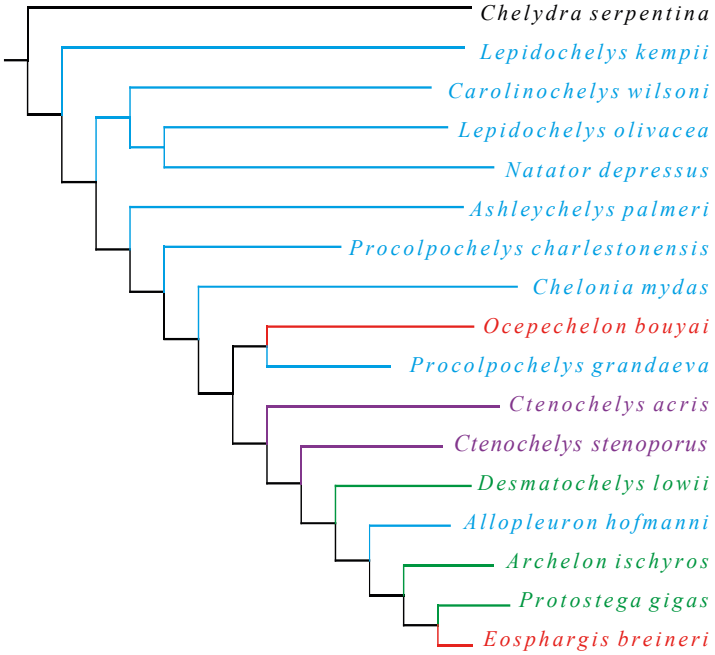

SKULL (DORSAL VIEW)

analysys par15 CD NT

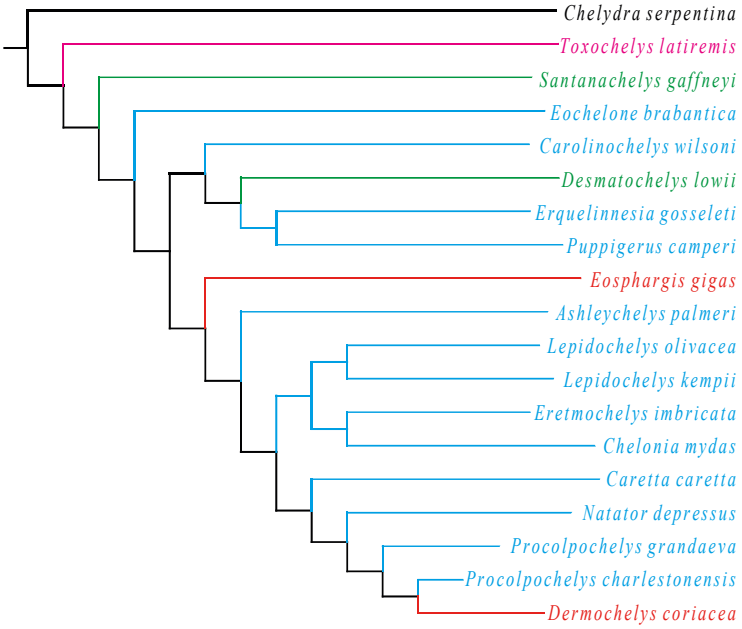

Figure 25. Cladograms of the most parsimonious trees of the carapace and skull (dorsal view) preliminary analyses. Legend: green – Protostegidae; blue – Pancheloniidae; red – Dermochelyidae; black – Chelydridae; purple – Ctenochelyidae; pink – *Toxochelys latiremis*.

SKULL (VENTRAL VIEW)

analysys par021 CV NT

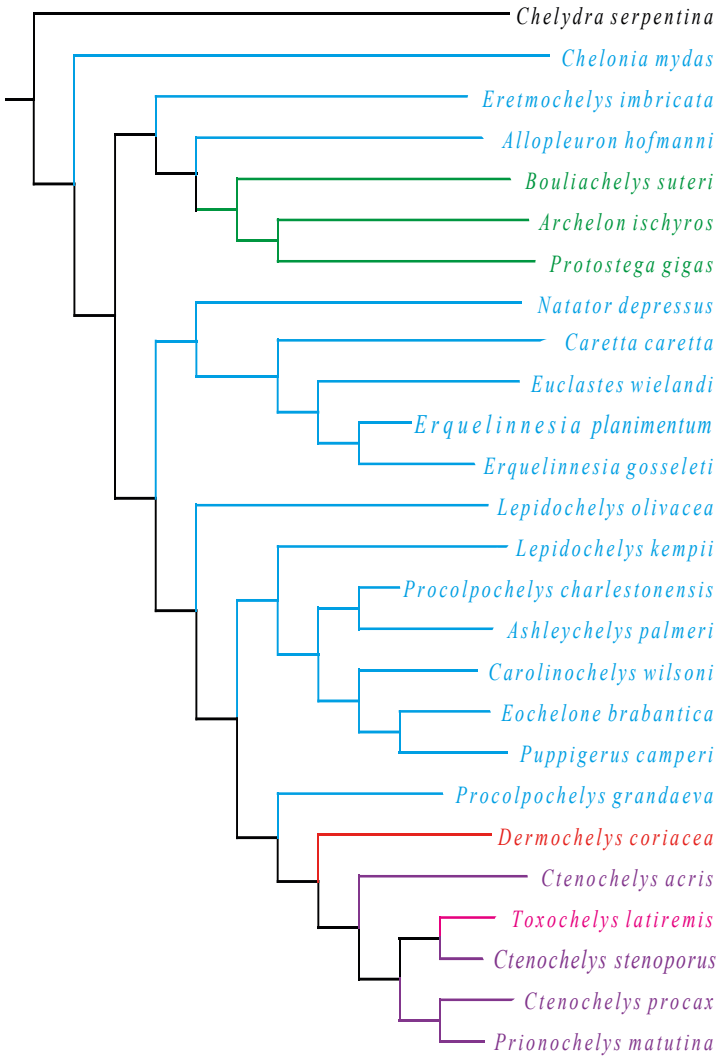

Figure 26. Cladogram of the most parsimonious tree of the skull (ventral view) preliminary analysis. Legend: green – Protostegidae; blue – Pancheloniidae; red – Dermochelyidae; black – Chelydridae; purple – Ctenochelyidae; pink – *Toxochelys latiremis*.

SKULL (LATERAL VIEW)

analysys par17 CL NT

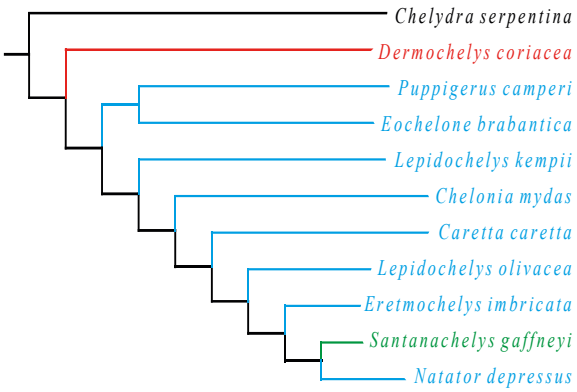

CORACOID

analysys par19 CO NT

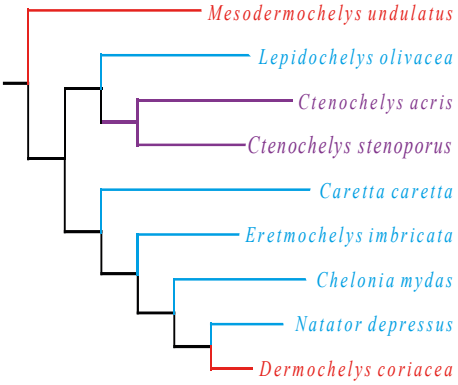

ILIUM

analysys par023 II NT

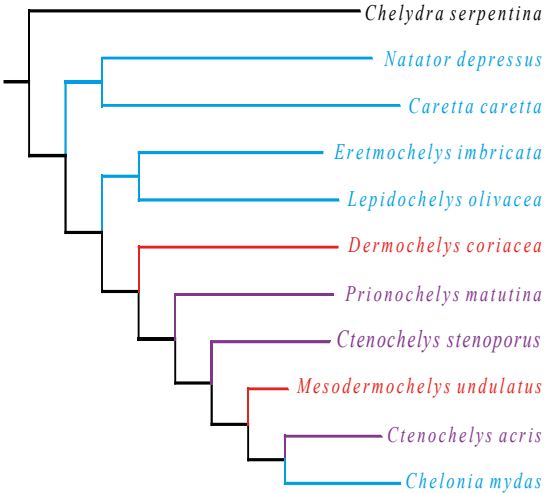

Figure 27. Cladograms of the most parsimonious trees of the skull (lateral view), coracoid and ilium preliminary analyses. Legend: green – Protostegidae; blue – Pancheloniidae; red – Dermochelyidae; black – Chelydridae; purple – Ctenochelyidae.

ISCHIUM

analysys par025 IS NT

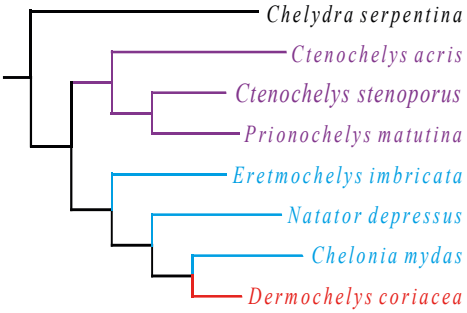

JAW

analysys par27 MD NT

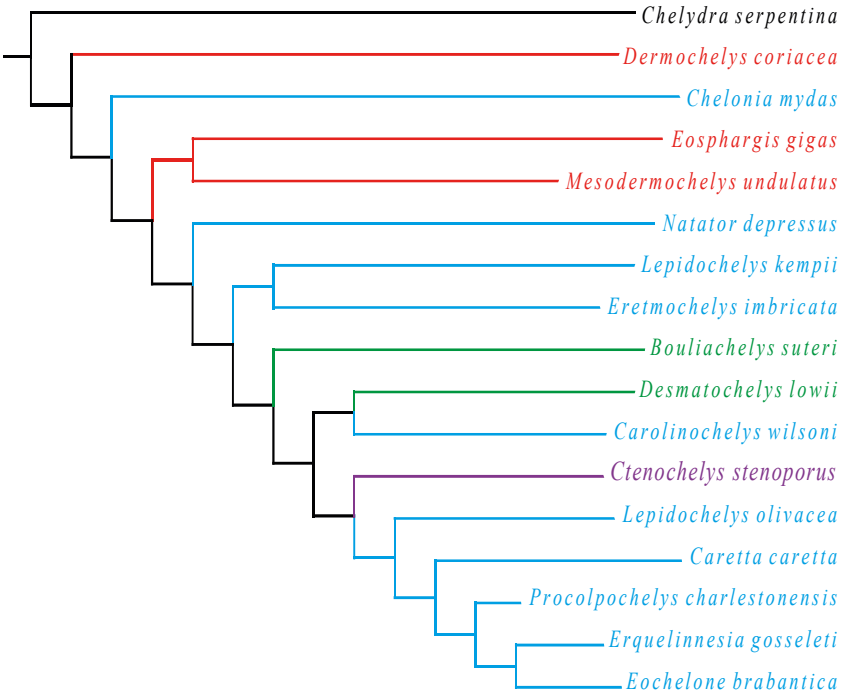

Figure 28. Cladograms of the most parsimonious trees of the ischium and jaw preliminary analyses. Legend: green – Protostegidae; blue – Pancheloniidae; red – Dermochelyidae; black – Chelydridae; purple – Ctenochelyidae.

PLASTRON

analysys par29 P NT

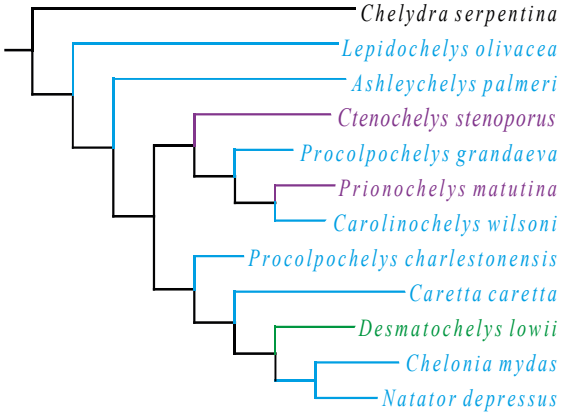

PUBIS

analysys par31 PU NT

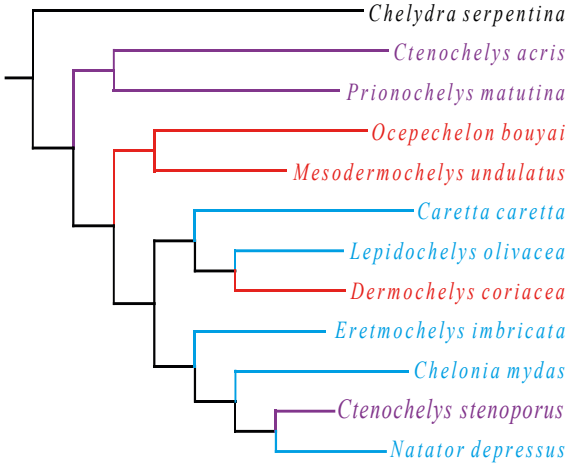

HUMERUS

analysys par33 UM NT

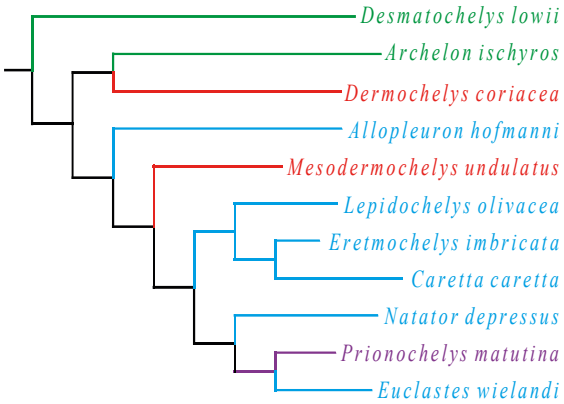

Figure 29. Cladograms of the most parsimonious trees of the plastron, pubis and humerus preliminary analyses. Legend: green – Protostegidae; blue – Pancheloniidae; red – Dermochelyidae; black – Chelydridae; purple – Ctenochelyidae.

HEAD (CD+CV+CL+MD)

analysys par35 HE NT

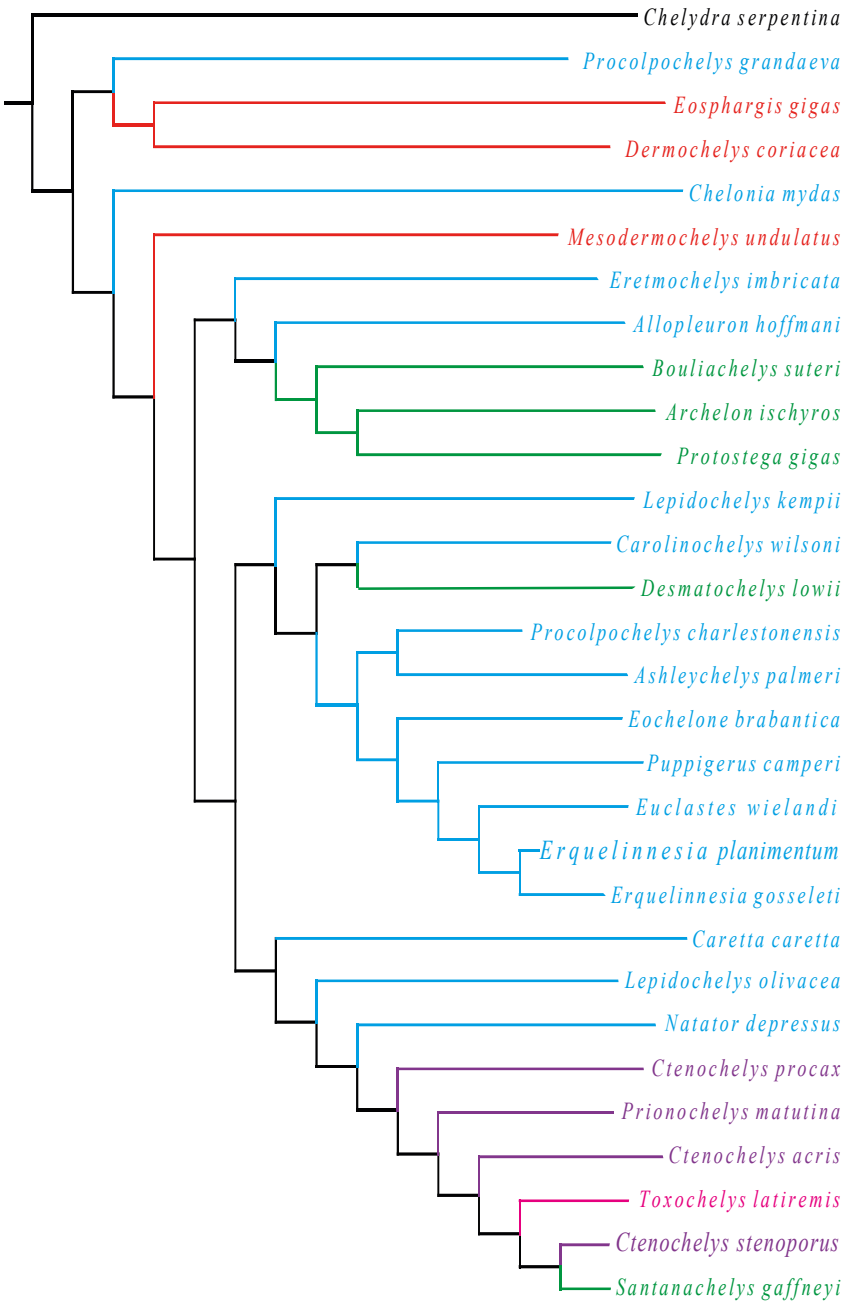

Figure 30. Cladogram of the most parsimonious trees of the "head" = skull (all views) + jaw preliminary analysis. Legend: green – Protostegidae; blue – Pancheloniidae; red – Dermochelyidae; black – Chelydridae; purple – Ctenochelyidae; pink – *Toxochelys latiremis*.

SHELL (CAD+P)

analysys par37 SH NT

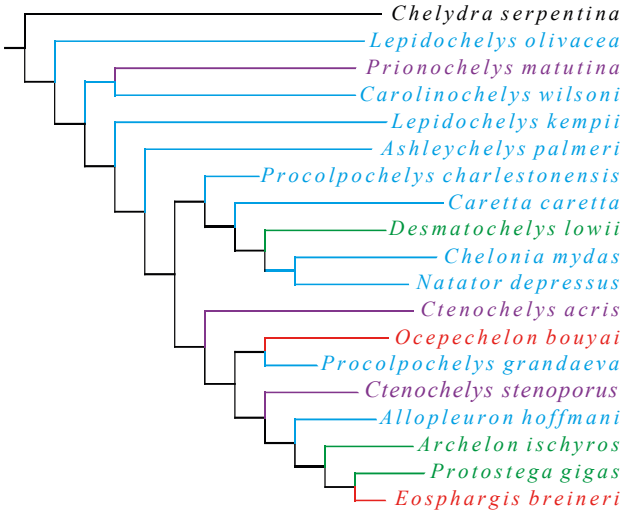

PELVIC GIRDLE (II+IS+PU)

analysys par39 PEG NT

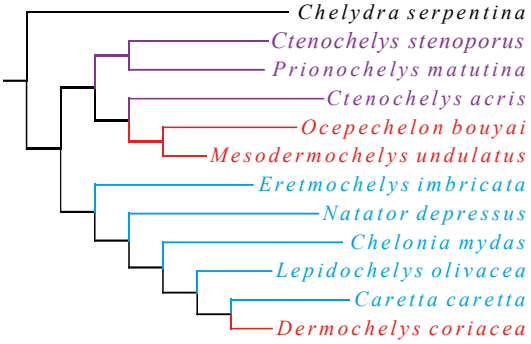

PECTORAL GIRDLE (CO+HU)

analysys par041 PCG NT

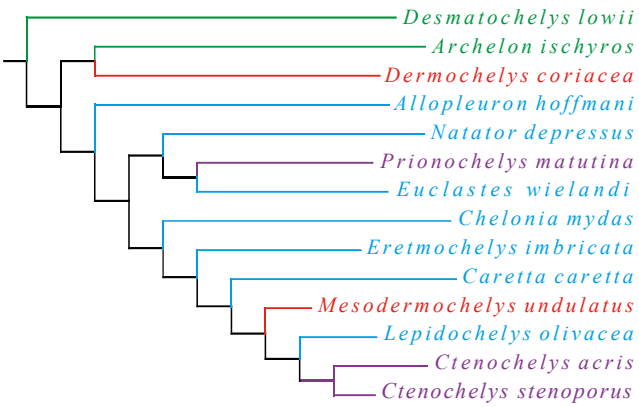

Figure 31. Cladograms of the most parsimonious trees of the shell = carapace + plastron, pelvic girdle = ilium + ischium + pubis, and pectoral girdle = coracoid + humerus preliminary analyses. Legend: green – Protostegidae; blue – Pancheloniidae; red – Dermochelyidae; black – Chelydridae; purple – Ctenochelyidae.

APPENDICES (PEG+PEC)

analysys par043 AP NT

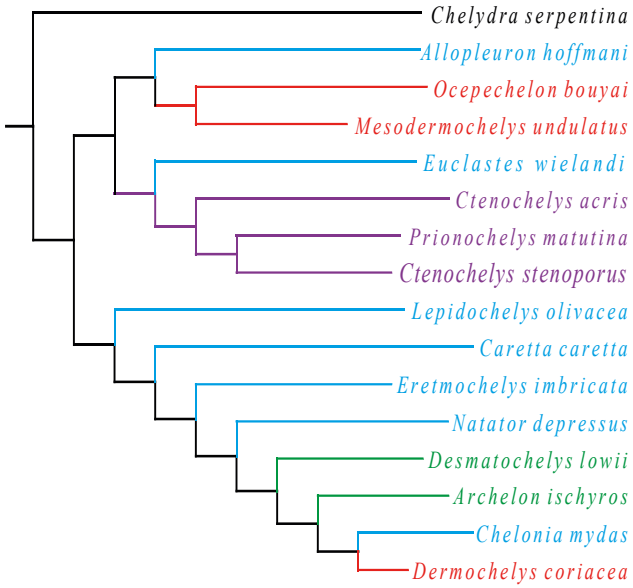

POST-CRANIUM (SH+AP)

analysys par045 PC NT

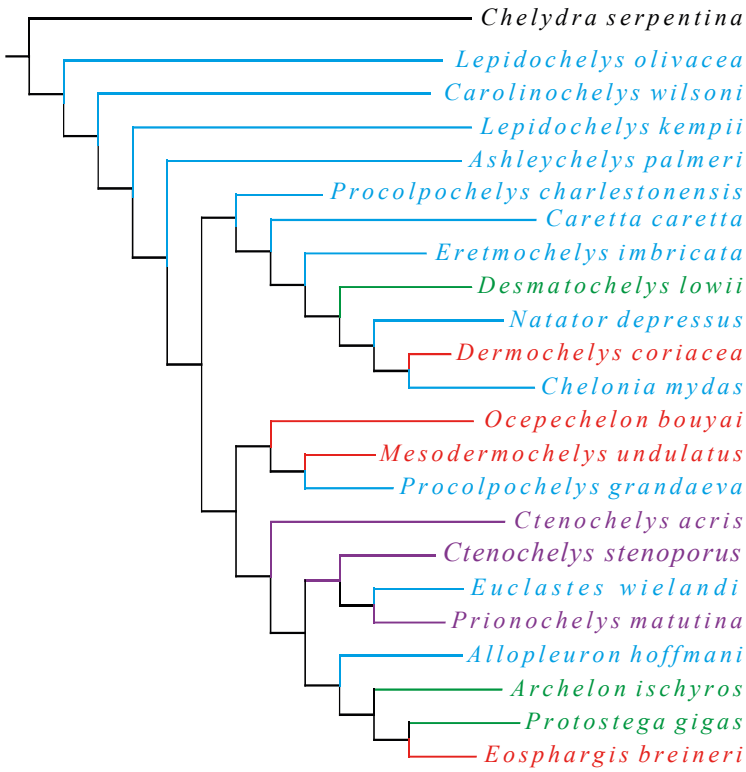

Figure 32. Cladograms of the most parsimonious trees of the appendices = pelvic + pectoral girdles, and post-cranium = shell + appendices preliminary analyses. Legend: green – Protostegidae; blue – Panchelo-niidae; red – Dermochelyidae; black – Chelydridae; purple – Ctenochelyidae.

TURTLE (HE+PC)

analysys par047 TU NT

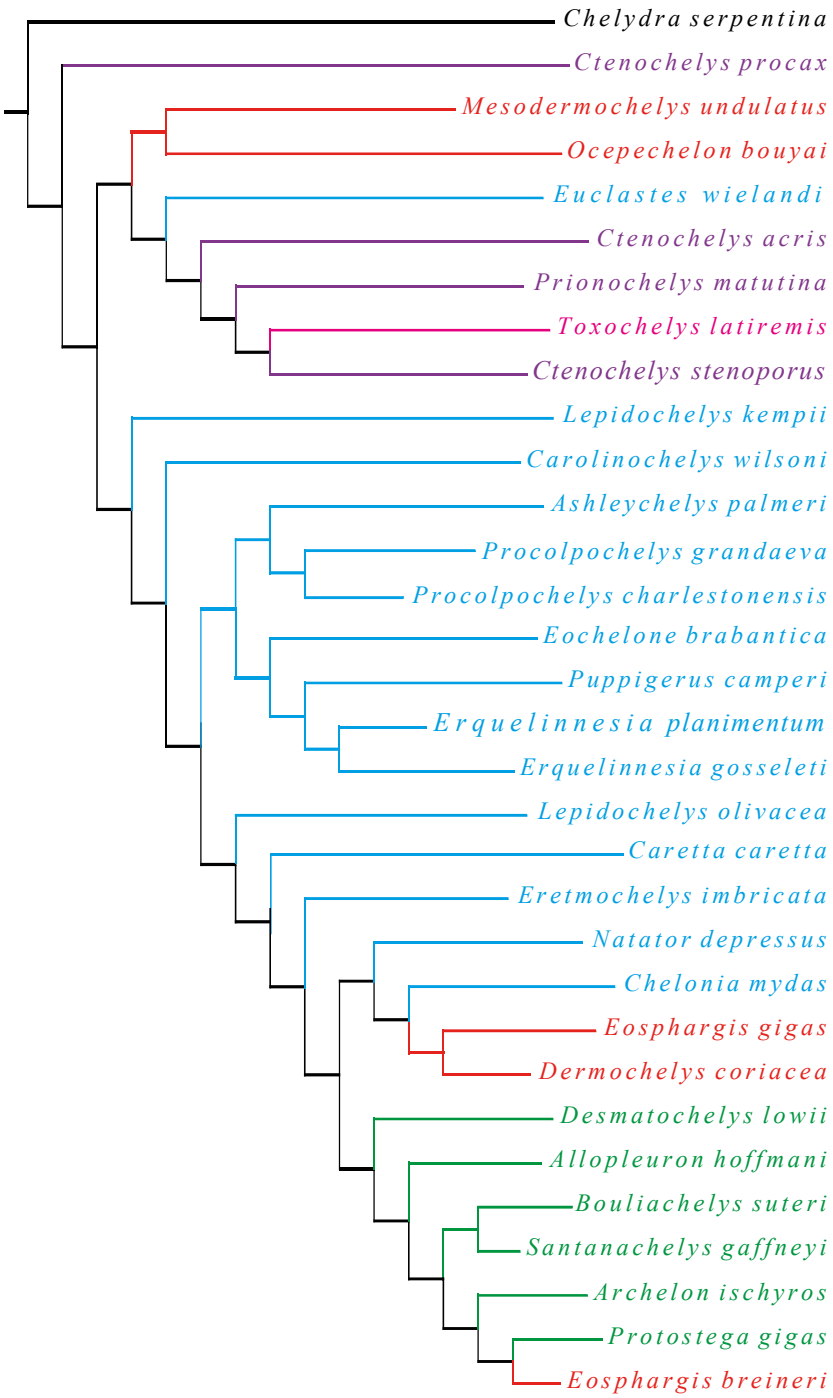

Figure 33. Cladogram of the most parsimonious trees of the "turtle" = all LM configurations preliminary analysis. Legend: green – Protostegidae; blue – Pancheloniidae; red – Dermochelyidae; black – Chelydridae; purple – Ctenochelyidae; pink – *Toxochelys latiremis*.

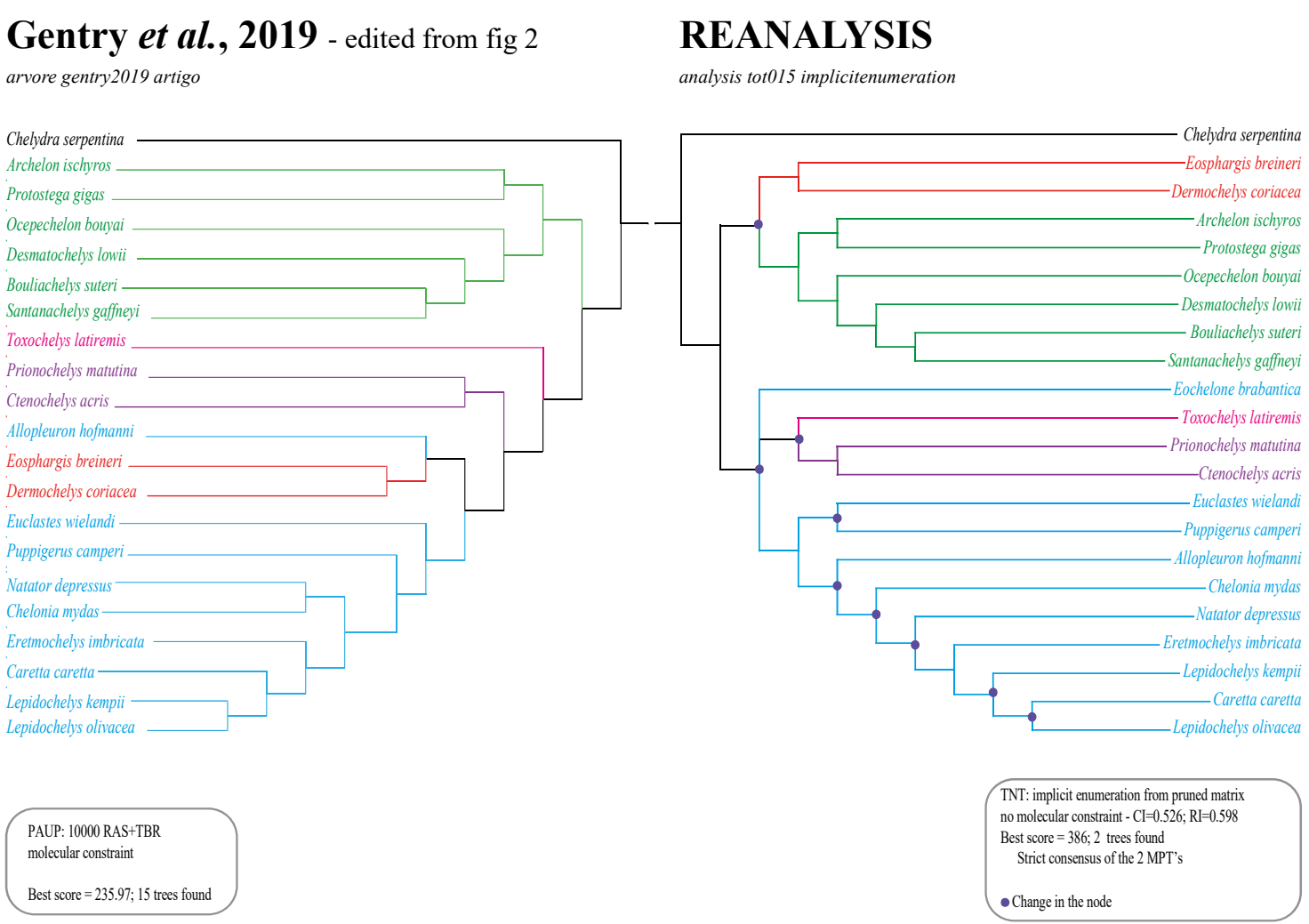

Figure 34. Strict consensus of the 2 most parsimonious trees of the reanalysis of Gentry *et al.,* 2019 pruned matrix. The purple dots point changes in the nodes in contrast to the original tree. Legend: green – Protostegidae; blue – Pancheloniidae; red – Dermochelyidae; black – Chelydridae; purple – Ctenochelyidae; pink – *Toxochelys latiremis.*

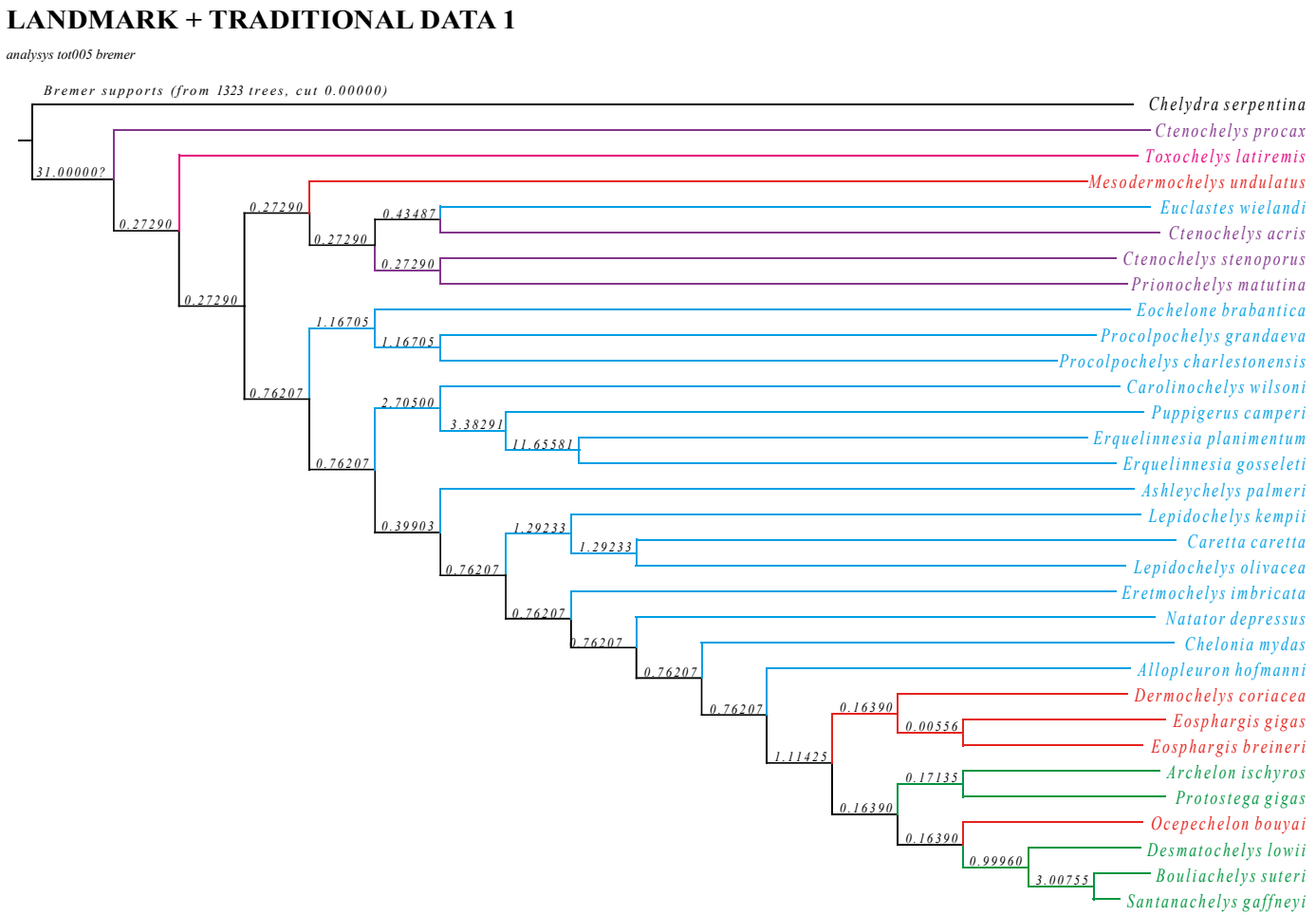

Figure 35. Cladogram of the most parsimonious tree of the first global preliminary analysis. Legend: green – Protostegidae; blue – Pancheloniidae; red – Dermochelyidae; black – Chelydridae; purple – Ctenochelyidae; pink – *Toxochelys latiremis*.

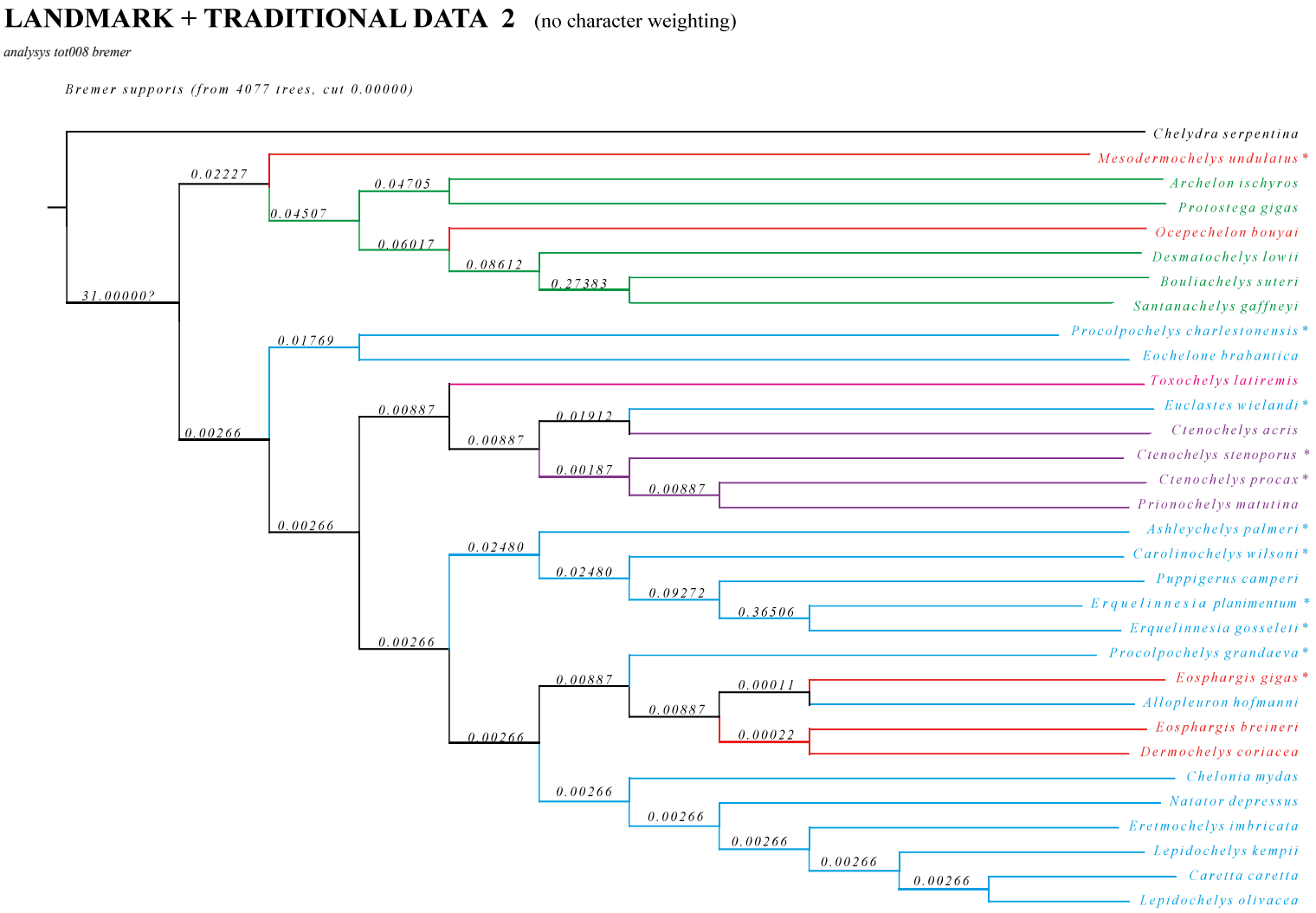

Figure 36. Cladogram of the most parsimonious tree of the second global preliminary analysis. Legend: green – Protostegidae; blue – Pancheloniidae; red – Dermochelyidae; black – Chelydridae; purple – Ctenochelyidae; pink – *Toxochelys latiremis*. Species with only LM data are marked with an asterisk.

LANDMARK + TRADITIONAL DATA 3 (without palatal view of the skull)

analysys tot011 bremer

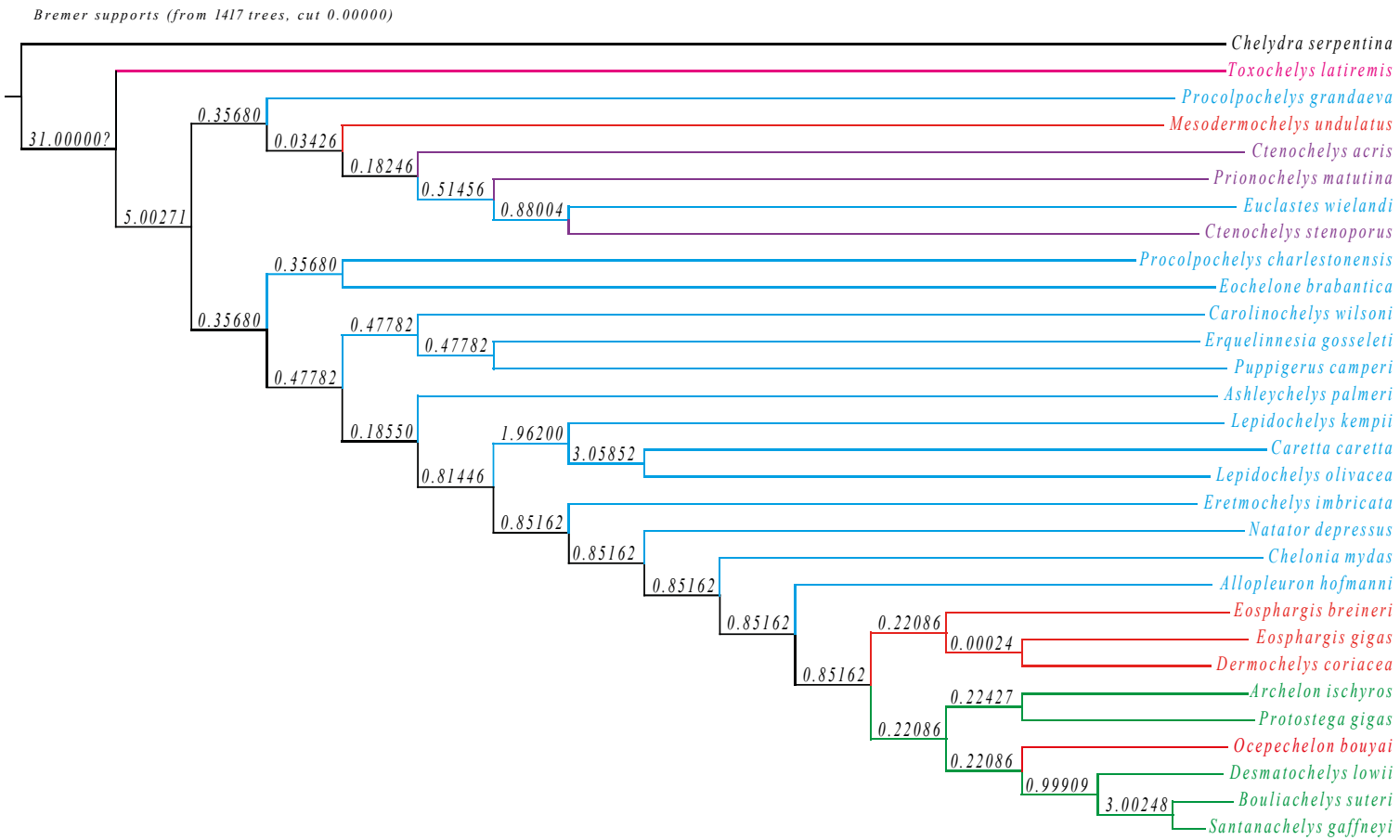

Figure 37. Cladogram of the most parsimonious tree of the third global preliminary analysis. Legend: green – Protostegidae; blue – Pancheloniidae; red – Dermochelyidae; black – Chelydridae; purple – Ctenochelyidae; pink – *Toxochelys latiremis*.

LANDMARK + TRADITIONAL DATA 4 (RFTRA against *L. olivacea*)

analysys tot014 bremer

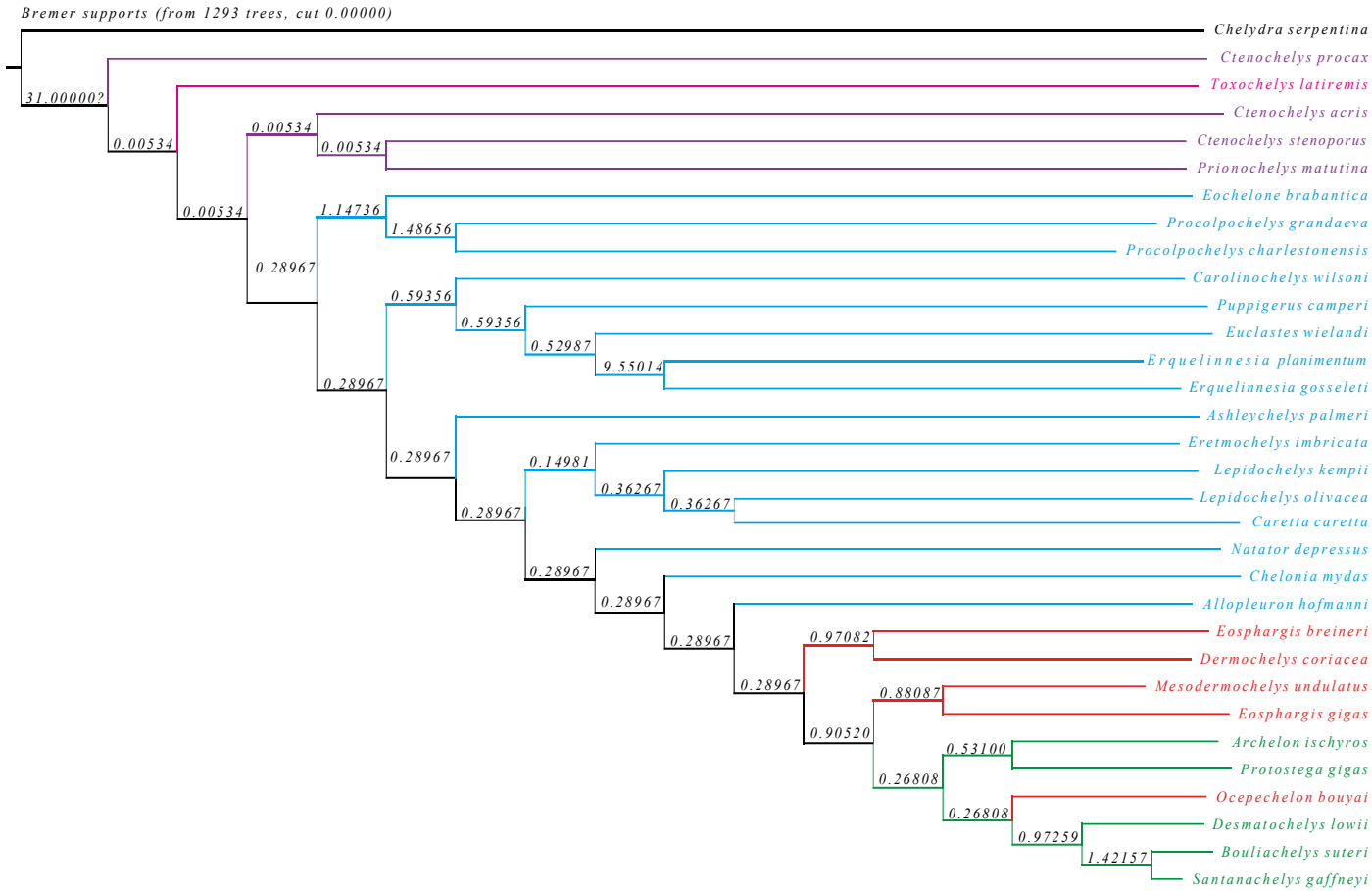

Figure 38. Cladogram of the most parsimonious tree of the fourth global preliminary analysis. Legend: green – Protostegidae; blue – Pancheloniidae; red – Dermochelyidae; black – Chelydridae; purple – Ctenochelyidae; pink – *Toxochelys latiremis*.

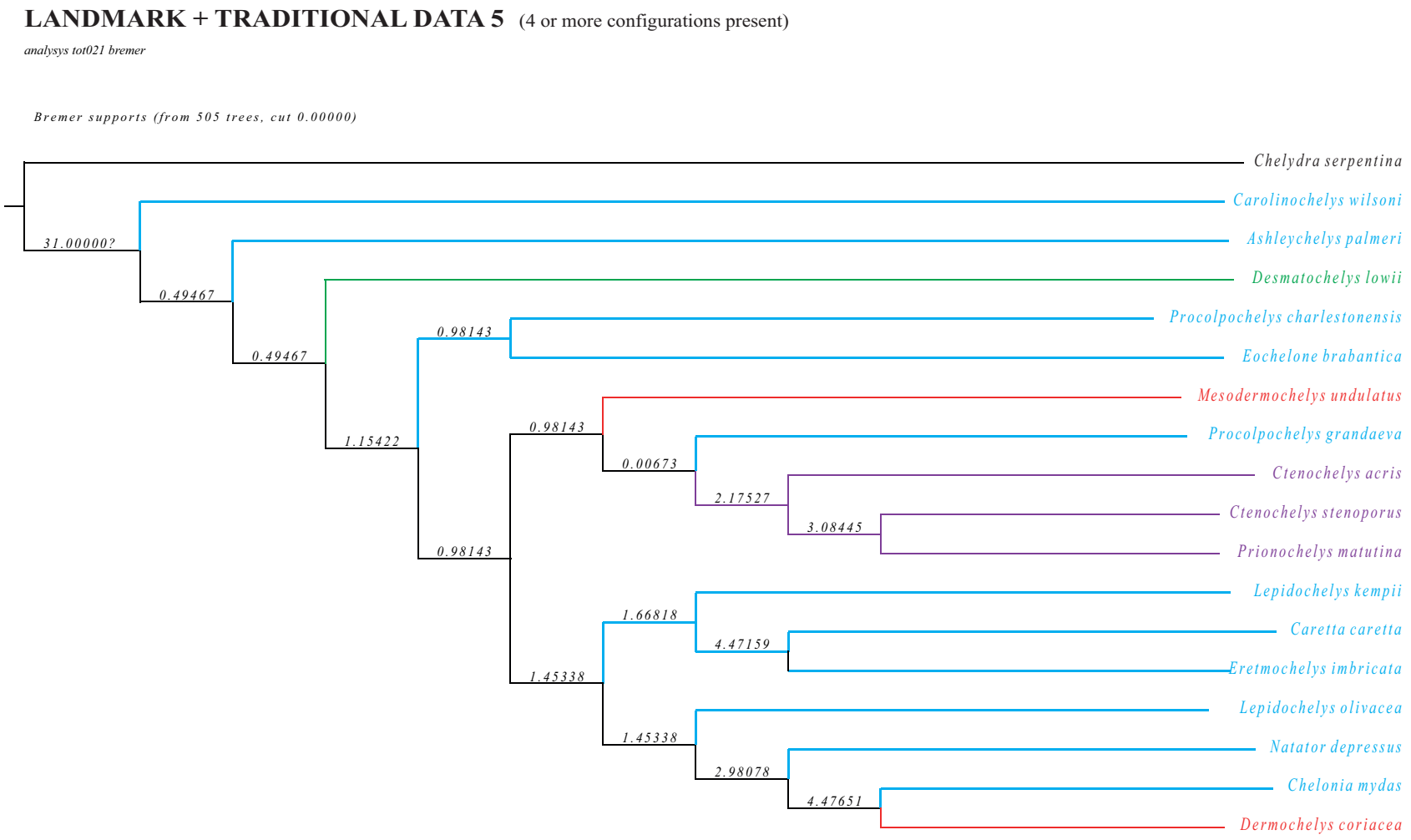

Figure 39. Cladogram of the most parsimonious tree of the fifth global preliminary analysis. Legend: green – Protostegidae; blue – Pancheloniidae; red – Dermochelyidae; black – Chelydridae; purple – Ctenochelyidae; pink – *Toxochelys latiremis*.

LANDMARK + TRADITIONAL DATA 6.1 (Ctenochelyidae and early diverging taxa)

analysys tot024 bremer

Bremer supports (from 78 trees, cut 0.00000)

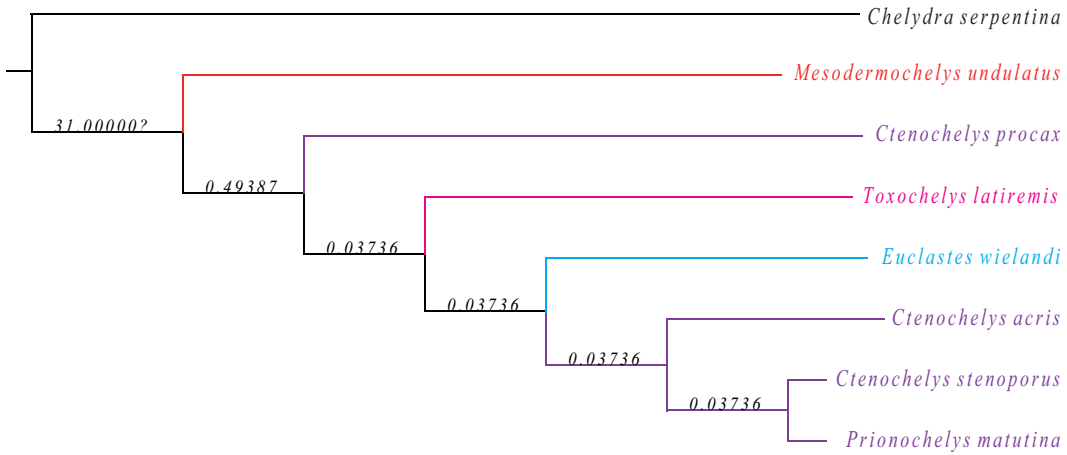

Figure 40. Cladogram of the most parsimonious tree of the sixth global preliminary analysis. Legend: blue – Pancheloniidae; red – Dermochelyidae; black – Chelydridae; purple – Ctenochelyidae; pink – *Toxochelys latiremis.*

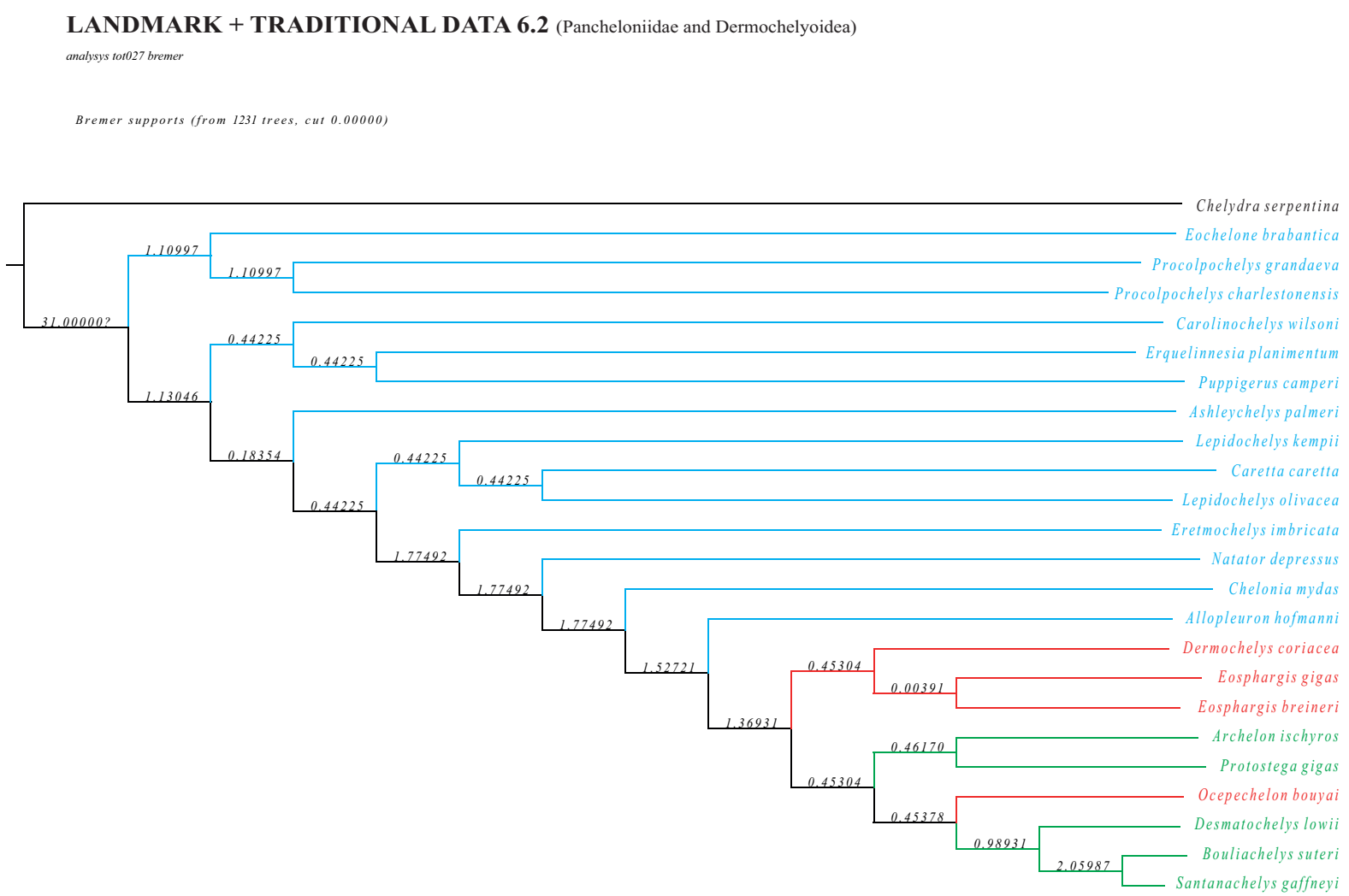

Figure 41. Cladogram of the most parsimonious tree of the sixth global preliminary analysis. Legend: green – Protostegidae; blue – Pancheloniidae; red – Dermochelyidae; black – Chelydridae; purple – Ctenochelyidae; pink – *Toxochelys latiremis*.